SYNTHESIS AND CHARACTERIZATION OF NANOENCAPSULATED FERULIC ACID FOR BIOMEDICAL USAGE

Ph.D. THESIS

by

RICHA PANWAR

DEPARTMENT OF BIOTECHNOLOGY
INDIAN INSTITUTE OF TECHNOLOGY ROORKEE
ROORKEE – 247667, INDIA
JUNE, 2016

SYNTHESIS AND CHARACTERIZATION OF NANOENCAPSULATED FERULIC ACID FOR BIOMEDICAL USAGE

A THESIS

Submitted in partial fulfilment of the requirements for the award of the degree

of

DOCTOR OF PHILOSOPHY

in

BIOTECHNOLOGY

by

RICHA PANWAR

DEPARTMENT OF BIOTECHNOLOGY
INDIAN INSTITUTE OF TECHNOLOGY ROORKEE
ROORKEE – 247667, INDIA
JUNE, 2016

INDIAN INSTITUTE OF TECHNOLOGY ROORKEE
ROORKEE

CANDIDATE'S DECLARATION

I hereby certify that the work which is being presented in this thesis entitled "**SYNTHESIS AND CHARACTERIZATION OF NANOENCAPSULATED FERULIC ACID FOR BIOMEDICAL USAGE**" in partial fulfilment of the requirements for the award of the Degree of Doctor of Philosophy and submitted in the Department of Biotechnology of the Indian Institute of Technology Roorkee, Roorkee is an authentic record of my own work carried out during a period from December, 2010 to June 2016 under the supervision of Dr. Vikas Pruthi, Professor, Department of Biotechnology and Dr. Dharam Dutt, Professor, Department of Pulp and Paper Technology, Saharanpur Campus, Indian Institute of Technology, Roorkee, Roorkee.

The matter presented in this thesis has not been submitted by me for the award of any other degree of this or any other Institute.

(**Richa Panwar**)

This is to certify that the above statement made by the candidate is correct to the best of our knowledge.

(Vikas Pruthi)
Supervisor

(Dharam Dutt)
Supervisor

Dated: _____

Abstract

Use of naturally occurring phytochemicals have attracted a great deal of interest as therapeutic agents against a wide range of ailments. Hydroxycinnamic acid derivatives are a major category of phenolic acids which provide significant benefits as natural antioxidants. Ferulic acid (FA; $C_{10}H_{10}O_4$) is the most abundant hydroxycinnamic acid bound to lignin and polysaccharides via ester/ether linkages in plant cell walls. FA is present in various cereals, fruits, crop residues (wheat bran, corn bran, sugarcane bagasse) and possess a potent antioxidant capacity due to its structural characteristics. It exhibits an array of therapeutic properties including anti-inflammatory, anticancer, anti-diabetic, antimicrobial along with prevention of cardiovascular disorders. Most of these activities could be directly attributed to the free radical scavenging potential of FA. Although having valuable therapeutic characteristics, this important plant derived nutraceutic display major drawback in the form of low bioavailability and clinical efficacy. FA exhibits a small plasma retention time both in rats and humans and is quickly eliminated from the body, mostly via urinary excretion. Polymeric encapsulation of FA would enhance its plasma retention time, bioavailability and stability against degradation in gastrointestinal tract. Chitosan (CS) is a non-toxic biocompatible polymer, used extensively for encapsulation of bioactive molecules. CS acts as a shell material to envelop these compounds bearing multiple negative charges via cationic crosslinking to generate stable, biodegradable nanosized particles through ionic cross linking when comes in contact with specific polyanions such as sodium-tripolyphosphate. These nanoparticles are extensively used to deliver various compounds including drugs, proteins, nutrients and phenolics into the biological systems. Present investigation was carried out to synthesize ferulic acid encapsulated chitosan nanoparticles (FANPs) having enhanced plasma retention time along with investigation of their effects in biological disorders such as cancers, diabetes, inflammations.

Chapter 2 deals with synthesis and characterization of FANPs at optimized CS conc. 1 mg/ml, CS:TPP mass ratio 4 and FA conc. 0.0528 and 0.1056 mg/ml. Particles diameter/morphology of resulting nanoparticles were measure and visualized through zeta sizer and field emission-scanning electron microscopy (FE-SEM) analysis. Approximately 50% encapsulation efficiencies were achieved for optimized nanoformulations that exhibited enhanced solubility, higher thermal degradation range along with stability of FA antioxidant potential during encapsulation.

Biochemical characterization of FANPs through the Fourier transform infrared spectra (FT-IR) provided an insight about its secondary interactions with chitosan nanoparticles (CSNPs). Proton nuclear magnetic resonance (^{1}H NMR) spectroscopy revealed the functional groups shifts in the chemical structures of different formulations that have taken place during encapsulation process while the X-ray diffractometry (XRD) established the successful encapsulation of FA. Subsequently, in Chapter 3, pharmacokinetic and urinary excretion profile analyses were carried out for FA in free form (non-encapsulated) and FANPs using healthy Wistar albino rats. FA in its free form was found to eliminate quickly from the circulation owing to its rapid and extensive metabolism and is mostly excreted through urine. The encapsulated FA displayed extended plasma retention time and maximum plasma conc. was recorded at 60 min which implied enhancement of T_{max} to four times higher compare to free FA. The elimination of compound from rat's body also displayed a similar pattern where the peak urinary excretion of FA from nanoformulations was measured at 4 h contrary to 2 h in case of free FA. In the same context, rats with carrageenan-induced paw edema showed a better recovery when treated with FANPs establishing them as a highly promising and cost-effective nutraceutical with commendable safety profile. The ability of FA to regulate cell growth and proliferation, scavenge free radicals, stimulate cytoprotective enzymes and inhibit cytotoxic systems in both *in-vitro* and *in-vivo* experimental models account for the potential adjuvant role of FA in cancer therapy. Nevertheless, the unfavorable pharmacokinetic and low bioavailability of FA necessitate its encapsulation into CS, in order to increase bioavailability and at the same time maintain or enhance its antiproliferative action. Chapter 4 emphasized on the *in-vitro* evaluation of anticancer potential of FANPs on ME-180 human cervical carcinomas and PC-3 human prostate cancer cell lines. Initially, the *in-vitro* release of FA from its nanoformulations was evaluated at different pH, followed by screening of both cell lines with different conc. of FANPs to estimate minimum dose required for their 50% inhibition (IC_{50}). Subsequently, the effect of nanoformulations on cell proliferation were assessed via MTT assay and flowcytometry. Morphological changes occurring within the formulation treated cells were visualized through FE-SEM and fluorescence microscopy. Finally, the cytocompatibility of corresponding formulations were checked on Human Embryonic Kidney (HEK-293) cell lines. Cytotoxicity evaluation of FANPs established them as strong antiproliferative agents against ME-180 human cervical and PC-3 human prostate cancer cell lines without any potential toxicity to normal healthy cells. In subsequent chapter testing of antibiofilm potential of FANPs against *Candida albicans* biofilms was performed. *C. albicans* is the major multidrug tolerant species,

causing life-threatening infections that display striking ability to form drug-resistant biofilms. *C. albicans* biofilms are reported to be 4000 times more resistant to antifungal drug fluconazole when compared to planktonic or to its free-floating counterparts. Compared to conventional synthetic antifungal drugs that have become unyielding towards the biofilm matrix, there was a less likelihood of the development of resistance by biofilm cells against naturally occurring FA. Hence, it was hypothesized that FANPs could easily penetrate the biofilm cells and matrix owing to their high surface area to volume ratio. These FANPs are believed to disrupt or alter the permeability of fungal cell plasma membrane and could reduce the cell population. Cytocompatible FANPs at conc. 40 µM and 80µM reduced *C. albicans* biofilm cells viability upto 30 and 21.4% respectively, thus emphasizing its potential as a powerful antifungal agent. Positive zeta potential of FANPs was proposed to be a crucial factor facilitating their binding with negatively charged membrane of fungal cell, thus disrupting its integrity which eventually lead to leakage of intracellular materials and biofilm inhibition. The intriguing synergistic effect of FANPs on prevention of *C. albicans* biofilm might offer a new hope in the management of biofilm related infections. Chapter 6 confined to the evaluation and comparison of *in-vivo* anti-diabetic activities of native FA and FANPs in streptozotocin (STZ) induced diabetic Wistar albino rats. Diabetes mellitus is a condition which is characterized by various pathological disorders, all or most of which are integrated with chronic hyperglycemia. The hyperglycemic disorders are very likely to cause overproduction of free radicals, giving rise to an oxidative stress inside the body tissues. FA displayed a strong anti-diabetic behavior by regulating a large number of biochemical or physiological pathways involved in hyperglycemia. It is found to stimulate insulin secretion by pancreatic β-cells while inhibiting lipid peroxidation in diabetic mice resulting in the improvement of hyperglycemia. FANPs with a higher cellular availability and enhanced plasma retention time exhibited a positive effects on diabetes associated symptoms such as lowering of blood glucose levels, enhancement in body weight along with reduction in total cholesterol, low density lipoprotein cholesterol and triglycerides conc. in diabetic rats. FANPs also resisted a sharp decline in insulin level, which allowed further regulation of cholesterol, triglycerides and overall lipid profile in induced diabetes. Positive impact of FANPs in improving the hyperglycemic condition prevalent in diabetic rats might provide new avenues for the treatment of diabetes mellitus and helps to avoid the secondary complications associated with synthetic drugs.

Acknowledgements

This is a perfect opportunity to express my sincere gratitude to my supervisors, Prof. Vikas Pruthi and Prof. Dharam Dutt for their constant guidance, constructive criticism, motivation and support through each and every step of my work. I have been able to complete my work with the help of their valuable suggestions and continuous boost throughout this venture.

I extend my sincere regards to my committee members, Prof. R. Prasad, Prof. Sanjoy Ghosh (Chairman, SRC), Department of Biotechnology and Prof. M. R. Maurya, Department of Chemistry, IIT Roorkee, for their time and valuable advices on my research work. The help provided by other faculty members of Department of Biotechnology and the staff at Institute Instrumentation Centre, IIT Roorkee to carry out data analysis is also highly appreciable.

I would also like to acknowledge the office staff of Department of Biotechnology, IIT Roorkee for their prompt support on quick calls. Here, I would also like to appreciate the help and support provided by my dear friend Ms. Mandeep Kaloti, Centre for Nanotechnology, IIT Roorkee. I also find this as an appropriate opportunity to thank all my labmates and seniors to help me to garner beautiful memories throughout my journey.

This is a time to show heartfelt gratitude to my ever supportive and most adorable parents for their love and perseverance all throughout my ordeal. It won't have been possible for me to achieve anything that I have today without their faith in me. It would never be enough to appreciate the constant support, patience and care bestowed upon me by my husband Mr. Vishal Sarawat and respected in laws who were constantly supportive and encouraging through my ordeal. This acknowledgement could not be completed without thanking my dear sister, nephew and brother in law for being there in all thick and thins throughout my journey.

Contents

Abstract ..... **i**

Acknowledgements ..... **iv**

Contents ..... **v**

List of Figures ..... **viii**

List of Tables ..... **xii**

List of abbreviations ..... **xiii**

Chapter 1 Introduction and Literature Review **1**

1.1. Ferulic acid 2

1.2. Natural sources and occurrences of FA 3

1.3. Therapeutic potentials of FA: linkage with antioxidant capacity 5

1.3.1. Free radical scavenging and lipid peroxidation 6

1.3.2. FA as an anticancer agent 8

1.3.3. FA in diabetes control 9

1.3.4. FA as an anti-inflammatory agent 11

1.3.5. FA against pathogens 12

1.3.6. Other biomedical uses of FA 12

1.3.7. Industrial applications of FA 13

1.4. Metabolism and pharmacokinetic of FA 13

1.5. Chitosan 15

1.5.1. Physico-chemical attributes of CS 16

1.5.2. Biological applications of CS 16

1.6. Chitosan based nanoencapsulation 18

1.7. Synthesis of CSNPs by ionic cross linking: An overview 20

1.8. Drug delivery and therapeutic applications of CSNPs 22

1.9. Objectives 24

Chapter 2: Synthesis and Characterization of Ferulic Acid Encapsulated Chitosan Nanoparticles **25**

2.1. Introduction 25

2.2. Materials and methods 26

2.2.1. Materials 26

2.2.2. Preparation of solutions 26
2.2.3. Synthesis of nanoparticles 26
2.3. Physicochemical characterization of nanoparticles 27
2.4. Free radical scavenging activity 28
2.5. Results and discussion 29
2.5.1. Synthesis of FA-CSNPs 29
2.5.2. Characterization of FANPs 37
2.6. Free radical scavenging activity 44
2.7. Conclusion 45
Chapter: 3: *In-vivo* Release Study of FANPs and their Anti-inflammatory Potential in Carrageenan-induced Paw Edema in Wistar Albino Rats 46
3.1. Introduction 46
3.2. Methodology 48
3.2.1. Animal care and handling 48
3.2.2. Acute oral toxicity studies 48
3.2.3. Pharmacokinetic study design 48
3.2.4. Analytical procedure 50
3.3. Anti-inflammatory activities 51
3.4. Results and discussion 52
3.5. Conclusion 60
Chapter 4: Evaluation of FANPs as an Anticancer Agent 61
4.1. Introduction 61
4.2. Materials and methods 62
4.2.1. In- vitro release analysis 63
4.2.2. Screening of formulations 63
4.2.3. Cytotoxicity analysis 64
4.2.4. Cytocompatibility evaluation 65
4.3. Results and Discussion 65
4.3.1. In vitro FA release analysis 65
4.3.2. Screening of FANPs effective conc. 66
4.3.3. Cytotoxicity evaluation 74
4.3.4. Cytocompatibility evaluation 84
4.4. Conclusion 88

Chapter 5: FANPs as Potent Antibiofilm Agents 89
5.1. Introduction 89
5.2. Material and methods 90
5.3. Results and discussion 91
5.4. Conclusion 100
Chapter 6: FANPs as Anti-diabetic Agents: *In-vivo* Studies 101
6.1. Introduction 101
6.2. Materials and methods 102
6.2.1. Experimentations 103
6.2.2. Biochemical studies 104
6.3. Results and discussion 109
6.4. Conclusion 115
Summary and Future Scope 116
References 117
List of Publications 142

List of Figures

Figure 1.1: Structural representation of FA 3

Figure 1.2: Hypothetical representation of ferulic acid ester linkages to arabinoxylan (A) FA linked to O-5 of arabinose chain of arabinoxylan. (B) A-1,4-linked xylan backbone. (C) B-1,2-linked L-arabinose. (Image source: Buanafina, 2009)..... 4

Figure 1.3: Resonance stabilization of FA radical (Image source: Srinivasan et al., 2007)..... 6

Figure 1.4: Pictorial representation of therapeutic capacities of naturally occurring FA associated with its free radical scavenging potential..... 6

Figure 1.5: Industrial applications of ferulic acid..... 13

Figure 1.6: Chemical structure of chitosan..... 16

Figure 1.7: Synthesis of CSNPs through intramolecular linkages..... 21

Figure 1.8: Schematic representation of the synthesis of FA encapsulated CS nanoparticles through CS-TPP ionic cross linking..... 21

Figure 2.1: Variations in (A) particles diameter (B) zeta potential of CSNPs at different CS-TPP mass ratio tested 30

Figure 2.2: FESEM micrographs of CSNPs at CS:TPP mass ratio 4 and CS conc. 1 mg/ml; Microscopic magnification 50KX, Scale bar 100 nm 31

Figure 2.3: FE-SEM images depicting A) Small particles at CS:TPP mass ratio 2, CS conc. 1mg/ml; Microscopic magnification 50KX, Scale bar 200 nm. B) larger aggregates at CS:TPP mass ratio 6, CS conc. 1mg/ml; (Microscopic magnification 50KX, Scale bar 1 µm) 32

Figure 2.4: FA standard curve for calculations of encapsulation efficiencies of FANPs at 319 nm..... 34

Figure 2.5: FESEM micrographs of FANPs obtained at nanoformulation NF2; CS conc. 1mg/ml, native FA conc. 0.0528 mg/ml; (Microscopic magnification 100KX, Scale bar 100 nm)..... 35

Figure 2.6: The auto-fluorescence micrograph of FANPs at NF2 at wavelength 470-510 nm; (Magnification 100KX, Scale bar 10µm)..... 36

Figure 2.7: Randomly distributed large FANPs visualized at NF4; (Microscopic magnification 50KX, Scale bar 2µm)..... 37

Figure 2.8: Fourier transform infrared spectrum of different formulations..... 38

Figure 2.9: A proposed mechanism of interaction between phenoxy groups of FA and amino group of CS..... 38

Figure 2.10: A) Thermogravimetric, B) derivative thermogravimetric, C) differential scanning calorimetric thermographs for different formulations..... 40

Figure 2.11: ^{1}H nuclear magnetic resonance spectra for test formulations 42

Figure 2.12: XRD patterns of different test formulations A) native FA, B) CSNPs and FANPs .43

Figure 2.13: Ascorbic acid standard curve for calculating DPPH radical scavenging capacities of test formulations at 517 nm.....44

Figure 3.1: FA standard curve 51

Figure 3.2: A) Induction of paw edema in rat by carrageenan, (B) Measurement of rat paw volume by Plethysmograph.....52

Figure 3.3: Schematic representation of pharmacokinetic analysis and interaction of FANPs to target cell membrane and their internalization. Upon entering the cell's internal environment nanoparticles might be attacked by lysosomal enzymes causing a sustained FA release.....54

Figure 3.4: **(A)** Plasma conc. of free FA and FANPs at different time intervals post oral administration **(B)** Area under chromatographic curve for both formulations at different time intervals **(C)** HPLC chromatogram for free FA corresponding to its C_{max} (1.774243) and T_{max} (15 min) 55

Figure 3.5: The HPLC chromatograms depicting FA release from rats treated with nanoformulation after (A) 0.5 h, (B) 1h, (C) 2h, (D) 6h 56

Figure 3.6: Urinary excretion profile of animals administered with free FA and FANPs 58

Figure 4.1: *In- vitro* release of FA from its nanoformulations over a period of 120 h in PBS at different pH values.....66

Figure 4.2: MTT metabolic activity assay for A) ME-180 B) PC-3 cells treated with different test formulations for 72 h. Error bars represent mean ± standard deviation for three independent experiments (n = 3).....67

Figure 4.3: Phase contrast micrographs showing the effect FANPs on ME-180 cell lines A) 10 µM, B) 20 µM, C) 40 µM; (Scale bar 10 µm, microscopic magnification 50X).....70

Figure 4.4: Phase contrast micrographs showing the effect FANPs on PC-3 cell lines A) 40 µM, B) 80 µM, C)120 µM; (Scale bar 10 µm, microscopic magnification 50X) 73

Figure 4.5: Graphs representing viability of cancer cells treated with different test formulation A) ME-180 B) PC-3 75

Figure 4.6: A possible mechanism of interaction of FANPs with tumor cells: FANPs might bind to the tumor cell membrane via electron interactions, entered the cell through endocytosis and release the encapsulated FA slowly into the cytosol 75

Figure 4.7: FE-SEM micrographs of cells cultured in presence of FANPs at corresponding IC50, showing reduction in cell numbers A) ME-180 cells B) PC-3 cells; (Scale bar 10 µm, microscopic magnification 10 KX).....78

Figure 4.8: Fluorescent micrographs of AO:EtBr stained ME-180 cells treated with different test formulations (A^1-A^3) control cells, (B^1-B^3) CSNPs treated, (C^1-C^3) 40µM native FA treated and (D^1-D^3) 40µM FANPs treated cells after 24 h incubation. Morphological changes such as chromatin condensation and damaged wrinkled cells are marked with white arrows; (Microscopic magnification 100KX) 79

Figure 4.9: Fluorescent micrographs of AO:EtBr stained PC-3 cells treated with different test formulations (A_1-A_3) control cells (B_1-B_3) CSNPs treated (C_1-C_3) 80µM native FA (D_1-D_3) FANPs at 80µM conc. after 48 h incubation. Morphological changes such as chromatin condensation and damaged wrinkled cells are marked with white arrows; (Microscopic magnification 100KX) 80

Figure 4.10: A) Flow-cytometric graphs showing induction and progression of apoptosis at varying stages for ME-180 cell lines treated with different formulations B) Graph showing percentage variations in cells density upon treatment with different formulations..... 82

Figure 4.11: A) Flow-cytometric graphs showing induction and progression of apoptosis at varying stages for PC-3 cell lines treated with different formulations B) Graph showing percentage variations in cells density upon treatment with different formulations..... 83

Figure 4.12: Cytocompatibility evaluation of test formulations on HEK-293 cell lines after 24 h incubation by MTT assay. Error bars represent mean ± standard deviation for three independent experiments (n = 3); *p< 0.02; **p< 0.05 85

Figure 4.13: Scanning electron micrograph of HEK-293 cell lines. A) untreated control cells, B) cells treated with NF_2, C) cells treated with NF5, D) cells treated with FA_1, E) cells treated with FA_2, F) cells treated with FA_5; (Scale bar 1µm, Magnification 50KX)86

Figure 4.14: Fluorescent micrographs of AO:EtBr stained HEK-293 cells. A1-A3) control cells, B1-B3) cells treated with NF_2, C1-C3) cells treated with NF_3, D1-D3) cells treated with NF_5 after 24 h incubation; (Scale bar 50µm, Magnification 10KX)..... 87

Figure 5.1: Proposed mechanism displaying binding of positively charged FANPs to negatively charged *C. albicans* cell membranes..... 93

Figure 5.2: XTT assay representing changes in *C. albicans* cell metabolic activity (%) after 24 h incubation with different test formulation. Error bars represent mean ± standard deviation for three independent experiments (n = 3), *p< 0.0005, **p< 0.002, ***p < 0.00001..... 93

Figure 5.3: FE-SEM images of Control *C. albicans* biofilm cells at different magnifications A) 10 µm, 1KX, B) 2 µm, 5KX..... 94

Figure 5.4: FE-SEM images of variation in cell density of *C. albicans* treated with CSNPs at different magnifications. A) 10 µm, 1KX, B) 2 µm, 5KX..... 95

Figure 5.5: FE-SEM images of variation in cell density of *C. albicans* treated with FANPs (NF_1) at different magnifications. A) 10 µm, 1KX B) 2 µm, 5KX..... 96

Figure 5.6: FE-SEM images of variation in cell density of *C. albicans* treated with FANPs (NF_2) at different magnifications. A) 10 µm, 1KX B) 2 µm, 5KX..... 97

Figure 5.7: Variation in cell density of *C. albicans* treated with FANPs (NF_3) at different magnifications A) 10 µm, 1KX B) 2 µm, 5KX..... 98

Figure 5.8: Scanning electron microscopic images of *C. albicans* A) Control biofilm cells embedded in exopolymeric substances (i, inset) indicated by white arrow, B) Biofilm formed in presence of unloaded CSNPs and white arrow indicates the rough cell wall (ii, inset), note that no exopolymeric matrix was observed, C) Inhibition of biofilm formation by NF_2, arrow (iii, inset) signify the cell membrane shrinkage, D) NF_3 treated cells showing distortion (iv, inset) due to leakage of cell contents by plasmolysis; (Scale bar 2 µM, Microscopic magnification 5KX).....100

Figure 6.1: **(A)** Lipid profiling of rat serum **(B)** Automated analyzer.....104

Figure 6.2: (A) Excision of rat pancreas, (B) Pancreas kept in 10% formalin 108

Figure 6.3: Effect of test formulations on blood glucose levels in glucose loaded normal rats. Values are mean ± standard error, where n=6, *p<0.05, **p<0.01 and ***p<0.001. a- Significance difference as compare to control group, b-significance difference as compare to diabetic control group, c-significance difference as compare to reference drug treated group 110

Figure 6.4: Variations in body weight of STZ induced diabetic rats treated with different formulations over 14 days along with percent decrease in body weight 111

Figure 6.5: Impact of different test formulations in STZ induced diabetic rats on A) blood glucose level, B) blood insulin level. Values are mean ± standard error, where n=6, *p<0.05, **p<0.01; a- Significance difference as compare to control group, b-significance difference as compare to diabetic control group, c-significance difference as compare to native FA 112

Figure 6.6: Histopathological representation of pancreas treated with hemotoxylin and Eosin A) control group; pancreas with normal islets of Langerhans (arrow) within normal pancreatic acini (arrow head), B) diabetic group; pancreas showing shrunken islets with deformed acini, C) groups treated with standard glibenclamide showing normal islets and acini, D) groups treated with FANPs showing recovered islets of Langerhans with higher cells mass. (Microscopic magnification 100X).....115

List of Tables

Table 1.1: Lipid peroxidation studies of FA associated with it free radical scavenging effect 7

Table 1.2: Biological activities of CS and their applications 17

Table 1.3: Modifications in biological activities of nanoencapsulated polyphenols..... 24

Table 2.1: Particle size, zeta potential and encapsulation efficiencies of FANPs at different FA loading conc.; CS:TPP mass ratio 4; CS conc. 1 mg/ml 35

Table 2.2: Enhancement in solubility (%) of FANPs at NF2, and NF3 in different solvents at room temperature 36

Table 3.1: Effect of native FA and FANPs on carrageenan induced paw edema rat groups, compared with standard diclofenac sodium. Values are mean ± standard error, where n=6, *p<0.05, **p<0.01 and ***p<0.001 59

Table 6.1: Serum lipid profile of animal groups treated with different test formulations. Values are mean ± standard error, where n=6, *p<0.05, **p<0.01 and***p<0.001. a-Significance difference compared to control group, b-significance difference compared to diabetic control group, c-significance difference compared to native FA treated group..... 113

List of abbreviations

Abbreviations	Description
4-AAP	4-aminoantipyrine
AO	Acridine orange
AV	Annexin V
CAT	Catalase
CE	Cholesterol esterase
CHOD	Cholesterol oxidase
CMC	Carboxy methyl cellulose
Conc.	Concentration
CPCSEA	Committee for the Purpose of Control and Supervision of Experiments on Animals
CS	Chitosan
CSNPs	Chitosan nanoparticles
DAP	Dihydroxyacetone phosphate
DM	Diabetes mellitus
DMEM	Dulbecco's modified Eagle medium
DMSO	Dimethyl sulfoxide
DPPH	2, 2-diphenyl-1-picryl-hydazyl
DSC	Differential scanning calorimetry
DTG	Derivative thermogravimetric analysis
EC_{50}	Effective conc. to achieve 50% antioxidant capacity
EE	Encapsulation efficiency
EtBr	Ethidium bromide
FA	Ferulic acid

FACS	Fluorescence activated cell sorter
FAEs	Ferulic acid esterases
FANPs	Ferulic acid encapsulated CSNPs
FBS	Fetal bovine serum
FE-SEM	Field-emission scanning electron microscopy
FFA	Free fatty acids
FITC	Fluorescein 5(6)-isothiocyanate
FTIR	Fourier transform infrared spectra
GK	Glycerol kinase
GPO	Glycerol 3-phosphate oxidase
H	Hour(s)
HDL	High density lipoprotein
HPLC	High performance liquid chromatography
IC_{50}	Conc. required for 50% cell inhibition
IFA	Iso-ferulic acid
LD_{50}	Lethal dose required for 50% death (animal or cells)
LDL	Low density lipoprotein
LPL	Lipoproteins lipase
Min	Minute(s)
MTP	Microtitre plates
MTT	3-(4,5-dimethylthiazol-2-yl)-2,5-diphenyltetrazolium bromide
NF	Nanoformulation(s)
NMR	Nuclear magnetic resonance
NO	Nitric oxide
OGTT	Oral glucose tolerance test

PBS	Phosphate buffered saline
PI	Propidium iodide
POD	Peroxidase
RNS	Reactive nitrogen species
ROS	Reactive oxygen species
SOD	Superoxide dismutase
STZ	Streptozotocin
TC	Total cholesterol
TG	Triglycerides
TGA	Thermogravimetric analysis
TPP	Sodium tri-polyphosphate
VLDL	Very low density lipoprotein
XRD	X-Ray diffraction
XTT	2,3,-bis(2-methoxy-4-nitro-5-sulfophenyl)-5-[(phenylamino)-carbonyl]-2H-tetrazolium salt
YPD	Yeast peptone dextrose

Chapter 1

Introduction and Literature Review

1.1. Background

Currently, there is a widespread consumer led trend to withdraw from chemically synthesized drugs and therapies due to their possible health hazards and instead search for natural alternatives for various chronic diseases. In this regard, plant-based foods, such as fruits, vegetables, and whole grains containing significant amounts of bioactive phytochemicals may provide desirable health benefits beyond basic nutrition (Liu, 2003). Among various phytochemicals, phenolic compounds have attracted great interest due to growing evidence of their beneficial effect on human health. Epidemiological studies have shown an inverse association between the intake of foods rich in phenolic compounds and the incidences of cardiovascular disease, diabetes mellitus, and cancer (Luana et al., 2012; Hertog et al., 1993). In plant kingdom, phenolic compounds are the secondary metabolites involved in plant defense against ultraviolet radiation or aggression by pathogens (Manach et al., 2004). These compounds are majorly classified in terms of phenols, coumarins, flavonoids and phenolic acids (Marian and Fereidoon, 2004). Phenolic acids are the compounds with one phenol ring bound to one or more hydroxyl groups, widely distributed throughout the plant kingdom. These naturally occurring phenolic acids consists of two distinctive classes: hydroxybenzoic acid and hydroxycinnamic acids. The basic skeleton remains same in both these groups, the difference is established by the numbers and positions of the hydroxyl groups on the aromatic ring. Hydroxybenzoic acids include gallic, p-hydroxybenzoic, protocatechuic, vanillic and syringic acids, having a common C_6–C_1 structure. Hydroxycinnamic acid are aromatic compounds having a three-carbon side chain (C_6–C_3), with caffeic, ferulic, p-coumaric and sinapic acids as the most common members of group (Bravo, 1998). Hydroxycinnamic acid derivatives are a major category of phenolic acids which provide important benefits as natural antioxidants. Among these, FA ($C_{10}H_{10}O_4$) is the most abundant hydroxycinnamic acid bound to lignin and polysaccharides via ester/ether linkages in plant cell walls. The compound has found wide applicability in the field of medicine in the form of an antimicrobial and anti-inflammatory agent, along with anticancer effect, cholesterol-lowering activity, prevention against thrombosis and

atherosclerosis since many decades (Graf, 1992; Smith and Hartley, 1983; Gorewit, 1983; Dutt, 1925). Most of the therapeutic properties of FA could be attributed to its potent antioxidant capacity. As a result, it has emerged as a natural molecule of choice in pharmaceutical, cosmetics, food and agrochemical industries. Recently 36 amide derivatives of FA have been screened for *in-vitro* antioxidant and anticancer agents (Kumar et al., 2016).

1.2. Ferulic acid

FA is a ubiquitous plant phenolic acid found in corn bran, wheat bran, maize bran, bamboo shoots, citrus fruits, extracts of various herbs and several other fruits and vegetables (Mattila and Hellstrom, 2007; Mattila, 2005; Kroon et al., 1999). Initially arising from the metabolism of phenylalanine and tyrosine, FA is the most abundant hydroxycinnamic acid in plant cell walls. It occurs in leaves and seeds either freely or covalently linked via ether/ester to lignin and/or polysaccharides (Smith and Hartley, 1983). FA nomenclature comes from *Ferula foetida*, a plant of Umbelliferae, from which it was first isolated in 1866 and later chemically synthesized in 1925 (Graf, 1992). FA functions in plants include defense from pests and microorganisms, indoleacetate enzyme inhibition and resistance towards seed bud breakage (Fazary and Ju, 2008; Mathew and Abraham, 2006; Li et al., 2003; Rosazza et al., 1995). The biological effect of FA came to notice in 1970s, when Yagi & Ohishi (1979) reported the antioxidant properties of FA steryl esters extracted from rice oil. Several medical studies carried out in China have established FA as an effective component of Chinese traditional medicine, such as *Angelica sinensis, A. cimicifuga and A. heracleifolia lignsticum chuangxiong* (Sakai et al., 1999). Additionally, FA salt namely sodium ferulate is reported to be used for treatment of cardiovascular and cerebrovascular diseases (Wang et al., 2004). Palacios et al. (1990) and Graf (1992) reported the role of phenolic nucleus and extended side chain of FA to forms a resonance stabilized phenoxy radical which accounts for its free radical-scavenging effect.

Organic and inorganic molecules/atoms containing one or more unpaired, independently existing electrons are termed as free radicals. These free radicals are found in all biological systems as they are continuously generated by several physiological processes. In addition to endogenous generation, various exogenous/environmental factors such as ultraviolet light, air pollutants and cigarette smoke contributes to the induction of potentially damaging free radicals. The property of terminating free radical chain reaction is conferred upon FA due to the presence of electron

donating groups on the benzene ring in its structure (Figure 1.1). The carboxylic group with an adjacent unsaturated C-C double bond also provides additional attack site to free radicals thus preventing the further reaction (Srinivasan et al., 2007). FA could thus provide a defensive system against the detrimental effects caused to human health by free radicals. Besides that, FA also augment the activities of enzymes such as superoxide dismutase (SOD) and catalase (CAT), at the same time inhibiting the enzymes that catalyzes free radicals production (Ou and Kwok, 2004). FA is also reported to suppress melanin generation by antagonizing tyrosine owing to similarities in their chemical structures. FA powerfully absorb the harmful long wave ultraviolet band hence becomes particularly effective for cosmetic use as a whitening agent and sunscreen (Lin et al., 2005; Chan et al., 2004; Saija et al., 1999). During last three decades, several researchers have documented FA ability to protect DNA and lipids against oxidation through reactive oxygen species (ROS), leading to prevention or treatment of oxidative stress linked disorders including disease such as Alzheimer, diabetes and cancers (Mori et al., 2013; Ohsaki et al., 2008; Srinivasan et al., 2006; Balasubashini et al., 2003; Kanski et al., 2002 Andreasen et al., 2001; Ohta et al., 1997; Bourne and RiceEvans 1997; Asanoma et al., 1994; Kuenzig et al., 1984).

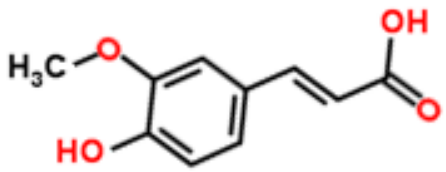

Figure 1.1: Structural representation of FA

1.3. Natural sources and occurrences of FA

FA is ubiquitously present in various commelinid plants such as wheat, rice, oats; in grasses; citrus fruits; sugar-beet; cereals along with many crop residues. It represents the most abundant hydroxycinnamic acid cross-linked with lignin and polysaccharides via ester and ether bonds in plant cell walls, forming lignin/phenolics–carbohydrate complexes. (Buranov and Mazza, 2009; Tilay et al., 2008; Buranov and Mazza, 2008). Ester linkage between the carboxylic acid group of

FA and the primary alcohol on the C_5 carbon of the arabinose side chain of arabinoxylans are the major sites for introduction of FA residues into the cell wall polysaccharides of grasses (Ralph and Helm, 1993; Hartley and Ford, 1989). In addition to esterified from, FA was also found covalently linked to lignin monomers via an ether linkage as described by Kondo et al (1990) and Scalbert et al (1985). Presence of FA in arabinoxylans may act as a nucleating site for lignin formation and its linkage to the xylan/cellulose network via lignin–ferulate–xylan complexes (Figure 1.2). This bonding between xylan and cellulose accounts for the low digestibility of most grass species as well as resistance of grass tissues towards degradation by simple mixtures of cellulases and xylanases (Buanafina, 2009).

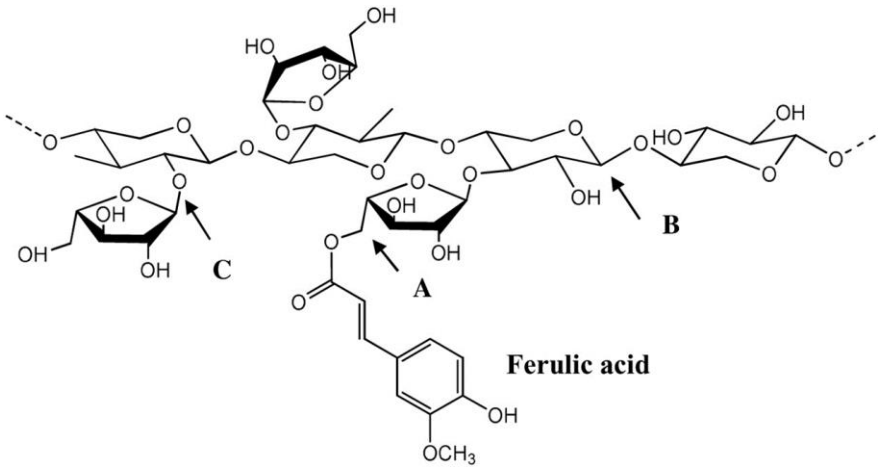

Figure 1.2: Hypothetical representation of ferulic acid ester linkages to arabinoxylan **(A)** FA linked to O-5 of arabinose chain of arabinoxylan. **(B)** A-1,4-linked xylan backbone. **(C)** B-1,2-linked L-arabinose. (Image source: Buanafina, 2009)

FA could generally be synthesized by either chemical method involving condensation of vanillin with malonic acid catalyzed by piperidine or it could be extracted from natural resources. Widespread occurrence of FA among the plant kingdom offers a great opportunity for its extraction from the plant sources thus establishing it as the most preferred method for FA synthesis. Different extraction methods involving alkaline, acidic and enzymatic procedures have been reported for FA extraction from various plant sources (Tilay et al., 2008; Lam et al., 2001). Enzymatic extraction method involves use of cell wall degrading enzymes such as hemicellulases,

xylanases, pecitnases and specific feruloyl esterase enzymes (FAEs) that plays key role in hydrolyzing ferulate ester group involved in cross linking between hemicelluloses or lignin-hemicellulose. However, because of covalent linkage of FA with lignin and other biopolymers, and the difficulty in obtaining pure FA from fermentation broth, its commercial production by enzymatic means becomes a challenging task. Alkaline extraction treatment essentially involves hydrolytic cleavage of ester linkages between lignin and plant polysaccharides thereby releasing FA (Lam et al., 1994).

1.4. Therapeutic potentials of FA: linkage with antioxidant capacity

In living cells, there are many cascades of events such as leakage of electrons from mitochondrial electron-chain reactions or from metal mediated reactions (transition metals) leading to production of various reactive oxygen species (ROS). These ROS differ in reactivity and lifetime and are capable of oxidizing proteins, lipids, DNA and in several cases, elevated levels of corresponding oxidative markers are reported (Kuenzig et al., 1984). Development of various chronic diseases such as cancer, neurodegenerative and cardiovascular diseases are also related to the production of ROS within tissues (Benzie, 2000). Essentially, preventive methods are required for capturing and scavenging these radicals and quenching of metal ions to inhibit them attacking the cellular targets. This could be achieved with the help of antioxidant that enhances cellular defense and prevent the oxidative damage to cellular components.

Recently, natural antioxidants have attracted considerable public and scientific interest as their administration may help in removing ROS, thus improving the overall clinical outcome (Itagaki et al., 2009). FA belongs to the family of phenolic acids and possess a potent antioxidant property which is usually attributed to its structural characteristics, such as the presence of phenolic nucleus and unsaturated side chain (Figure1.1). Upon collision with a reactive free radical, FA absorbs an H atom from it and generate a low energy, highly stabilized resonating structure (Srinivasan et al., 2007; Graf 1992; Palacios 1990). The electron present in this structure is not bound to oxygen only, rather it is free to delocalize across the entire molecule (Figure 1.3). Subsequently, instead of initializing any further radical chain reaction this resonating structure undergo collisions and condensations to yield dimeric ferulate. Some of the important functions of FA which could directly attributed to its free radical scavenging potential (Srinivasan et al., 2007) are summarized in Figure 1.4.

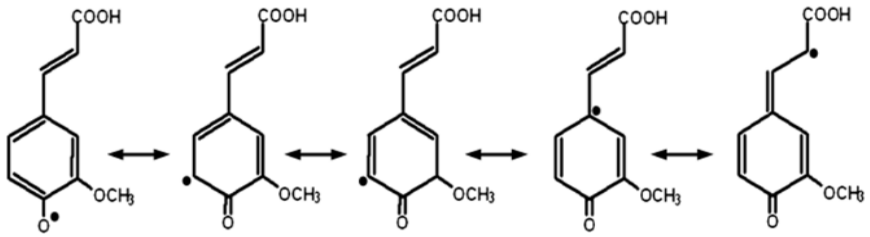

Figure 1.3: Resonance stabilization of FA radical (Image source: Srinivasan et al., 2007)

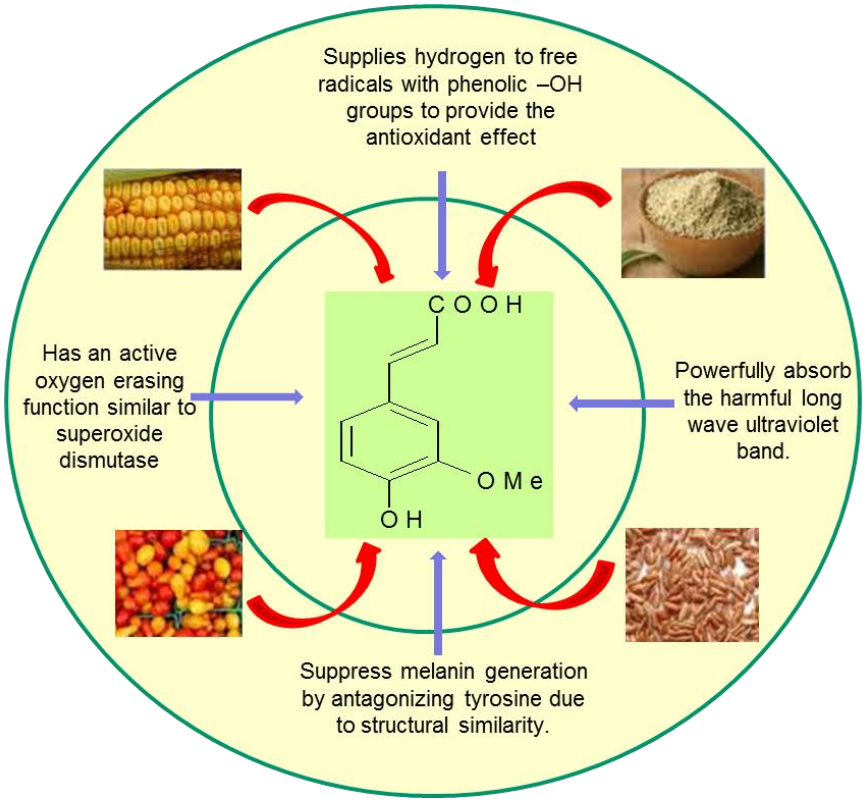

Figure 1.4: Pictorial representation of therapeutic capacities of naturally occurring FA associated with its free radical scavenging potential

1.4.1. Free radical scavenging and lipid peroxidation

The resonance stabilized phenoxy radical intermediate and carboxylic acid group (with the adjacent unsaturated carbon–carbon double bond) present in FA makes it an efficient scavenger of

both ROS and reactive nitrogen species (RNS). Along with this, the carboxylic acid group present in FA structure also acts as an anchor by which it binds to the lipid bilayer, conferring certain level of protection against lipid peroxidation (Kanski et al., 2002). Besides augmenting the activity of enzymes such as SOD and CAT, FA is also found to enhance cell stress response in co-ordination with the members of heat shock protein family. FA is indirectly involved in up regulation of heme oxygenase-biliverdin reductase system which in turn activates endogenous free radical scavenging mechanism. Presence of FA is also attributed to down-regulation of certain pathways involved in cell death such as inducible nitric oxide synthase (Mancuso and Santangelo 2014). Researchers have provided various line of evidences over time that are suggestive of a direct correlation between lipid peroxidation and free radical scavenging ability of FA (Table 1.1).

Table 1.1: Lipid peroxidation studies of FA associated with it free radical scavenging effect

S. No.	Antioxidant mechanism	Reference
1	Inhibition of peroxyl radicals initiated lipid peroxidation in reconstituted rat brain microsomes	Trombino et al., 2013
2	Modulation of nitric oxide synthase expression in focal cerebral ischemia in rat model	Koh, 2012
3	Inhibition of free radical-induced lipid peroxidation in the organ of Corti of guinea pigs	Fetoni et al., 2010
4	Reduction in H_2O_2 induced lipid peroxidation in peripheral blood mononuclear cells	Khanduja et al., 2006
5	Inhibition of toxicity associated with carbon tetrachloride generated secondary free radicals	Srinivasan et al., 2005
6	Regulating the over-expression of iNOS induced by amyloid-b-peptide in mouse	Cho et al., 2005
7	Peroxyl radical-induced cell death in synaptosomal and neuronal cell culture systems	Kanski et al., 2002
8	Inhibition of peroxynitrite dependent tyrosine nitration	Pannala et al., 1998
9	Improvement in the viability and motility of sperm, enhancement in intracellular levels of cAMP and cGMP, reduction in lipid peroxidation of cell membranes	Zheng and Zhang, 1997

1.4.2. FA as an anticancer agent

A variety of endogenous and exogenous factors are considered important in the initiation, progression and metastasis of neoplasms. These include ROS generation and subsequent damage to DNA and cell proteins, imbalance within intracellular signaling pathways that regulate cell proliferation and response to oxidative stress, resistance to apoptosis and chronic inflammations. FA's anti-carcinogenic activity is attributed to its capability of scavenging ROS along with inhibition of lipid peroxidation, stimulation of cytoprotective enzymes and regulation of cell growth and proliferation. Hirosi *et al*. (1999) related the anti-cancer activity of FA against heterocyclic amine-induced carcinogenesis to its antioxidant property. In the same context, Mori *et al*. (1999) reported a significant reduction in the incidences of tongue carcinomas and preneoplastic lesions in rats. Subsequently, Kawabata *et al*. (2000) observed lower incidence of colon carcinomas in azoxymethane induced colon carcinogenesis in F344 rats fed on FA diet. The activity of several detoxification enzymes which was otherwise blocked due to interference of azoxymethane was also found to be enhanced in this study.

Octyl and dodecyl esters of FA were reported to block the growth of lung, colon, breast and central nervous system tumor by inhibiting tumor cell proliferation, cyclooxygenase enzyme, and lipid peroxidation (Jayaprakasam et al., 2006). Increased intracellular levels of SOD, CAT along with vitamin A, C and E in FA administered rat peripheral blood lymphocytes were reported to confer protection from nicotine-induced DNA damage and lipo-peroxidation (Sudheer et al., 2007). Pathohistological evaluation carried out by Adluri et al. (2008) provided additional insight against nicotine-induced tissue damage and altered lipid levels in experimental rats. They reported a dose dependent effect of ferulic acid (10–40 mg/kg *per os* for 22 weeks) in nicotine-treated rats and observed a significant reduction in plasma markers of tissue damage namely, lactic dehydrogenase and alkaline phosphatase. Alias *et al*. (2009) evaluated the chemopreventive potential of topically applied as well as orally administered FA in Swiss albino mice with dimethylbenz(a)anthracene induced skin cancers. Their study reported the preventive effects of orally administered FA on to formation of skin tumor as well as its modulating effect on the status of detoxification agents, lipid peroxidation byproducts and cellular antioxidant. Regulation of phase II detoxification enzymes by FA in Sprague–Dawley rats induced with mammary carcinogenesis has also been reported (Baskaran 2010). Antiproliferative potential of FA was observed in Caco-2 colon cancer cells through modulation of various cell cycle proteins. It was reported to up-regulate centrosome

assembly and S phase checkpoint protein, whilst down regulating the proteins required for cell cycle progression in the S-phase (Janicke et al., 2011). Radiosensitizing effect of FA was documented by Karthikeyan et al. (2011) in HeLa and ME-180 cervical cancer cell lines by decreasing cell viability, survival, increasing intracellular ROS, lipid peroxidation and DNA damage in the cell lines. Role of FA as an adjuvant to chemotherapy or radiotherapy was further elucidated on HeLa cells where it potentiated the cytotoxicity of 5-fluorouracil (Hemaiswarya and Doble, 2013). The results of study carried out by Bandugula and Prasad (2013) suggested induction of cell death in NCIH460 lung cancer cell lines through a combinatorial effect of 2-Deoxy-D-glucose and FA. Both these compound initiated a multifaceted mechanism involving alteration in expression of p53, p21, NF-κB, Bax, and caspase-3 along with cell redox status. Recently, a further insight into cell cycle mediated anticancer mechanism of FA was provided by Eroğlu et al. (2015) in their study on human prostate cancer cells PC3. In their study, a significant increase in gene expression of TP53 (p53), BAX, BIK, and CYCS and a significant decrease in gene expression of BCL2 were seen in FA-treated PC3 cell lines.

1.4.3. FA in diabetes control

Diabetes mellitus (DM) is a most common endocrine disorder of multifactorial origin which is characterized by hyperglycemia i.e. an increased conc. of glucose in blood. Hyperglycemia originates as a result of impaired insulin secretion and variable degrees of peripheral insulin resistance, causing an overproduction of free radicals leading to oxidative stress inside the cells. During oxidative stress, the balance between the prooxidants and antioxidants is compromised inside the cell, thereby triggering cellular injury. In many cases, hyperglycemia leads to several other complications most severe of which include cognitive dysfunctions and cardiovascular disease (Jangra et al., 2013). Natural antioxidants with potent clinical efficacy must be developed to reduce oxidative stress associated with hyperglycemia, similar to their synthetic counterparts (Saini et al., 2007). FA, owing to its free radical scavenging activity was found useful in alleviating oxidative stress and attenuating the hyperglycemic response in streptozotocin induced diabetic KK-Ay mice. FA also inhibited lipid peroxidation in brown adipose tissue of diabetic mice thus establishing its utility for improvement of hyperglycemia in diabetes (Ohnishi 2004). Earlier it has been reported that amides derivatives of FA stimulated insulin secretion by pancreatic β-cells Noumura et al. (2003). Experiments conducted on Wistar female rats showed the activities of antioxidant enzymes glutathione peroxidase, SOD and CAT to be elevated in liver of FA

administered diabetic rats as compared to control group (Balasubashini *et al*., 2004). Further, a reduction in blood glucose level and increase in body weight was observed in groups which received FA, as a result of its anti-hyperglycemic effect.

An overall reduction in oxidative stress caused during diabetes correlated with decline in thiobarbituric acid reactive substances, hydroperoxides and free fatty acids in liver. Histopathology of pancreatic islets also demonstrated FA capacity to increase islet cells mass. Subsequently, Jung et al. (2007) demonstrated a significant reduction in blood glucose levels, plasma total cholesterol and low density lipoprotein cholesterol conc. in Type 2 diabetic mice administered with FA and its ethyl extract fraction. Elevated plasma insulin levels, hepatic glycogen synthesis and glucokinase activity were also noted in groups administered with these FA fractions. A noteworthy preventative effects of FA on diabetic nephropathy via suppression of TGF-β1 upregulation was validated on type 2 diabetic mice along with significant lowered urinary protein level compared to the control group (Fujita et al., 2008).

Another investigation conducted to assess the effect of FA on obese diabetic rats yielded a protective and therapeutic effects on diabetic nephropathy by reducing blood glucose, oxidative stress markers and inflammation. In renal histopathology, FA-treated rats showed decreased glomerular basement membrane thickness, glomerular volume, and mesangial matrix expansion (Choi et al., 2011). Previously, FA was shown to inhibit rat intestinal maltase and sucrase, thus acting as a natural alpha glucosidase inhibitor (Adisakwattana et al. 2009). Roy et al. (2013) and Ramar et al. (2012) studied and validated the role of FA in oxidative stress reduction, expression of pro-inflammatory cytokines and apoptosis on alloxan-induced diabetic mice and STZ induced diabetic rats. They further reported a substantial decrease in lipid peroxidation levels and reduced glutathione enzyme activities in liver, kidneys and pancreatic tissues in FA treated groups. Down-regulation of IL-1β and TGF- β1 expression and inhibition of the pro inflammatory factor NF-kB by FA were documented to be the underlying mechanism in these studies. A recent study testified the role of FA in improving diabetes-evoked hypertension through inhibition of ROS formation, improvement of NO production and endothelial relaxation (Badawy et al.2013). In their investigation, FA was also reported to inhibit aldose reductase in STZ induced diabetic rats. An interesting aspect of FA as an anti-diabetic agent was reflected from its synergistic interaction with commercially available anti-hypoglycemic drugs (Prabhakar et al. 2013).

The potentiality of FA as a supplement to reduce the side effects associated with metformin and thiazolidinedione in STZ induced diabetic rats was evaluated. Blood glucose, plasma lipid profiles levels, liver function and kidney function markers were measured along with the histopathological analysis of the pancreas. Results revealed the positive synergism of FA with both the drugs for all the analyzed experimental markers along with decreased side effects.

1.4.4. FA as an anti-inflammatory agent

During last two decades, there has been an extensive research that signified the role of chronic inflammation in various illnesses including cancer, diabetes, Alzheimer's, cardiovascular and pulmonary diseases. Macrophages play a central part in the process of chronic or acute inflammation by managing several phenomenon including overproduction of pro-inflammatory cytokines and inflammatory mediators (ROS, nitric oxide and prostaglandin E_2).

FA and its ester derivatives have been found to decrease the expression and levels of certain inflammatory mediators such as TNF-α, prostaglandin E_2 and inducible nitric oxide synthase (iNOS) (Fazary and Ju. 2007; Balasubashini *et al*., 2004; Li et al., 2003). Effect of FA and isoferulic acid (IFA) was studied on Murine interleukin-8 (IL-8) production in response to influenza virus infections *in vitro* and *in vivo* using the ELISA assay. IL-8 is a protein of cytokine family which acts as a mediator in the inflammatory process and is also expressed in tumor cells. Both drugs were found to reduce the IL-8 levels in comparison with control in a dose-dependent manner (20-h conditioned medium) *in-vitro* as well as *in-vivo*. Interestingly, both acids significantly reduced the number of neutrophils exuded in bronchoalveolar lavage during *in vivo* study (Hirabayashi, 1995). Later, the anti-inflammatory effect of FA and IFA as active components of *Cimicifuga heracleifolia* extract was further verified through the inhibition of macrophage inflammatory protein-2 (Sakai,1999). Akihisa (2000) demonstrated the striking anti-inflammatory activity of various trans and cis FA esters of natural and synthetic origin against 1,2-O-tetradecanoylphorbol-1,3-acetate induced inflammation in mice. Subsequently, the role of different FA derivatives was found to be central in regulating certain pathways leading to inflammation and tumors. Among others, the suppression of lipopolysaccharide, iNOS, cyclooxygenase-2 (COX-2), TNF-α constitutes the important paradigm *in-vitro*, at the same time, *in-vivo* suppression of inflammation and skin tumor were also observed (Murakamia, 2002; Hosoda, 2002).

1.4.5. FA against pathogens

A wide array of antimicrobial/antibacterial activities of FA have been reported against Gram-positive/negative bacteria and yeasts (Jeong et al., 2000). The growth inhibitory effect of FA on different organism including *Escherichia coli*, *Helicobacter pylori*, *Klebsiella pneumonia*, *Shigella sonnei*, and *Enterobacter aerogenes* was attributed to the inhibition of bacterial arylamine *N*-acetyltransferase in human gastrointestinal microflora by the compound (Tsou et al., 2000; Lo and Chung, 1999). In a study conducted by Saini et al. (2012) on *Setaria cervi*, FA present as an active component in ethyl acetate fraction of *Hibiscus mutabilis*, displayed noteworthy micro/macrofilaricidal activities in worm mortility and MTT reduction assays. Recently, FA and its derivatives have also been screened for their antibiofilm potential against *Candida albicans* (Alavarce et al., 2015; Raut et al., 2014).

1.4.6. Other biomedical uses of FA

The spectrum of FA therapeutic efficacy could be further expanded into various other arenas, most of which are also attributable to its potent antioxidant capacity. FA was suggested to inhibit cholesterol synthesis by competitive modulation of hydroxymethylglutaryl CoA reductase activity in the liver and increasing excretion of acidic sterol (Ou and Kwok, 2004). The authors also reported the usage of FA as an herbal cure for thrombosis, since it has been shown to inhibit the activity of thromboxane A2 synthetase and blood platelet aggregation.

As a result of its preventive effects against thrombosis and atherosclerosis as well as cholesterol lowering activity, FA is considered as an effective cardio-protective agent (Hiramatsu et al., 1990). Besides, it was also found to play an important role in neurodegenerative disorders such as Alzheimer's disease, which are mainly induced by chronic inflammation resulting from ROS and RNS (Mori, 2013; Mamiya, 2008). Their studies have shown the reduction of oxidative stress induced brain damage through various mechanisms such as deprivation of reduced glutathione or modulation of β-secretase in mice upon administration of FA at different doses. As a consequence of these modulations a significant increase in the cognitive activity of test animals was observed.

1.4.7. Industrial applications of FA

As discussed previously (sections 1.3), superior antioxidant capacity of FA compared to synthetic molecules makes it an alternate compound of choice to be used in various industries including food, cosmetics and pharmaceuticals. An overview of industrial applications of FA is provided in Figure 1.5.

Figure 1.5: Industrial applications of ferulic acid

1.5. Metabolism and pharmacokinetics of FA

Total serum and plasma conc. of hydroxycinnamates including FA are generally low which could be attributed to their limited absorption coupled with fast metabolism and quick elimination from the circulation (Zhao and Moghadasian, 2010). Daily FA intake in a normal healthy individual according to typical Mediterranean diet was calculated approximately 16–24 µM/kg body weight. However, the exact amount ingested cannot be calculated specifically since the intake varies from individual to individual and also according to diet servings. All the more, low bioavailability further limits its required conc. which is required to elicit the *in-vivo* therapeutic effect. Peak plasma conc. (C_{max}) and time taken to reach this conc. (T_{max}), are important parameters which are routinely used to calculate the plasma retention and on site availability of a bioactive compound.

Various *ex-vivo* as well as human studies have suggested a fast gastric absorption of FA wherein the compound was detected as early as 5 to 10 min of oral administration in rats and humans,

respectively (Yang et al., 2007; Konishi et al., 2006). Earlier, Zhao et al. (2004), suggested a quick elimination of more than 70% of administered FA within 25 min of *in-situ* incubation in rat's stomach model. Similarly, Spencer et al. (1999) also reported a rapid disappearance of FA from jejunum in an isolated rat intestinal model.

The high absorption rate of FA remained largely unexplained in-spite of several theories put forward in many literature reports such as passive diffusion across gastric mucosa and an H^+ driver transport system (Itagaki et al., 2005; Zhao et al., 2004). The conjugation reactions of FA primarily takes place in liver where glucuronic acid and sulfate were reported to be its major conjugation partners. FA-glucuronide, FA-sulfate, FA-sulfoglucuronide, dihydroferulic acid and vanillic acid were recovered as major metabolites of FA metabolism (Zhao and Moghadasian, 2010; Zhao et al., 2004 and 2003). The conjugation process of FA in liver is suggested to be responsible for its low tissue bioavailability, since it affect the fate of its orally absorbed form in GI tract (Zhao et al., 2004**)**.

Urinary excretion constitutes the major elimination pathway for FA followed by bile excretion, which accounts for a meagre 4-6% of total elimination (Zhao et al., 2004; Adam et al., 2002). Significantly low degree of toxicity upon oral administration of FA in their study on female and male F344 rats has been reported (Tada et al., 1999). In this regard, an LD_{50} equivalent to 2445 mg/kg for male rats and 2113 mg/kg for female rats were suggested subsequently (Ou and Kwok, 2004; Tada et al., 2001).

Several epidemiologic studies have suggested the role of polyphenol rich diet for overall health and benefits of human body but their therapeutic applications remain hampered due to markedly low absorption rate (Kanaze et al., 2006; Labrecque et al., 2005; Cai et al., 2004). The *in-vitro* effective conc. of polyphenols are several magnitude higher than the levels actually present *in-vivo* systems. The *in vivo* conc. of FA to generate a required amount of response against various chronic infections is dependent upon its absorption and tissue distribution. As already discussed, the low bioavailability of FA post oral administration has restricted the number of clinical trials thus limiting its use as a potential nutraceutic. In general, the low tissue availability of polyphenolic compound is ascribed to a variety of factors including limited/poor solubility, restricted permeability due to passive diffusion or sometimes their back transportation into lumen due to active efflux action (Li et al., 2015). Poquet et al. (2008) have reported that passive diffusion is

mostly involved in absorption of FA (~90%) in colon, whereas a very small amount is transported actively through monocarboxylic acid transporter (MCT).

To overcome bioavailability limitations, phenolic phytochemicals should be stabilized before their clinical trials or oral administration. These stabilization methods must be able to maintain the structural integrity as well as physiological characteristics of bioactive molecules. Polymeric encapsulation and/or conjugation of phenolic compounds with the material of natural or synthetic origin presents an interesting stabilization rationale (Jain et al., 2013; Punyani and Singh, 2008; Kumar et al., 2007). Encapsulated or conjugated bioactives are currently finding applications in various domains including food, pharmaceutics, agro-chemical industries, biomedical trials, biotechnology and sensor industries (Munin and Levy, 2011). Amidst a variety of available polymers, CS has strongly emerged as a material of choice for encapsulating a variety of biomolecules, including polyphenols (Woranuch and Yoksan, 2013b).

1.6. Chitosan

CS is a cationic polysaccharide which has received an increasing attention during the last decade by virtue of its biocompatibility, low-immunogenicity and biodegradability (Luo and Wang, 2013). It is commercially synthesized by N-deacetylation of chitin which is an abundant biopolymer generally isolated form exoskeleton of crustaceans. CS consists of repeating units of acetylated and deacetylated β-(1-4)-linked glucopyranose units in its structure (Figure 1.6). It exhibits antimicrobial property; high encapsulation potential; gelling and film forming nature along with antioxidant capacity. Owing to these properties, a plethora of applications have been discovered for CS including their use in cosmetics/ pharmaceutics industries, water purification, food packaging, edible films, and encapsulation of biologically active molecules.

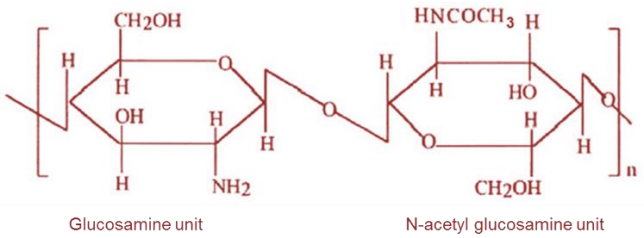

Figure 1.6: Chemical structure of chitosan

1.6.1. Physico-chemical attributes of CS

CS is a hydrophobic, weakly basic biological polymer which is generally insoluble in water at high pH, but dissolves in dilute acetic acid solution at lower pH and also has the capacity to form gel (Qin et al., 2006). The degree of deacetylation of CS has a major impact on molecular weight and physico-chemical properties of CS, which in turn determines its applicability. At acidic pH and 50% deacetylation degree, CS becomes water soluble due to protonation of its amine functional group (Luo and Wang, 2013). It is a linear polyamine with reactive amino and hydroxyl groups facilitating its binding with a variety of biomolecules and chelation of transition metal ions. These reactive groups could easily be amended by different chemical and enzymatic methods, thereby unraveling the scope of CS applicability in diverse fields.

1.6.2. Biological applications of CS

CS and its derivatives possess several biological properties including antimicrobial, antioxidant, hypocholesterolemic, antitumor and immunity enhancing effects. However, all these effects are not produced by a single type of CS, since its physico-chemical and biological aspects are dependent upon molecular weight and deacetylation degree. Several advancements that have been made towards the applications of CS in various fields, utilizing its biological activities are summarized in Table 1.2.

Table 1.2: Biological activities of CS and their applications

Biological activities	Applications	References
Antioxidant	CS from crab shells showed hydroxyl and DPPH scavenging, reducing power, ferrous ion chelation CS from larvae of Musca domestica L. displayed scavenging of hydroxyl and superoxide anion, DPPH scavenging, reducing power Dietary CS exerted antiaging effect by diluting the oxidative stress in rats heart tissues Enhancement in serum level of antioxidant enzymes in hyperlipidemic rats	Yen et al., 2008 Ai et al., 2012; Anandan et al., 2013 Xia et al., 2011
Hypocholesterolemic	Elevation in antioxidant enzyme level Prevention of oxidative stress in STZ induced diabetes in rats High *in-vitro* fat and bile-salt-binding capacity; hypolipidemic activities *in-vitro* Significant reduction in plasma total cholesterol, triglycerides and low density lipoproteins, increase in high density lipoprotein levels	Yuan et al., 2009 Liu et al., 2008 Wydro et al., 2007 Zhou et al., 2006 Maezaki et al., 1993
Antimicrobial	Broad spectrum antimicrobial effects of CS in food preservation and on fungal cell walls Higher growth inhibition of gram positive and gram negative bacteria by CS compared to its oligomers Molecular weight dependent inhibition of *Staphylococcus aureus* and *Escherichia coli*	Allan and Hadwiger, 1979 Zheng and Zhu, 2003
Antitumor, Anticancer	Charged CS oligosaccharides exerted anticancer effect against HeLa, Hep3B and SW480 cancer cell lines by reducing cell viability and induction of necrosis Inhibition of tumor growth via immunity enhancement by hexa-N-acetylchitohexaose and chitohexaose against ascites cancer in BALB/c mice	Huang et al., 2006 Tokoro et al., 1988 Suzuki et al., 1986

Presence of amine and hydroxyl functional groups in CS structure renders it an attractive and amenable molecule to be modified and improvised its applications in various fields. Modifications of CS such as its alkylation, hydroxy/carboxy alkylation and thiolations etc. have aided in the further enrichment of its already existing attributes (Luo and Wang, 2013). CS based electrospun nanofibers and hydrogels have also been reported for their cytocompatibility and controlled, localized drug delivery (Bhattarai et al., 2010, 2005).

Several researchers have reported different conjugation of CS with hydroxycinnamic acids, especially FA, for enhancement of its characteristic properties such as antimicrobial capacity and antioxidant potential (Liu et al., 2014; Lee et al., 2014). Successful grafting of FA onto CS through hydroxyl radical mediated mechanism to yield water soluble derivatives was reported by Liu et al. (2014). The antioxidant activities (*in-vivo* and *in-vitro*) of grafted product were found to be enhanced in comparison to their native forms. Earlier they have reported the synthesis and characterization of FA grafted carboxymethyl CS using the similar mechanism, with a higher *in-vitro* antioxidant activity. Subsequently, Lee et al. (2014) showed an improvement in the antimicrobial and antioxidant properties of cytocompatible CS-FA conjugates than unmodified CS. The conjugates were reported to significantly inhibit lipid peroxidation besides antimicrobial activity against methicillin-resistant and susceptible strains of *Staphylococcus aureus*. In the same perspective, Woranuch and Yoksan (2013a) have synthesized FA grafted CS with superior aqueous solubility compared to unmodified FA and CS. They utilized carbodiimide-mediated coupling reaction to generate the grafted product with an improved radical scavenging activity, compared to native FA.

1.7. Chitosan based nanoencapsulation

Among several other modifications of CS, its nanoparticles formulations have received a wide acceptance among the scientific fraternity due to their green synthesis, reproducibility, feasibility in term of low cost, and ease in controlling the physicochemical factors. In general, the term “polymeric nanoparticles” is used to describe solid, colloidal particles within the size range of 10-1000 nm (Couvreur, 1998). Binding and entrapment of bioactive molecules takes place within hydrophobic cores of polymeric nanoparticles. As a result of their small sizes and high surface to volume ratio, these nanoparticles have become an important aspect in targeted drug delivery of biologically active molecules such as genes, peptides, drugs and polyphenolic compounds.

Nanoparticles mediated drug delivery assists the drug to reach the intended target, thereby preventing normal tissues from any undesirable side effects. As a result, the clinical efficacy and bioavailability of nanoparticles encapsulated molecule is enhanced manifold in comparison with their free forms. Apart from injected delivery, nanoparticles formulation (nanoformulations) or nanosuspensions are also administered orally to facilitate the absorption of poorly absorbable drug as well as prevent their degradation in gastro-intestinal medium (Singh et al., 2015; Bansal et al., 2014; Ghosh et al., 2012; Vrignaud et al., 2011; Liu et al., 2008). These nanoformulation have an edge over traditional medicines in terms of cell membrane interaction and penetration, reaching specific targets, controlled release and enhanced therapeutic impact. Cationic surfaces of CSNPs promotes the adherence and internalization of encapsulated drug with oppositely charged target membrane, such as bacterial or tumor cells membranes (Kumari et al., 2010). All the more, solubility of CS in aqueous acetic acid solution allows fabrication of nanoparticles without using precarious organic solvents, hence justifying their use in living systems. Recently, self-assembled FA- glycol chitosan nanoparticles (FA-GC) with high neuroprotective effects against spinal cord injury were synthesized Wu et al. (2014). Use of FA-GC in their study generated inflammatory responses at lesion sites and led to full functional recovery in spinal cord contusion injury model. Earlier, nanoencapsulated FA was found to decrease the cell viability of NCI-H460 lung carcinoma cell lines *in-vitro* (Merlin et al., 2012). Anselmi et al. (2008) reported that complexation of FA into the hydrophobic core of α-cyclodextrins could improvise the chemical stability of FA under UV-B stress. The complexation product also caused an increase in FA bioavailability, resulting in a slower and controlled skin delivery. Elevation of antioxidant potential of FA was observed following its encapsulation in solid lipid nanoparticles, which resulted in a dose dependent reduction in the lipid peroxidation of rat brain microsomes (Trombino et al., 2013). Other phenolic compounds such as eugenol and catechins have also been encapsulated in CSNPs to achieve controlled release and to improvise on their intrinsic physiological properties such as antioxidant capacity or thermal stability (Woranuch and Yoksan, 2013b).

CS based micro and nanoparticles have gained advantage due to their low toxicity and simplistic preparation approach. Among various approaches employed to synthesize CSNPs, ionic cross linking, microemulsions and ployelectrolyte complex methods are frequently used (Kumari et al., 2010). In microemulsion method, CS amine groups are usually conjugated with gluteraldehyde which is then mixed with surfactant/hexane mixture. The ployelectrolyte complex method makes

use of electrostatic interaction between positively charged amine groups of CS and anionic groups present in sodium alginate or dextran sulfate. Here, self-assembled particles are spontaneously synthesized, however their hydrophilicity is low due to charge neutralization. Likewise, the use of chemical crosslinking agents such as gluteraldehyde as in microemulsion method, may lead to mucosal irritation and other undesirable side effects. To avoid the toxicity associated with the use of chemical cross linking agents, non-toxic multivalent anion sodium tri-poly phosphate (TPP) has been used extensively (Ko et al., 2002). The cationic nature of CS, and presence of a large number of free amine groups in its backbone, allows a rapid and spontaneous ionic cross-linking with phosphate groups of TPP.

1.8. Synthesis of CSNPs by ionic cross linking: An overview

Ionic cross linking of CS with TPP exploits the mutual binding forces between oppositely charged cations and anions in their structure, respectively. According to hypothesis presented by Kaloti and Bohidar (2010), binding of OH^- ions to CS may result in softening of polymeric chain structure and allows intramolecular binding of tripolyphosphoric ions (Figure 1.7). The preparation method essentially involves a fusion of CS in acidic phase (generally CS+1% v/v aqueous acetic acid; pH 4-6) and TPP in alkaline phase (pH 7-9). To achieve a successful nanoformulation it is necessary to consider a dropwise addition of TPP into CS solution. The mixture is continuously stirred at room temperature and nanoparticles (CSNPs) are spontaneously generated through cationic and anionic inter/intra molecular adhesive forces of principal components (Figure 1.8). Trial and error methods involving different molecular weight CS with varying pH and CS:TPP mass ratio are routinely tested to obtain nanoformulations of diverse sizes. Introduction of compounds altering the ionic strength of CS-TPP solution (such as KCl) have also been tested for their effect on swelling and disintegration behaviors of CSNPs (Elgadir et al., 2015; Nagpal et al., 2010). CS also exhibits an interesting property of gel formation by virtue of counter-ion cross linkage with TPP, under specific preparation parameters and pH values, hence the process is referred as “ionic gelation” (Ko et al., 2002). In an experiment conducted by Mi et al. (1999), ionic gelation characteristic was exploited for the synthesis of CS-TPP beads by dropwise addition of CS to 10% (w/v) TPP at pH 8.4. Subsequently, the beads were produced through polyelectrolyte complexation of CS and TPP, which were later utilized for encapsulation of anticancer agent. Kaloti and Bohidar (2010) have reported that at CS conc. < 0.5mg/ml, CS:TPP volumetric mixing ratios < 2 and pH

5.5, the system was driven away from CSNPs formation. Instead, the reaction parameters lead to the spontaneous generation of natural coacervates. However, particles of diameter 150- 350 nm were formed at same pH with CS conc. higher than 0.5 mg/ml and CS:TPP mixing ratio >2.

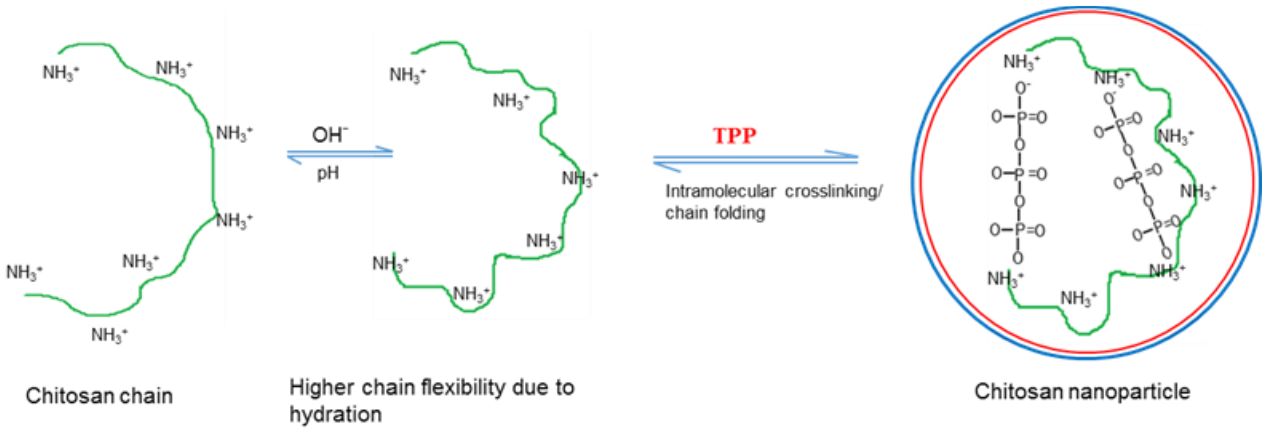

Figure 1.7: Synthesis of CSNPs through intramolecular linkages

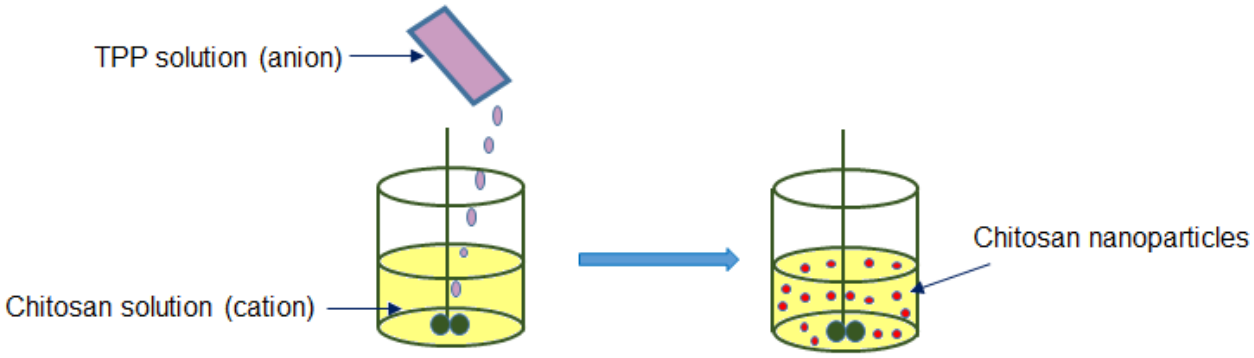

Figure 1.8: Schematic representation of the synthesis of FA encapsulated CS nanoparticles through CS-TPP ionic cross linking

1.9. Drug delivery and therapeutic applications of CSNPs

Owing to their simple and mild synthesis process, CSNPs have been extensively utilized for drug encapsulation and delivery in both *in-vitro* and *in-vivo* systems. CS based nanoformulations and drug delivery systems have shown an elevated therapeutic efficacy, compared to free/native drug (Park et al., 2010). The observed enhancement in healing aspect of encapsulated phenolic phytocompounds is quintessentially dedicated to a number of factors including better solubility; better permeation across target cell membrane; enhanced absorption; target specificity and biocompatibility (Li et al., 2015; Park et al., 2010).

Phenolic phytochemicals remain confined to nanoparticles core through hydrophobic interactions and H-bonds. The outer polar surfaces of these polymeric nanoparticles remain stable in dispersion medium through sufficient surface charges and hydration properties (Li et al., 2015). Higher aqueous solubility have been reported earlier for curcumin encapsulated CSNPs (Duan et al., 2010). Polymeric encapsulation of phenolic compound is also associated with lower incidences of damage or degradation in hostile conditions prevailing in upper gastrointestinal tract. For example, encapsulated epigallocatechin-3- gallate (EGCG) showed two times higher stability in simulated stomach fluid than free EGCG (Onoue et al., 2011).

Two different modes of transportation viz. paracellular and transcellular, have been described for penetration of nanoparticles through intestinal epithelium (Li et al., 2015). Transcellular transportation is an energy requiring pathway, found to be mediating the transport of CS independent nanoparticles (Benfer and Kissel, 2012). In paracellular pathway, nanoparticles mediated controlled disruption of epithelial tight junctions facilitates the transport of bioactive compound across the epithelial cell membrane and the original form of tight junctions is restored afterwards (Li et al., 2015). CSNPs were involved in modulation of tight junction protein activity, leading to opening of tight junctions in Calu-3 cells (Vllasaliu et al., 2010). The ability of CS to reversibly dislocate the tight junctions along with mucoadhesive property was supposed to be responsible for its absorption promoting behavior (Artursson and Lindmark, 1994). Positively charges amino groups in CS and negatively charged sialic acid groups on mucus membrane allowed the effective interface and increased the contact time of encapsulated agent and absorptive surface (Soane et al., 1999). The ease of permeation with elevated contact time and higher absorption offered a higher blood circulation time to the encapsulated bioactive (Park et al., 2010).

As discussed earlier, the mechanism of ionic/chemical cross linking and ionic complexation are responsible for encapsulation and controlled release of bioactives from CSNPs several physiological signals including changes in temperature, pH and ionic strength indicates the presence of disorders in biological systems. Signals such as higher temperature or low pH values have been reported in tissues showing necrosis or inflammations (Park et al., 2010). Therefore, specific drug carrier could be fabricated which detect these signals and allows the delivery of encapsulated drug/bioactive agent to their desired locations. Specific surface charge characteristics of CSNPs have enabled their use in site specific targeting, along with negligible toxicity against healthy cells. Binding and internalization of CSNPs to negatively charged tumor cell surfaces results in higher mutual interaction which has been considered a major factor responsible for their cytotoxic activities *in-vivo* (Qi et al., 2006).

The role of CSNPs in apoptosis induction, membrane disruption, changes in fatty acid composition of membranes and DNA fragmentation was reported in a study conducted on human gastric carcinoma cells MGC-803 (Qi et al., 2005). Investigation performed on human hepatocellular carcinoma in a mouse xenograft model suggested inhibition of tumor antiangiogenesis by CSNPs through modulation in vascular endothelial growth factor receptor 2 (Xu et al., 2010). Another report also suggested both *in-vitro* and *in-vivo* antitumor effect of CSNPs on human hepatoma cell line BEL-7402 (Qi et al., 2007). Oral delivery of insulin and other bioactive molecules through CS encapsulation have also been reported for improvement in their therapeutic indices (Chaudhury and Das, 2011). Table 1.3 lists an overview of polyphenols encapsulated in CSNPs along with modifications in their therapeutic activities upon nanoencapsulation.

Table 1.3: Modifications in biological activities of nanoencapsulated polyphenols

Polyphenols	Activities	Modifications in activity	Reference
Ellagic acid	Anti-haemorrhagic, Antioxidant	Encapsulation in CSNPs aided in significantly faster blood clotting compared to its free form	Gopalakrishnan et al., 2014
Chlorogenic acid	Antioxidant, Anti-inflammatory	Controlled *in-vitro* release with preserved antioxidant capacity of nanoparticles bound form	Nallamuthu et al., 2014
Eugenol	Antioxidant, Antimicrobial	CSNPs encapsulation improved thermal stability and antioxidant capacity	Woranuch and Yoksan, 2013b
Carvacrol	Antioxidant, antimicrobial	Controlled *in-vitro* release, higher antimicrobial action of nanoencapsulated form	Keawchaoon and Yoksan, 2011
***Elsholtzia splendens* extract**	Antioxidant	Encapsulation in CSNPs resulted in enhanced lipid peroxidation inhibition	Lee et., 2010
Tea catechins	Antioxidant, Antitumor	Controlled release *in-vitro*	Hu et al., 2008

1.10.Objectives

The objectives of present study were:

1. Selection of process parameters for successful synthesis of ferulic acid encapsulated chitosan nanoparticles (FANPs).
2. Morphological evaluation and characterization of FANPs.
3. Evaluation of free radical scavenging and anticancer potential of FANPs and their anti-candida biofilm efficacy *in-vitro*.
4. Study of *in-vitro* release along with *in-vivo* pharmacokinetics of FANPs.
5. *In-vivo* assessment of anti-inflammatory and anti-diabetic potential of FANPs.

Chapter 2

Synthesis and Characterization of Ferulic Acid Encapsulated Chitosan Nanoparticles

2.1. Introduction

Ferulic acid (4-hydroxy-3-methoxycinnamic acid), is the most abundant hydroxycinnamic acid found in plant cell walls forming covalent ester linkages to polysaccharides and ether or ester linkages to lignin. It is reported to have antioxidant, antimicrobial, anti-inflammatory, cholesterol-lowering and anticancer activities, as well as ability to prevent thrombosis and atherosclerosis (Wilson et al., 2007; Akihisa et al., 2000; Kayahara et al., 1999; Mori et al., 1999). Being capable of absorbing UV radiations, FA is finding place as a photoprotective constituent in many skin lotions and sunscreens (Saija, 2000). However, the efficiency of polyphenols, in general is substantially limited due to their low bioavailability and integrity. Insufficient gastric residence time, low permeability and/or low solubility and instability in gastrointestinal tract limits the activity and the potential health benefits of polyphenols. Despite having valuable health advantages, bioavailability and clinical efficacy of FA is also inadequate due to its partial aqueous solubility and a short plasma retention time (Yang et al., 2007; Konishi et al. 2006; Zhao et al., 2004). To increase its stability, bioavailability and efficacy, FA has been stabilized through encapsulation in biodegradable polymeric nanoparticles (Salmaso et al., 2007; Vemula et al., 2006). Significant advantages of nanoparticles lies in their small dimensions that allow them to penetrate tissue or gastrointestinal barriers allowing facilitated transportation through aqueous biological environments. Among other polymers, CS which is a deacetylated form of chitin (2-amino-2-deoxy-(1-4)-D-glucopyranan) is comprehensively used for nanoparticles synthesis. Universal applicability of CS relates to its excellent biodegradability, biocompatibility and antimicrobial activity (Liu et al., 2006). CSNPs are extensively used to deliver bioactive compound including drugs, vitamins, proteins, nutrients and phenolics into the biological systems (Hu et al., 2008; Jang et al., 2008). CS acts as a wall/shell material to envelop these compounds bearing multiple negative charges via cationic crosslinking to generate stable, non-toxic, biodegradable nanosized particles (Keawchaoon and Yoksan, 2011). CS forms inter and intramolecular cross linkages when comes in contact with specific polyanions such as sodium tripolyphosphate (TPP) for drug encapsulation (Sofia et al.,

2008). Woranuch and Yoksan, (2013b) studied the thermal stability of eugenol by encapsulation into CS-TPP nanoparticles. Similarly Sofia et al. (2008) synthesized CS-TPP nanoparticles loaded with tea catechins by ionotropic gelation method. In this chapter, FANPs were prepared using ionic cross linking method, which is a low cost and environment friendly technique. Interactions among different components of FANPs were characterized and established through FTIR, TGA-DTG and DSC. The stability of encapsulated FA was assessed using ^{1}H NMR and XRD techniques. Finally, DPPH radical scavenging assay was performed to assess the *in-vitro* antioxidant potential of FANPs.

2.2. Materials and methods

2.2.1. Materials

Medium molecular weight chitosan (190-310 kDa) with 75-85% deacetylation degree, TPP, FA, cell culture-grade dimethyl sulfoxide (DMSO), DPPH (2, 2-diphenyl-1-picryl-hydazyl) and all analytical grade chemicals were purchased from Himedia (Himedia, India).

2.2.2. Preparation of solutions

CS stock solution (2% w/v) was prepared by dissolving CS in 1% acetic acid using a magnetic stirring at ambient temperature. In order to remove undissolved chitosan this solution was filtered through 8µm filter paper using a vacuum system and pH adjusted to 5 (2M NaOH). Similarly, 1 mg/ml TPP stock solution was prepared by dissolving it in Milli-Q purified water. Varying conc. of FA viz. 0.0264 (FA1), 0.0528 (FA2), 0.1056 (FA3), 0.2112 (FA4), 0.4224 (FA5) mg/ml were used to prepare nanoformulations as well as native FA solution in 2% DMSO.

2.2.3. Synthesis of nanoparticles

For synthesis of unloaded CSNPs (i.e. nanoparticles without FA encapsulation), CS stock solution was diluted using Milli-Q purified water to 1mg/ml and 1.5mg/ml conc. (pH 5). On the basis of CS conc., required amount of TPP was added separately to each CS solution to yield final CS:TPP mass ratios of (1:1, 2:1, 4:1, 6:1). For successful accomplishment of nanoparticles synthesis with a stable suspension, it is extremely necessary to add TPP slowly to the CS solution with constant stirring. Nanoparticles thus formed as a result of interaction between the negatively charged groups of TPP and the positively charged amino groups of CS. The effect of each CS conc. and CS to TPP mass ratio was studied with respect to particles diameter and zeta

potential. FANPs were prepared using the optimized CS:TPP mass ratio by following an earlier described protocol with certain modifications (Dhillon et al., 2014). Briefly, 10 µl each of varying FA conc. as mentioned above were added to 1 ml chitosan solution with intermittent vortexing (MX-F, Dragon Lab instruments, China). To this mixture, TPP was added drop-wise to yield nanoformulations designated as NF_1, NF_2, NF_3, NF_4, NF_5 based on FA conc. used. Nanoparticles thus obtained were centrifuged at 40000g for 30 min at 4°C, pellet rinsed with distilled water and freeze dried. To determine the encapsulation efficiency (EE) of nanoparticles, supernatant was collected and non-encapsulated FA was quantified spectrophotometrically at 319 nm using FA standard curve (Lasany double beam LI-2800). The EE (%) was calculated by the following equation:

EE (%) = (Total FA loaded- non-encapsulated FA/Total FA loaded) ×100

FA extinction coefficient (ε) was calculated using Beer–Lambert equation:

$\varepsilon_{319} = A/(c.b)$

Where, ε_{319} is extinction coefficient at 319 nm; A is absorbance; c is conc. of native FA (mol/l); b is thickness of cuvette (1 cm).

After freeze drying, a small fraction of FANPs was desiccated under vacuum for 180 days in order to assess their stability in terms of particle size, zeta potential and polydisperity index. Auto-florescence property of FA was utilized in order to validate its encapsulation into CSNPs using fluorescent microscope equipped with GFP light cube at 470-510 nm (EVOS-FL,AMG,USA). Solubility of FANPs was tested by dissolving 1 mg of dried pellet in 1 ml acetic acid (1 % v/v) and water followed by 5 min vortexing. The mixtures were then kept in a magnetic stirrer for 12 h and the percent enhancement in solubility was recorded using native FA as control.

2.3. Physicochemical characterization of nanoparticles

Morphology and size measurement

Field-emission scanning electron microscopy (FESEM; Quanta 200F Model, FEI, Netherland) was used to examine the morphology of nanoparticles by fixing them onto glass slides and sputter coated (sputter coater: Biotech SC005, Switzerland) with gold for 1 min. CSNPs and FANPs diameters were measured over 50-100 different points of FESEM images using “Image

J" analyzer software. Zeta potential values of the synthesized nanoparticles were recorded using zetasizer (Malvern Nano ZS; Malvern Instruments Ltd., U.K.).

Fourier transformation-infrared spectroscopy

The Fourier transform infrared (FT-IR) spectra of the nanoparticles were analysed by an IR spectrometer (FTIR; Thermo Nicolet Nexus 6700, US). Average values of 32 scans were recorded with 4,000–400 cm^{-1} wavelength scanning range and resolution of 4 cm^{-1} for each sample.

Thermogravimetric and Derivative thermogravimetric analyses

TGA and DTG analyses of native FA and nanoparticles preparations (CSNPs, FANPs) were performed in a simultaneous DTA-TG Apparatus (EXSTAR, TG/DTA 6300). Samples (2-8 mg) were heated from 20 to 500 °C at a scanning rate of 10 °C/min. Nitrogen was used as the purge gas at a flow rate of 20 ml/min.

NMR spectroscopy and X-Ray Diffraction analyses

Stability of FA upon encapsulation was evaluated by performing ^{1}H NMR spectra analysis with 500-MHz NMR spectrophotometer (Bruker, Germany) at 25 °C with deuterated DMSO as solvent. For further validation of stability and integrity of encapsulated FA, X- ray diffractograms were recorded from 5 ºC to 100 ºC with scanning rate of 2º min^{-1} at a voltage of 45 kV with CuKα radiations at 0.1542 nm wavelength (Brucker D-8 Advance X-ray diffractometer system).

2.4. Free radical scavenging activity

DPPH (2, 2-diphenyl-1-picryl-hydazyl) assay was used to determine radical scavenging activity of free FA and FANPs using earlier reported protocol with necessary modifications (Lee et al., 2010). Stock solution of DPPH was prepared by dissolving 16 mg DPPH in 100 ml ethanol and 100 ml distilled water. Different conc. (20, 40, 60, 80 and 100 µg/ml) of free FA and FANPs were prepared and from each of them 200 µl sample was added separately to 0.8 ml of DPPH stock solution. Each mixture was shaken and left for 30 min at room temperature, and the absorbance of the resulting solution was measured at 517 nm with spectrophotometer (Agilent Cary 60). Radical scavenging activity was calculated according to the following equation:

Free radical scavenging activity (%) = Ac-As/Ac × 100

Where Ac = control absorbance; As = sample absorbance.

Statistical analysis

All experiments were carried out in triplicate and the results represented are mean value ± Standard deviation of individual values. Significant difference between the mean values of different data sets was obtained by performing t-test and $p < 0.05$ was considered as statistically significant value.

2.5. Results and discussion

2.5.1. Synthesis of FA-CSNPs

Particle size and zeta potential predominantly governs the formation of a stable nanosuspension since they greatly influences the electrostatic repulsion between particles. The ratio between CS and TPP is critical in controlling the size as well as size distribution of nanoparticles thereby affecting their biological performances (Pan et al., 2002). In the present work, synthesized nanoparticles were investigated for their size and zeta potential using dynamic light scattering technique (zeta sizer); while their morphology were visualized through FESEM. Two different CS conc. (1 mg/ml and 1.5 mg/ml) were utilized to attain the optimum CS:TPP mass ratio for synthesis of stable particles with narrow size distribution. To provide an overview of synthesis process, the effects of CS:TPP mass ratio at each CS conc. were studied on particle's diameter and zeta potential. Particles diameter generally increased with increasing CS:TPP mass ratio for both the tested CS conc. However, the difference in particles diameter was almost double at CS:TPP mass ratio 4, when CS conc. was increased from 1 mg/ml to 1.5 mg/ml (Figure 2.1A). Zeta potential of a nanoformulation is reflective of particles' surface charge as well as the stability of colloidal suspensions. The zeta potential measurement of each CS:TPP mass ratio (both CS conc.) were found positive for the present investigation due to positive surface charges of CS. For mass ratios 1 and 2, the zeta potential value was measured to be lower, which might be a result of neutralization of positive surface charges of CS by anionic forces as previously discussed. At higher mass ratios, zeta potential also rose consistently for both CS conc. thus re-established the idea that nanoparticles structure is mainly composed of CS (Figure 2.1B).

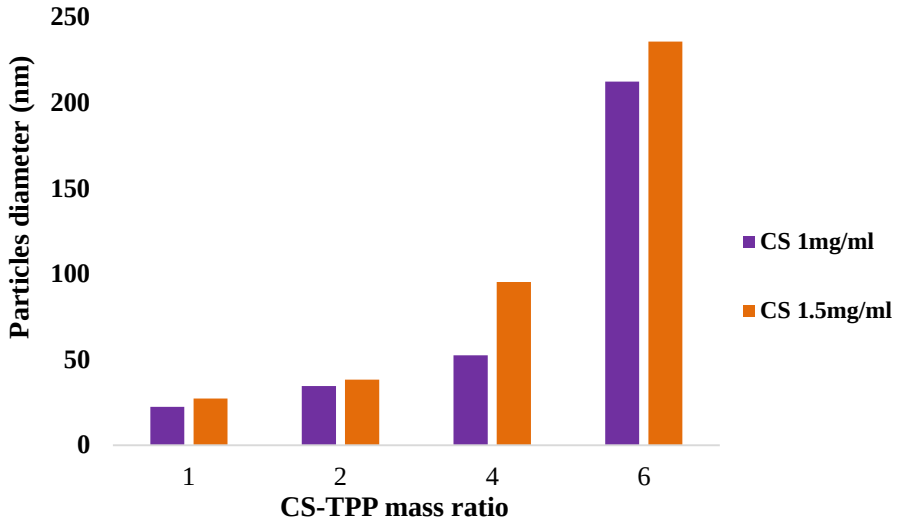

(A)

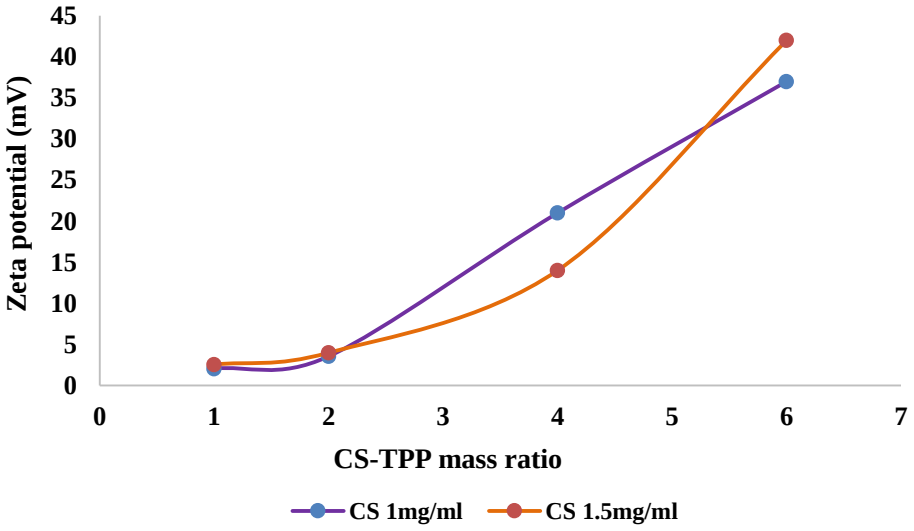

(B)

Figure 2.1: Variations in **(A)** particles diameter **(B)** zeta potential of CSNPs at different CS-TPP mass ratio tested

Well distributed (Polydisperity Index= 0.368), spherical CSNPs with average particle diameter 52.54 ± 0.22 nm were obtained at CS:TPP mass ratio 4, with 1 mg/ml CS conc. (Figure 2.2). Kaloti and Bohidar (2010) have described a minimum threshold conc. of 0.5 mg/ml for CSNPs synthesis, below which the nanoparticles system was driven towards natural coacervation, instead of particles formation. Small, non- distinguishable particles arranged into dense clusters were obtained at mass ratio 2 while larger aggregates instead of desired particles were visualized at mass ratio 6 at 1 mg/ml CS conc. (Figure 2.3A and B). At 1.5 mg/ml CS conc. the

particles with size distribution profiles similar to 1 mg/ml CS were reported. Strong mutual interactions of cationic and anionic forces between CS and TPP at mass ratios 1, 2 might be responsible for the formation of very small particles clustered densely. At higher CS:TPP mass ratio of 6, these forces might have weakened due to lower anion (TPP) conc. hence inhibiting the particles formation. From the obtained data, it was concluded that the CS:TPP mass ratio of 4, at 1 mg/ml CS conc. provided the most desirable results in terms of particles size, zeta potential, size distribution and morphological characteristics. Hence, this ratio was optimized to be used for further analysis.

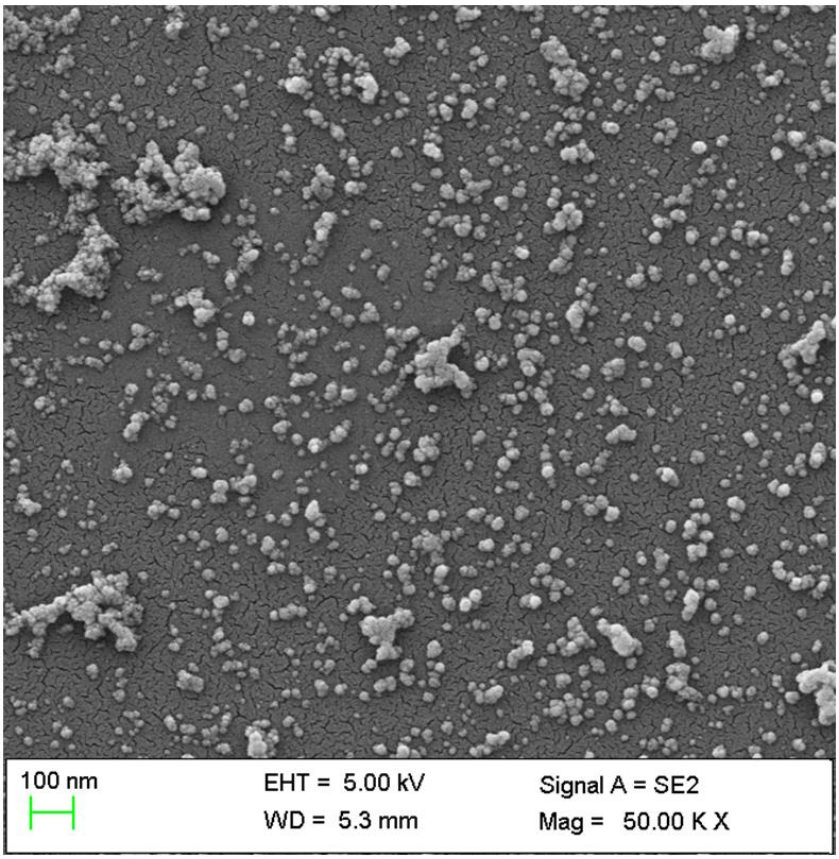

Figure 2.2: FESEM micrographs of CSNPs at CS:TPP mass ratio 4 and CS conc. 1 mg/ml; Microscopic magnification 50KX, Scale bar 100 nm

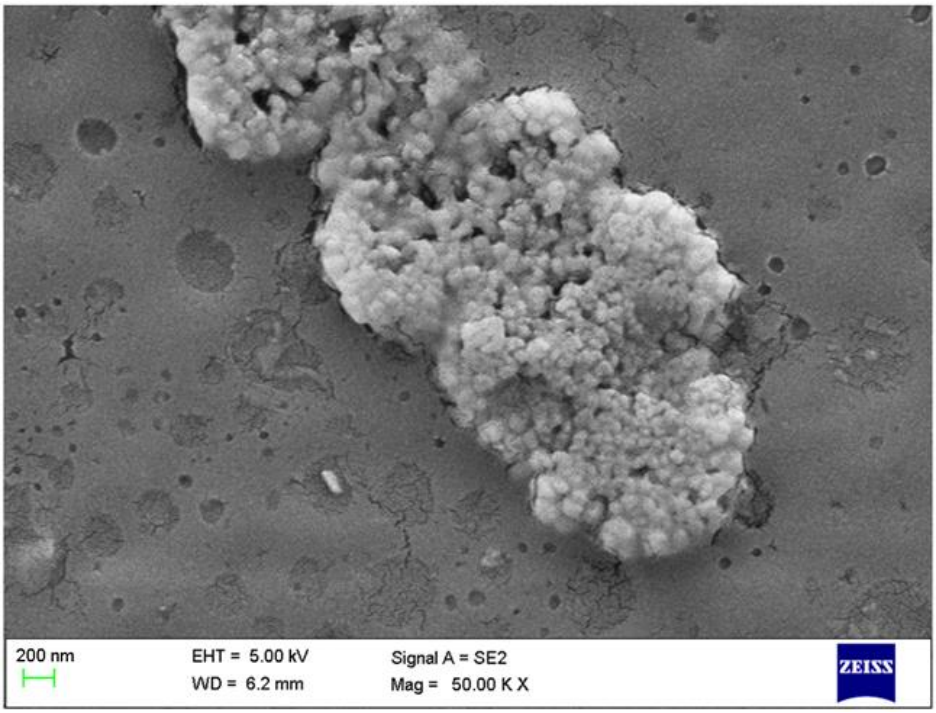

(A)

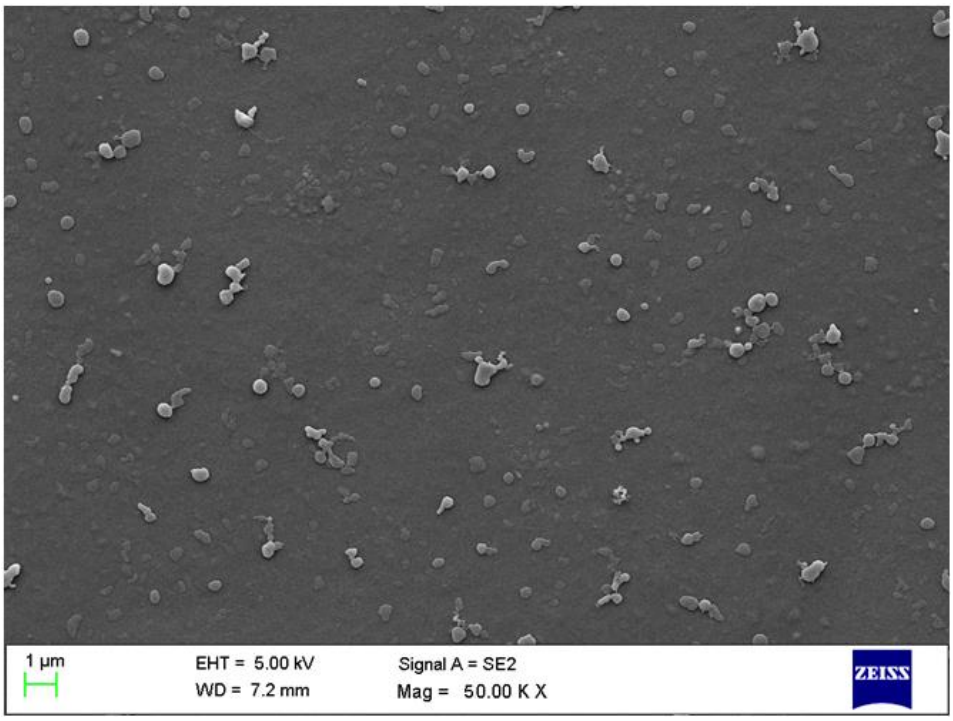

(B)

Figure 2.3: FE-SEM images depicting **A)** Small particles at CS:TPP mass ratio 2, CS conc. 1mg/ml; Microscopic magnification 50KX, Scale bar 200 nm. **B)** larger aggregates at CS:TPP mass ratio 6, CS conc. 1mg/ml; (Microscopic magnification 50KX, Scale bar 1 µm)

Encapsulation of different conc. of FA (FA_1-FA_5) into CS was achieved via formation of an oil-in-water emulsion wherein, the FA droplets were subsequently solidified by ionotropic interaction between positively charged CS and negatively charged TPP. The amount of compound encapsulated within the nanoparticles was calculated using FA standard curve (Figure 2.4). Molar extinction coefficient or molar absorptivity is the parameter that measure the strength of a substance to absorb light at a given wavelength. In the present study, the extinction coefficient for FA calculated using standard curve was 14,684 M^{-1} cm^{-1} at 319 nm.

Average particle diameter and EE of FANPs obtained at different formulations are summarized in Table 2.1. No significant size enhancement upon FA encapsulation in NF_1 was observed as compared to unloaded CSNPs. However, with the increase in initial FA content (FA_2-FA_5) average particle diameter increased consistently from NF_2 to NF_5. EE (%) tended to increase with initial FA content, starting from 14.71 ± 1.33% and reached a maximum value of 56.45 ± 2.47% at NF_3. Decline in EE (%) was observed in NF_4 and NF_5 which may partially be attributed to encapsulation limitations of CS. The above observations were in agreement with previous reports which revealed an increase in size and EE (%) of chitosan nanoparticles upon initial encapsulation phenolic compound carvacrol (Keawchaoon and Yoksan, 2011).

FESEM image of particles obtained at nanoformulation NF_2 is depicted in Figure 2.5. Particles of approximately 114.02 ± 1.24 nm diameter and 9.33 ± 2.05 mV zeta potential were obtained at this formulation. The mean particles size of FANPs measured using dynamic light scattering technique in zeta sizer was slightly greater than the size observed in FESEM micrograph. The increase in size so observed could be due to the swelling of CS layer or aggregation of individual particles in aqueous medium (Keawchaoon and Yoksan, 2011).

Decline in zeta potential value from 21.47 ± 0.35 mV (unloaded CSNPs) to 9.33 ± 2.05 mV upon encapsulation (NF_2) is suggestive of reduction in surface charges of nanoparticles upon FA loading. This reduction in zeta potential might have occurred through neutralization of some of the positive surface charges of CSNPs brought about by adsorption of excess FA remaining in the nanoparticles surfaces. The decrease, in part, could also be attributed to the retardation of electrophoretic mobility of the nanoparticles as a result of their size enhancement upon FA encapsulation. It has been reported earlier that decrease in surface charges leads to less repulsive forces between particles hence higher tendency to aggregate, which may also be a factor for the increase in mean particle size of nanoparticles upon FA encapsulation (Lee et al., 2010). To visualize nanoencapsulated FA at NF_2, its auto-florescence characteristics were

exploited and imaged (Figure 2.6). The changes in particle size, zeta potential and polydisperity index were almost negligible for both NF_2 andNF_3 after 180 days, indicating the stability of these formulations.

The solubility of FANPs at these formulations (NF_2, NF_3) was enhanced in water and 1 % acetic acid (v/v) at room temperature (Table 2.2). The observed enhancement in solubility may be attributed to the combined effect of interfacial adsorption and enhanced bioavailability of FA in the aqueous phase following encapsulation within CS. Interaction of phenolic phytochemicals with hydrophobic sites of nanoparticles through hydrogen bonds and hydrophobic forces is well established (Li et al., 2015). Sufficient surface charges and suitable hydration property keep phenolic phytochemical encapsulated NPs stable in aqueous system, which enhances the water solubility of phenolic phytochemicals.

Randomly distributed larger particle in the size range of several microns were obtained at NF_4 and NF_5 which were unstable since the components of mixture precipitated down within a week, giving a biphasic solution (Figure 2.7). Instability of particles at formulations NF_4 and NF_5 could partially be attributed to the lower zeta potential value since it did not suggest a stable nanosuspension (Müller et al., 2001).

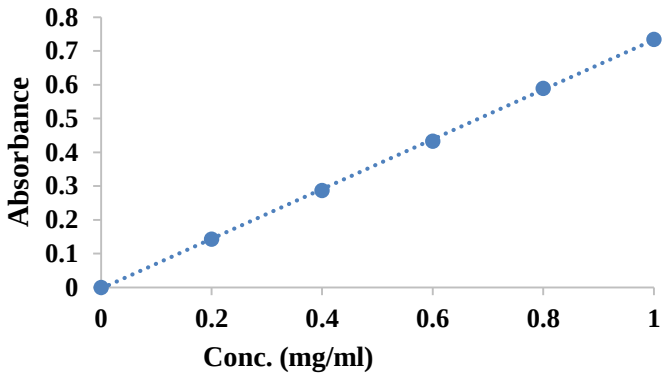

Figure 2.4: FA standard curve for calculations of encapsulation efficiencies of FANPs at 319 nm

Table 2.1: Particle size, zeta potential and encapsulation efficiencies of FANPs at different FA loading conc.; CS:TPP mass ratio 4; CS conc. 1 mg/ml

Nanoparticles formulation (NF)	Initial FA loaded (mg)	Particle diameter (nm)	Zeta potential (mV)	Polydisperity Index	Encapsulation efficiency (%)
CSNPs	0.0264(FA_1)	52.54±0.22	21.47±0.35	0.378	14.71±1.33
NF_1		57.39±0.57	33.55±1.15	0.453	
NF_2	0.0528(FA_2)	114.02±1.24	9.33±2.05	0.471	47.34±2.07
NF_3	0.1056(FA_3)	203.41±2.39	14.22±0.23	0.406	56.45±2.47
NF_4	0.2112(FA_4)	3902.00±2.43	0.34±1.47	0.366	47.76±1.21
NF_5	0.4224(FA_5)	4102.00±1.54	0.09±2.09	0.472	41.22±1.98

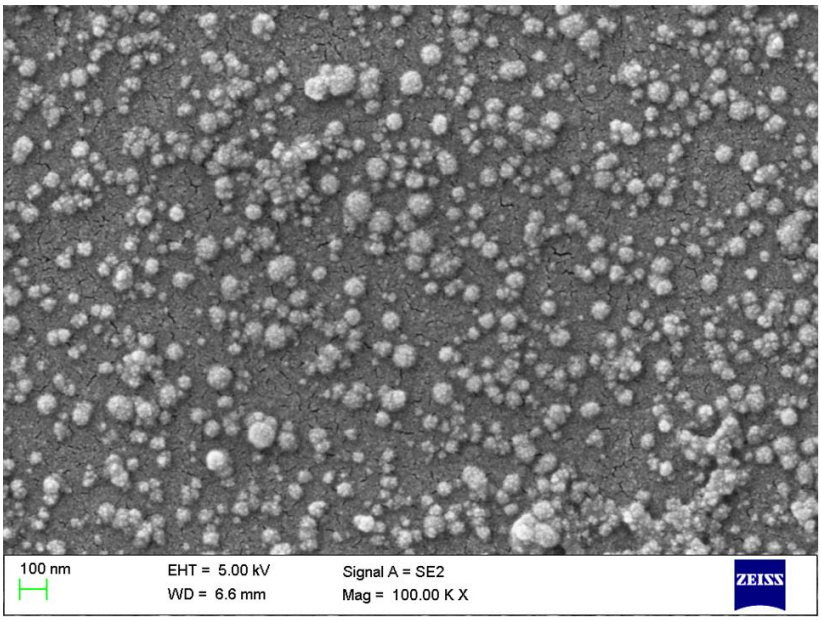

Figure 2.5: FESEM micrographs of FANPs obtained at nanoformulation NF2; CS conc. 1mg/ml, native FA conc. 0.0528 mg/ml; (Microscopic magnification 100KX, Scale bar 100 nm)

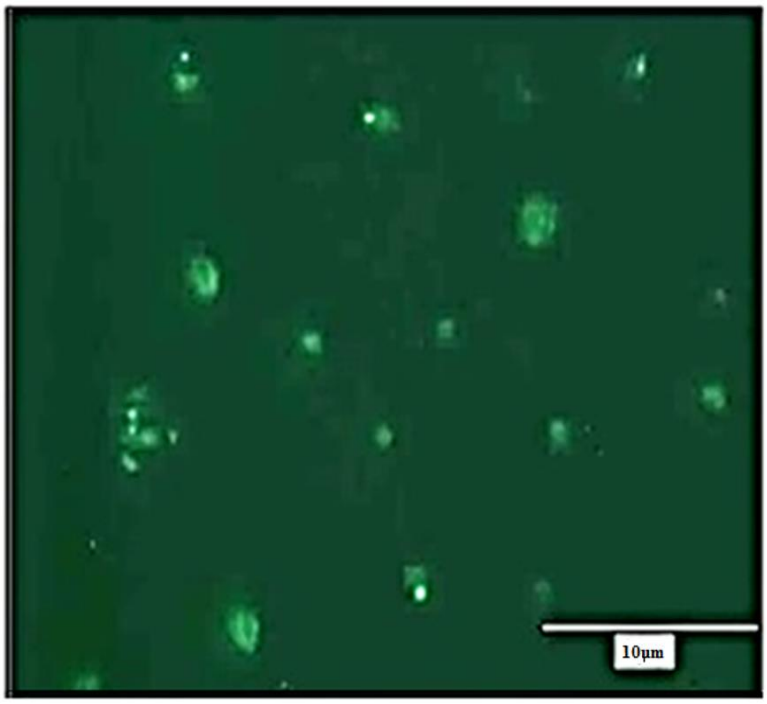

Figure 2.6: The auto-fluorescence micrograph of FANPs at NF2 at wavelength 470-510 nm; (Magnification 100KX, Scale bar 10µm)

Table 2.2: Enhancement in solubility (%) of FANPs at NF2, and NF3 in different solvents at room temperature

NFs	Enhancement in solubility	
	Water	**Acetic acid (1%)**
NF_2	28	25
NF_3	21	19

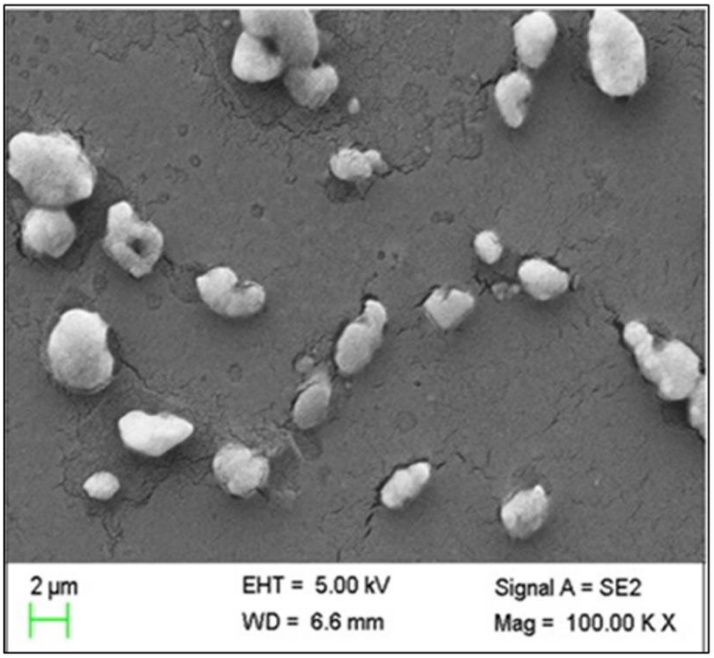

Figure 2.7: Randomly distributed large FANPs visualized at NF4; (Microscopic magnification 50KX, Scale bar 2µm)

2.5.2. Characterization of FANPs

Physicochemical characterization techniques involving FTIR, TGA/DSC and NMR were employed to evaluate the success of FA loading into CSNPs. FTIR spectra of native FA, CSNPs and FANPs (NF_2) displaying physicochemical interactions is represented in Figure 2.8. FA showed characteristic peaks at 3436 cm^{-1}, 2245 cm^{-1}, 1568 cm^{-1}, 1417 cm^{-1}, 1021 cm^{-1}, data obtained is in accordance with the earlier reports (Woranuch and Yoksan, 2013a). Absorption bands corresponding to NH_2 and OH groups stretching vibrations at 3422 cm^{-1} in chitosan nanoparticles indicated hydrogen bonding between chitosan and TPP. Bands at 1642 cm^{-1}, 1576 cm^{-1}, 1096 cm^{-1}, 893 cm^{-1} correspond to amide I, amide II, C-O-C and pyranose ring, respectively. In comparison with unloaded CSNPs, the band of NH_2-OH group stretching in FANPs has been broadened and shifted to 3374 cm^{-1} as a results of hydrogen bonding. Presence of bands at 1568 and 1417 cm^{-1} corresponding to C=C aromatic ring both in native FA as well as FANPs indicated their successful interaction. A possible mechanism of interaction between CS and FA is depicted in Figure 2.9. In addition to the hydrogen bonding and other covalent interaction, certain electrostatic forces are also believe to act between positively charged CSNPs and negatively charged FA in order to facilitate its loading. Data reported in above discussion implies formation of CSNPs and successful encapsulation of FA into them.

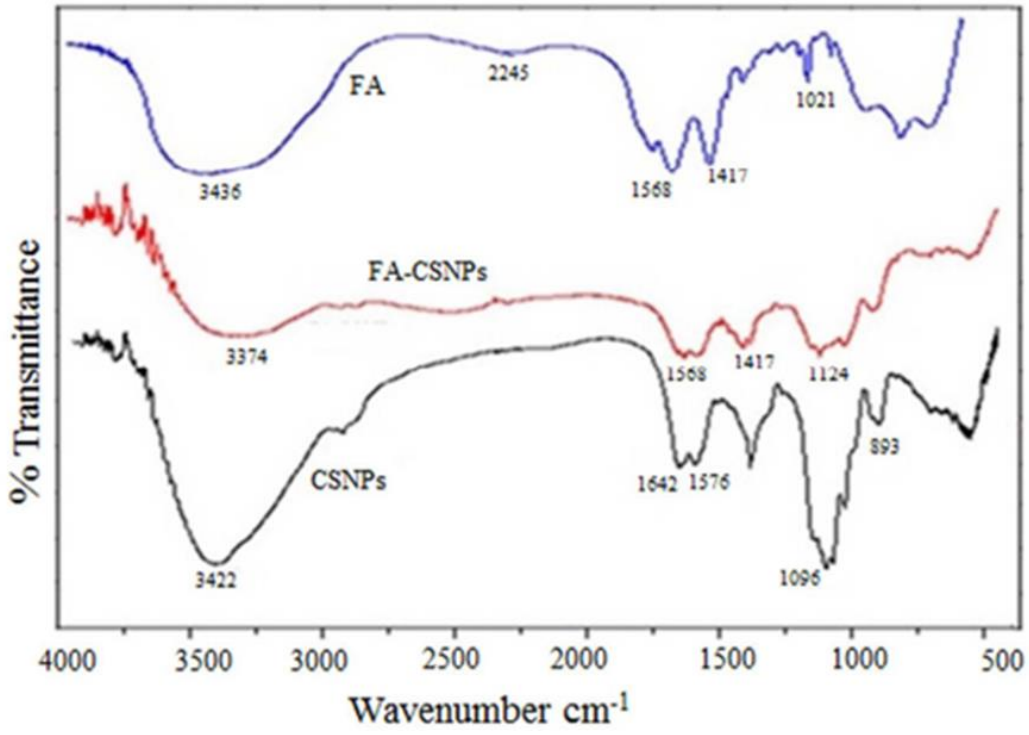

Figure 2.8: Fourier transform infrared spectrum of different formulations

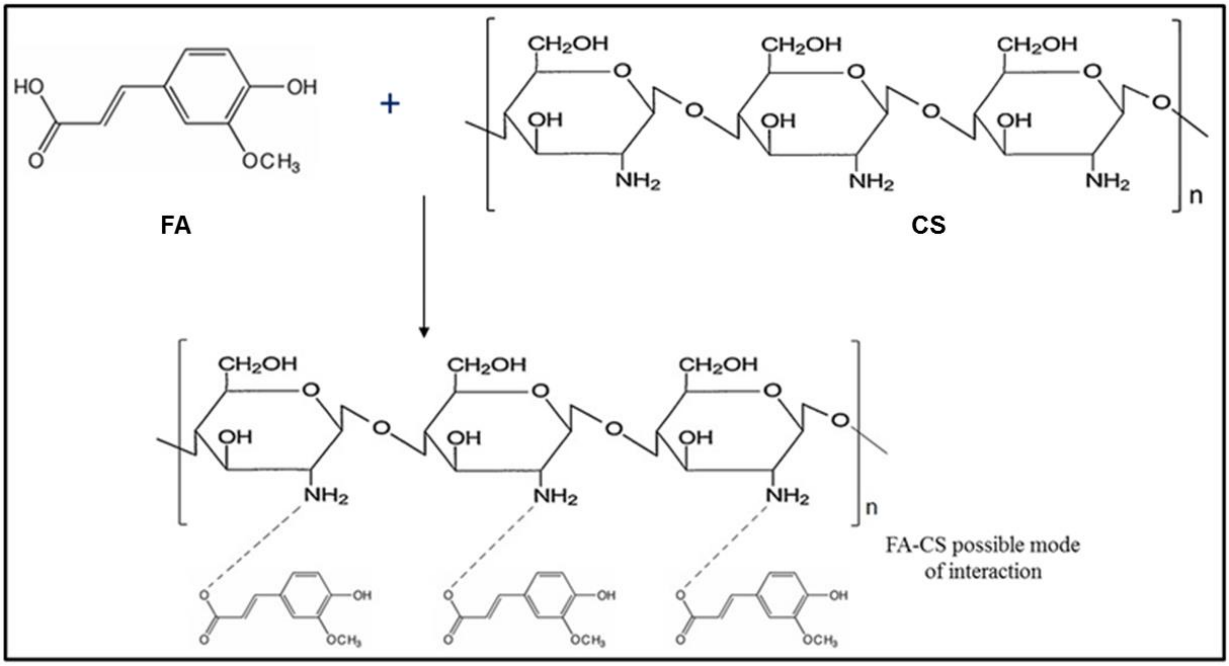

Figure 2.9: A proposed mechanism of interaction between phenoxy groups of FA and amino group of CS

The TGA curve of native FA, CSNPs and FANPs (NF_2) depicted percent loss of mass as a function of temperature at a constant heating rate (Figure 2.10A). Data represents a single stage mass decomposition curve for FA, starting around 174°C and continued linearly till its complete degradation around 520°C. Similar patterns of thermal degradation were also reported earlier for native FA by Mathew and Abraham (2008).

The degradation of unloaded CSNPs started around 51°C with a higher mass loss peak at 70°C and then followed a linear mass loss culminating at 500°C. The lower initial temperature for CSNPs degradation attributes to the lowering of acetylation degree of CS due to depolymerization following interaction with TPP molecules. For FANPs, the initial mass loss temperature was about 105°C which could be due to water evaporation while peak at 225°C indicated the loss of crystalline structure of CSNPs upon FA binding. Enhancement of initial degradation temperature and higher weight loss peaks for FANPs in comparison to unloaded CSNPs demonstrated the success of FA encapsulation.

The DTG curve of FA and CSNPs showed peak maximum decomposition at 250ºC and 253ºC, respectively; while FANPs exhibited decomposition temperatures at 223, 261 and 365ºC approximately (Figure 2.10B). The distribution of peak maxima in encapsulated FA may be a result of its interaction with polymeric components of CS.

Further evidences towards the accomplishment of encapsulation process could be drawn from DSC thermograph showing thermal transition profile for different formulations (Figure 2.10C). Sharp endotherm obtained at 175°C for FA is typical for the melting of its crystalline anhydrous form, followed by its decomposition at higher temperatures. Similar differential scanning calorimetric profile has been reported earlier for native FA (Mathew and Abraham, 2008; Rossi et al., 2005). CSNPs displayed endothermic band around 70°C, indicating a loss of bound water causing the onset of melting. Small endothermic peak around 210°C for FANPs signified melting and decomposition of FA and CS present in nanoparticles structure.

Data represented by DSC thermograph of nanoformulations could be correlated with their corresponding TGA curves (Figure 2A and C). From above discussion it could be concluded that the initial melting temperature of CSNPs was effectively enhanced upon FA encapsulation.

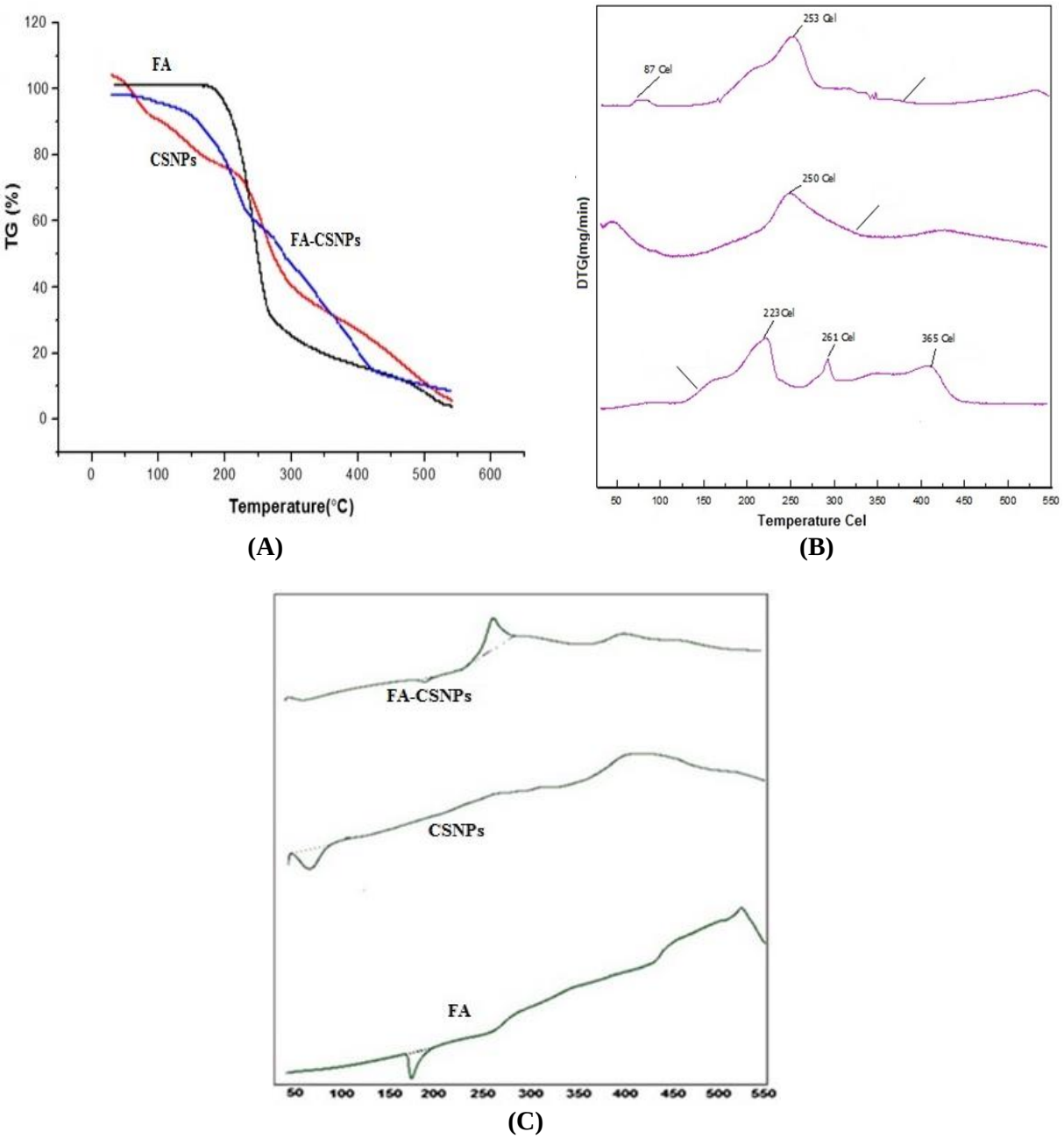

Figure 2.10: **A)** Thermogravimetric, **B)** derivative thermogravimetric, **C)** differential scanning calorimetric thermographs for different formulations

To evaluate the stability of FA upon encapsulation, chemical structure of formulation were analyzed and compared by using ^{1}H NMR spectrum. FA showed proton signal around 3.82 ppm ($-OCH_3$) and multiple peaks between 6.33-7.49 ppm corresponding to methine proton of FA (Figure 2.11).

Unloaded CSNPs exhibited proton signals at 2.50 ppm for the methyl protons of acetylated glucosamine residues, around 3.44 ppm for protons of pyranose ring and at 5.00-6.55 ppm for phenyl protons characteristics of CS. Additional peaks observed at 9.65 ppm and 10.76 ppm indicated the interaction of chitosan with TPP resulting in the formation of nanoparticles. Considering FANPs (NF_2), multiple peaks characteristics of ferulic acid between 6.34-7.51 ppm and proton signals at 9.54 and 12.11 suggested that the integrity of FA was not compromised significantly upon nanoencapsulation. Literature reports similar ^{1}H NMR spectral data for native FA, chitosan-FA conjugates and FA grafted chitosan (Liu et al., 2014; Sohn and Oh, 2003; Müller et al., 2001).

To determine physical state and distribution of FA in the synthesized FANPs, XRD technique was employed. Characteristic peaks obtained for FA at 2θ = 9.0, 10.3, 12.5, 15.5, 17.2, 21.0, 24.2, 29.3, 35.7 are depicted in Figure 2.12A. Similar XRD patterns were also observed earlier for native FA by Yu et al. (2013). The XRD pattern of CSNPs revealed typical CS crystalline peak intensities at 2θ = 10.1 and 21.8, similar to those reported earlier (Qi et al., 2004). Compared to CSNPs, broader XRD patterns were observed for FANPs at 2θ = 10.2, 21.8, 24.2, 25.8 and few minor peaks (Figure 2.12B). It may be attributed to breaking of inter and intra-molecular H-bonds present in CS structure due to loading and encapsulation of bulky FA (Woranuch and Yoksan, 2013). The data represented in Figure 2.12A and B, showed the presence of various common peaks in FA and FANPs diffractogram which is an indication of successful encapsulation of FA within CSNPs. Data also revealed that the typical crystalline structure of FA was not completely compromised during the encapsulation process.

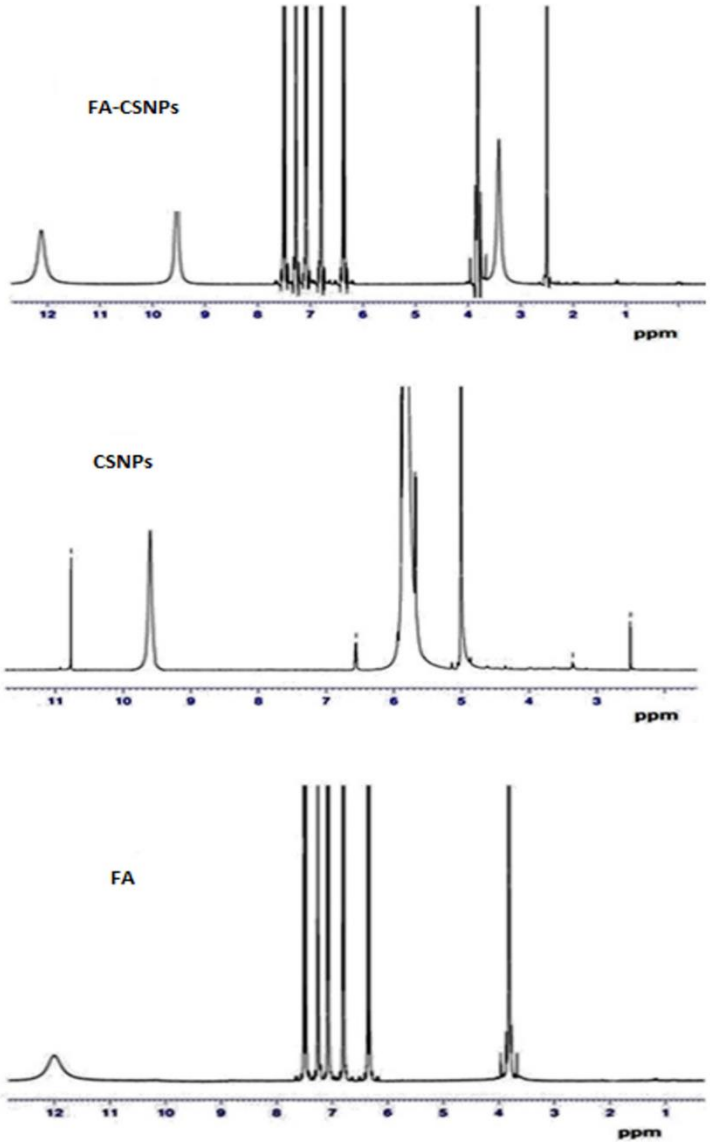

Figure 2.11: ^{1}H nuclear magnetic resonance spectra for test formulations

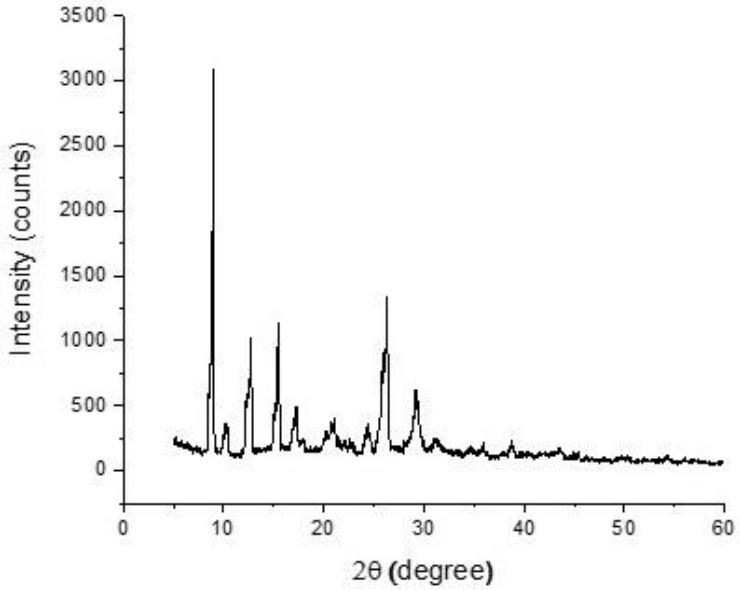

(A)

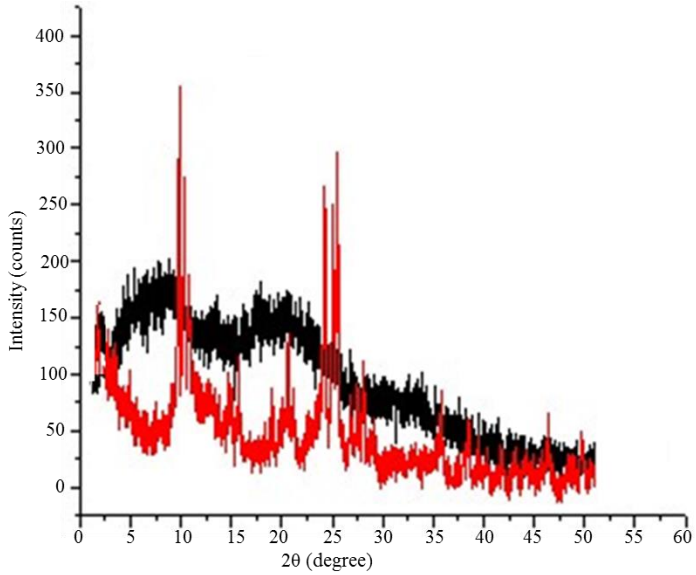

(B)

Figure 2.12: XRD patterns of different test formulations A) native FA, B) CSNPs and FANPs

2.6. Free radical scavenging activity

DPPH is a nitrogen centred free radical which gives strong absorption maximum at 517 nm. The change in color of solution from yellow to purple occurs as the singlet electron in DPPH free radical becomes paired with hydrogen, from free radical scavenging antioxidant to form the reduced DPPH-H.

Free radical scavenging effect (antioxidant potential) of free FA and FANPs was calculated by plotting conc. (20, 40, 80, 100 and 200 µg/ml) with respect to percentage inhibition, taking ascorbic acid as a standard (Figure 2.13). Dose dependent radical scavenging activity with EC_{50} values corresponding to 80.7 ± 1.2 µg/ml, 139.7 ± 0.9 µg/ml and 145.4 ± 0.5 µg/ml for standard (ascorbic acid), native FA and FANPs respectively were measured. EC_{50} value is defined as the effective conc. of a compound at which it exhibit 50% radicle scavenging. The EC_{50} values of test samples clearly indicated that the free radical scavenging property of FA upon encapsulation into CSNPs was not compromised noticeably with respect to native FA. This observation could be attributed to the fact that CS itself possess antioxidant property, and has been reported to scavenge hydroxyl radicals in DPPH assays (Luo and Wang, 2013).

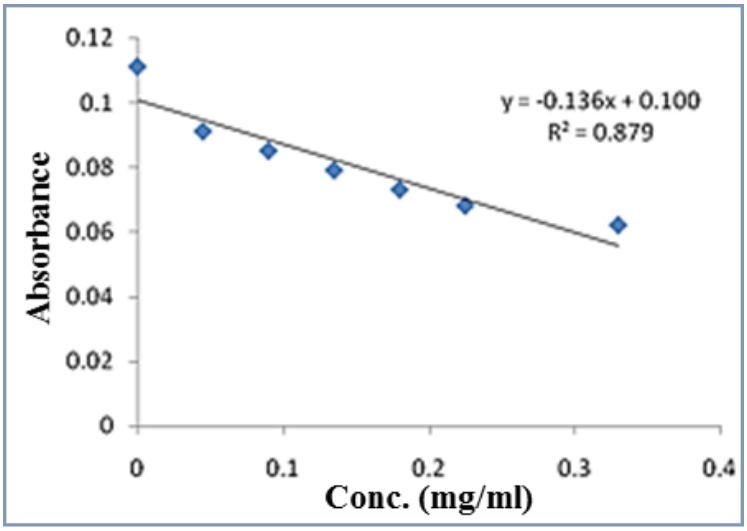

Figure 2.13: Ascorbic acid standard curve for calculating DPPH radical scavenging capacities of test formulations at 517 nm

2.7. Conclusion

In the present chapter, a plant polyphenolic compound FA, with potent antioxidant activity was encapsulated into CSNPs to develop polymeric nanocarriers. Medium molecular weight CS at a conc. of 1 mg/ml, with CS:TPP mass ratio of 4 provided the most suitable parameters for stable FANPs. Approximately 50% encapsulation efficiency was achieved for optimized nanoformulations. Biochemical characterization of FANPs through FTIR provided an insight about its secondary interactions with CSNPs while TGA/DTG analyses revealed enhanced thermal degradation range of FANPs. NMR spectroscopy revealed the functional groups shifts in the chemical structures of different formulations that have taken place during encapsulation process while the X-ray diffractometry established the successful encapsulation of FA. The EC_{50} values obtained for native FA (139.7 ± 0.9 µg/ml) and FANPs (145.4 ± 0.5 µg/ml) in DPPH radical scavenging assays indicated the stability of FA antioxidant potential during encapsulation.

Chapter: 3

In-vivo Release Study of FANPs and their Anti-inflammatory Potential in Carrageenan-induced Paw Edema in Wistar Albino Rats

3.1. Introduction

FA is one of the significant polyphenolic compounds widely present in plant kingdom which is positively co-related to various health benefits in human body. It has found noteworthy applications in food, cosmetics, nutrition and pharmaceutical industries (Tilay et al., 2008). Presence of phenolic nucleus and an extended side chain in FA structure bestow it the ability to form a resonance stabilized phenoxy radical. This highly unstable radical structure with an ability to quench hydroxy, phenoxy, peroxide and various other free radicals, underlines the basis of strong antioxidant potential possessed by FA (Adluri et al., 2008; Srinivasan et al., 2007; Kawabata et al., 2000). As discussed previously, various studies have reported the ability of FA to prevent cellular oxidative stress, DNA damage and lipid peroxidation (Sudheer et al., 2007; Balasubashini et al., 2004). In this regard, FA has been endowed with a strong cytotoxic activity *in-vitro* against different cancer cell lines as well as *in-vivo* causing a significant reduction in plasma markers of tissue damage; and in skin cancers (Hosoda et al., 2002; Murakamia et al., 2002). It has shown improvement of hyperglycemia in rats with induced diabetes and enhanced levels of antioxidant enzymes (SOD, CAT) in the liver of diabetic rats administered with FA as compared to control groups (Ohnishi et al., 2004; Hiramatsu et al., 1990). Studies have also reported the anti-inflammatory effect of FA by positively enhancing the production of anti-inflammatory proteins such as murine interleukin-8 and macrophage inflammatory protein-2 (Sakai et al., 1999; Hirabayashi et al., 1995).

Nevertheless, this highly beneficial plant nutraceutical present peculiar shortfalls related to its limited aqueous solubility, poor gastrointestinal stability and low bioavailability. Pharmacokinetic studies have shown that FA is quickly absorbed following oral ingestion and reaches its peak plasma conc. within 5-15 min in rats and 30 min in humans (Mancuso and Santangelo, 2014). The main route of FA excretion in rats is through urine, therefore, a marked first pass effect significantly lowers its plasma conc. i.e., the urinary excretion of FA reaches its

plateau within 1.5 h of oral ingestion in rats and about 7 h in humans (Rondini, 2004). As a consequence of this unfavorable pharmacokinetics, the lower *in-vivo* plasma conc. of FA might remain inadequate to elicit the required amount of biological responses (mainly antioxidant) necessary for prevention of chronic diseases. To overcome this disadvantage, FA could be stabilized through encapsulation into polymeric nanocarriers thereby improving its pharmacokinetic and pharmacodynamic profiles.

Nanoscale size and high surface-to-volume ratio are some of the distinctive properties of these nanocarriers which allow their favorable interface with encapsulated polyphenols through various physico-chemical interactions. Recent studies have reported that loading of polyphenols and bioactive compounds into polymeric nanoparticles significantly enhanced their absorption and bioavailability in addition to providing them stability against degradation in gastrointestinal tract (Wicki et al., 2015; Li et al., 2015; Khan et al., 2013).

CS is a naturally occurring polymer with positive surface charges that renders CSNPs an attractive choice for loading of polyphenols having negatively-charged sites on their cell surfaces. Other than macromolecular retention, cationic surface of CSNPs also allow their sustained release over an extended period of time (Vrignaud et al., 2011). TPP has been extensively used as an anionic binding force for preparation of CS-TPP nanoparticles through ionotropic gelation process. In the same context, CSNPs loaded with tea polyphenols and *Elsholtzia splendens* extract have shown their effectiveness as potential nanocarriers with slow drug release, while maintaining the integrity of encapsulated material (Liang et al., 2011; Lee et al., 2010). Recently, chlorogenic acid loaded CSNPs were prepared to allow control release of encapsulated drug along with preserving its antioxidant property (Nallamuthu et al., 2014).

In the previous chapter, we have reported successful synthesis of FANPs (1 mg/ml CS, CS:TPP mass ratio 4) with approximately 50% EE, without any noticeable damage to encapsulated FA. Present chapter provides an illustration of pharmacokinetics of free and encapsulated FA in the plasma of Wistar albino rats. This study would aid in comparing both form of FA in terms of their release profiles, thereby facilitating to establish FANPs as a useful pre-clinical nutraceutic. Finally, FANPs were tested for their anti-inflammatory potential with respect to free FA in carrageenan-induced rat paw edema model.

3.2. Methodology

3.2.1. Animal care and handling

The experiment were carried out on Wistar albino rats of 4 months, of both sexes, weighing between 110 to 190 g. They were provided from Sapience Bio-analytical Research Lab, Bhopal, (M.P.). Animals were acclimatized to the standard laboratory conditions one week prior to study in cross ventilated animal house at 25 ± 2°C, relative humidity 44–56% and light:dark cycles of 12:12 h. The animal were fed with standard pallet diet and water *ad libitum* during the course of experiment except for fasting overnight prior to pharmacokinetic analysis. The animal testing protocol was approved by the Institutional Ethics Committee and was performed as per CPCSEA guidelines (approval no. 1413/PO/a/11/CPCSEA).

3.2.2. Acute oral toxicity studies

Oral acute toxicity of test formulations were evaluated as per OECD guidelines (Organisation for Economic Co-operation and Development) on Wistar albino rats. Three animals were selected for maximum tolerable dose (LD_{50} equal to 2445 mg/kg) of FA and observed individually for any toxicity sign of gross changes like convulsion, tremor, circling, depression and mortality. All observations were systematically documented with individual records being maintained for each animal. No toxic signs were noticed in animals, hence administered dose was considered tolerable.

3.2.3. Pharmacokinetic study design

A single dose complete cross over method was employed for the study of pharmacokinetics of FA present in nanoformulation (FANPs) with respect to native FA.

Grouping and treatment of animals:

Group I: Native FA, used as standard sample

Group II: Nanoformulation (FANPs), used as test sample

Dose: A dose of 10 mg/kg was selected for the given protocol

Route of administration: p.o. (mouse oral gavage)

Preparation of 0.5% CMC Solution

Accurately weighed 250 mg of carboxy methyl cellulose (CMC; Himedia, India) was dissolved in Milli Q purified water and final volume was made up to 50 ml to give a conc. of 0.5%.

Preparation of Standard formulation of FA

Native FA stock suspension of 10 mg/ml conc. was prepared by dissolving 100 mg FA in 0.5% CMC solution to make the volume up to 10 ml.

Preparation of test formulation

A suspension of nanoformulation was prepared separately by dissolving 100 mg/ml FANPs (lyophilized powered sample) in 0.5% CMC solution and finally volume was made up to 10 ml to give a conc. of 10 mg/ml.

Treatment of animals:-

- Native FA was administered orally to the rats.
- The tube of oral gavage was inserted through mouth into the stomach, extra care was taken so as not to perforate the esophagus that would have led to instant death of animal.
- Once properly inserted, the syringe was attached to the tube and dose was administered.
- To assure the complete delivery of dose, a small volume (2 ml) of water was used to flush the tube.

Blood Sampling

Blood samples for pharmacokinetic procedure were obtained from peri-orbital venous sinus via retro-orbital puncture of rats (Hui et al., 2007). In this procedure, rat was restrained with one hand and microhematocrit tube was inserted through conjunctiva into the orbital sinus by quickly rotating the tube. Extreme care must be taken while inserting, and the tube must pass under the eye to avoid any possible damage to animal. The bleeding usually ceases by the orbit pressure, but if required the eye could be wiped. The withdrawn blood (≈0.5 ml) was collected in polyethylene vials containing 22 mg/ml disodium EDTA at different time intervals viz. 0, 30, 60, 120, 240, 360, 480 and 600 min. The collected samples were centrifuged at 3000 rpm for 15 min and the plasma samples were stored at -20°C until analyzed.

3.2.4. Analytical procedure

Apparatus

HPLC apparatus (Waters; Milford, MA, USA) fitted with a model 600 controller, model 600 pump, UV absorbance detector in combination with a data module integrator (Data ace work station) and a model 7725I rheodyne manual injector. An ODS C18 (Waters, MA, USA) analytical column (5µm i.d., 4.6mm X 250 mm) coupled with C18 guard column were employed for chromatographic separation.

Reagents and Chemicals

FA, acetic acid, methanol, HPLC grade acetonitrile and water, carrageenan and sodium diclofenac and other standard analytical chemicals were procured from Himedia (Himedia, India) and Merck (Merck Ltd, Mumbai, India).

Mobile phase and standard Solutions

The mobile phase consisted of acetonitrile: water (15:85) with 0.5% (v/v) glacial acetic acid (pH 2.5) and was run isocratically with a flow rate of 1 ml/min during the entire analysis. FA stock solution was prepared by dissolving it in methanol upto a conc. of 1 mg/ml, followed by further dilution with mobile phase to obtain working solution of 2, 4, 6, 8 and 10 µg/ml.

Initially, 20 µl of FA solution of each conc. (as above) were injected into the column and UV spectra recorded at 322 nm. Subsequently, the peak height ratios of each sample were plotted against their respective conc. to obtain FA standard curve (Figure 3.1). In succession, blank plasma sample was filtered through 0.2 µm membrane filter and run to identify any interference of plasma peaks with native FA. Likewise plasma samples of animals from both groups were analyzed and the conc. of FA in each sample at different time points was calculated using the regression parameters obtained from FA standard curve.

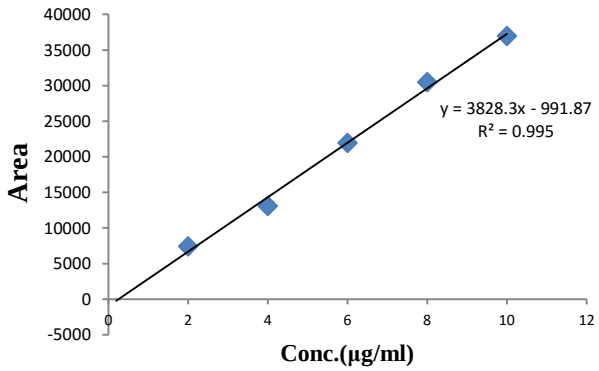

Figure 3.1: FA standard curve

3.3. Anti-inflammatory activities

The animals used for anti-inflammatory activities were habituated and housed in the condition as described previously for pharmacokinetic analysis (section 3.2.1).

Grouping and dosing

In this investigation, 24 rats were used which were divided into 4 groups comprising 6 animals in each as follows:

Group **I:** Control, vehicle treated (1 ml/100g water), injected with carrageenan (0.1 ml).

Group **II:** Standard, treated with diclofenac sodium, (10 mg/kg, p.o.) 1h prior to carrageenan injection.

Group **III:** Test 1, treated with native FA (10 mg/kg p.o.) 1h prior to carrageenan injection.

Group **IV:** Test 2, treated with FANPs (10 mg/kg p.o.) 1h prior to carrageenan injection.

Induction and measurement of paw edema in rats

Acute inflammation was caused by injecting 0.1 ml of 1 % (w/v) carrageenan (Hi-Media, India) prepared in saline into the sub-plantar region of the left hind paw of each rat. Edema was expressed as mean increase in paw volume relative to control animals (Figure 3.2A and B). The percentage inhibition of edema was calculated by the following equation:

Inhibition of edema (%) = 100 (1-Vt/Vc),

Where, Vc is the edema volume in the control group and Vt is the edema volume in test groups (Fernández et al., 1998).

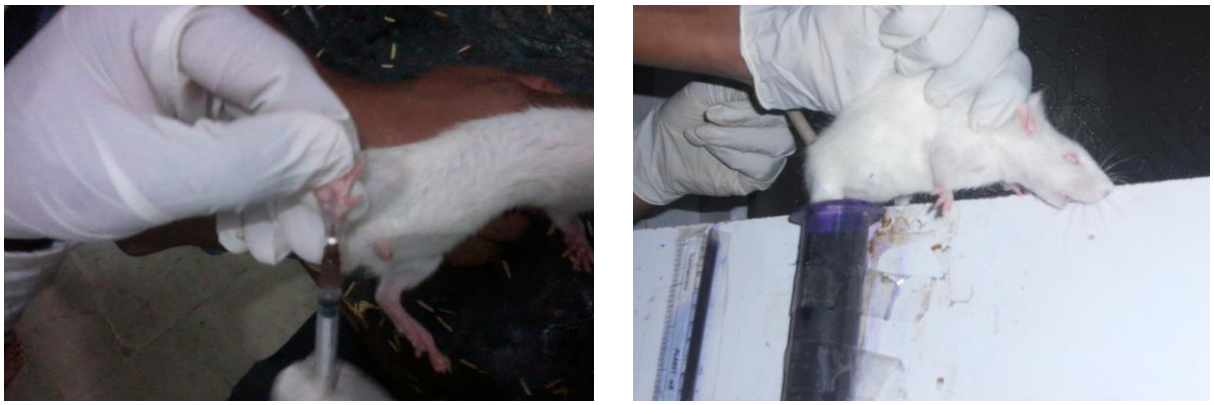

(A) **(B)**

Figure 3.2: **A)** Induction of paw edema in rat by carrageenan, **(B)** Measurement of rat paw volume by Plethysmograph

Statistical analysis

All values were expressed as mean±standard error of mean and analyzed through ANOVA and posthoc Tukey-Kramer Multiple Comparisons Test using "GraphPad InStat 3" statistical software. Differences between groups were considered significant at $P < 0.05$.

3.4. Results and discussion

Bioavailability of a compound is an indirect indication of the time period during which it stayed in plasmatic compartment before it is metabolized and excreted (Rondini et al., 2004). A decrease in urinary excretion of a compound over a period of time might suggest higher bioavailability.

The adsorption of polyphenols into nanocarriers provide them with an extended blood circulation time with increased *in-vivo* stability thus allowing their controlled release with in biological systems as hypothesized in Figure 3.3. Our data presenting the plasma conc. of free and encapsulated FA at different time intervals post oral administration and their respective area under HPLC chromatogram is depicted in Figure 3.4A and B. Results showed that FA in its free form was absorbed quickly and appeared very early in plasma, wherein the peak of

maximum plasma conc. (C_{max}=1.774243) was detected within 15 min (T_{max}) of oral administration. Upon attaining its maximum plasma conc., FA levels started to decline from the system (Figure 3.2A). There was a slight increase in 2-4 h plasma conc. level which may be due to the interference of plasma proteins. The conc. reached it minimum level after 6 h of dosing, beyond which no FA was detected.

Zhao et al. (2003) reported the maximum plasma conc. of free FA and its sulphate ester 30 min after their oral administration in rat plasma. Yang et al. (2007) and Konishi et al. (2006) also suggested a fast gastric absorption of FA where the maximum plasma conc. of free FA was achieved within 5 to 10 min of administration in rats and humans respectively. The early appearance of FA in plasma upon oral intake of free form could be related to its fast absorbance in jejunum or stomach. Spencer et al. (1999) in his studies conducted on isolated rat intestine model, described quick disappearance of FA from jejunum and recovered a very small amount in ileum.

HPLC chromatogram obtained for free FA corresponding to its C_{max} and T_{max} is presented in Figure 3.4C. Contrary to free form, FANPs depicted a different course of absorption with a much delayed release of FA from its nanoformulation (Figure 3.2A). Its maximum plasma conc. level was detected approximately 1 h post administration with a C_{max} of 0.549018 µg/ml corresponding to T_{max} (60 min). The plasma FA conc. levels remained almost stable from 2-6 h, however release was higher in case of nanoformulation than the free form during 4-6 h. After 6 h, the plasma conc. declined slowly, notwithstanding the fact that the measurable amounts of FA were still detected upto 8 h (unlikely of free form).

Upon oral delivery, CSNPs aids in a higher absorption of encapsulated drug due to its mucoadhesive property and the transportation of CS-drug nanoparticles is facilitated across mucosal cells membrane through a momentary opening of tight junctions (Vllasaliu et al., 2010). Also, the opposite surface charges of CSNPs (positive) and mucin (negative), offers an extended period of contact between drug and target cell surface thus assisting in better absorption (Nagpal et al., 2010). The HPLC chromatograms depicting FA release from nanoformulation at 0.5, 1, 2 and 6 h are presented in Figure 3.5A-D.

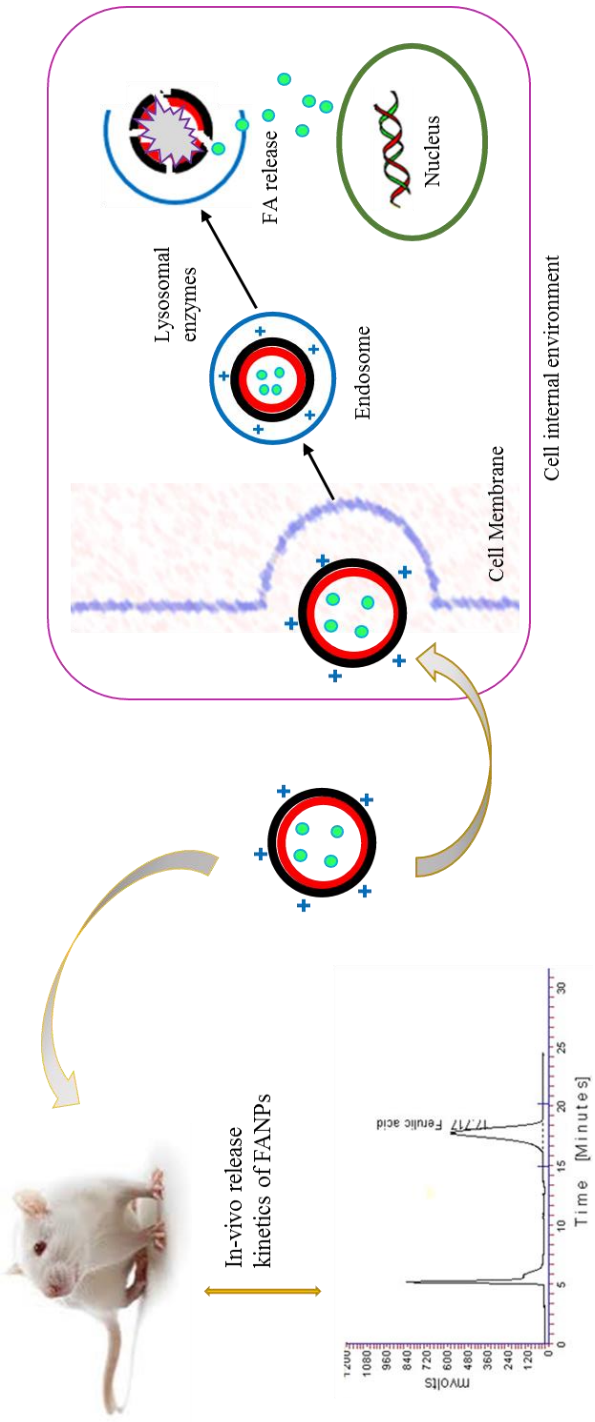

Figure 3.3: Schematic representation of pharmacokinetic analysis and interaction of FANPs to target cell membrane and their internalization. Upon entering the cell's internal environment nanoparticles might be attacked by lysosomal enzymes causing a sustained FA release

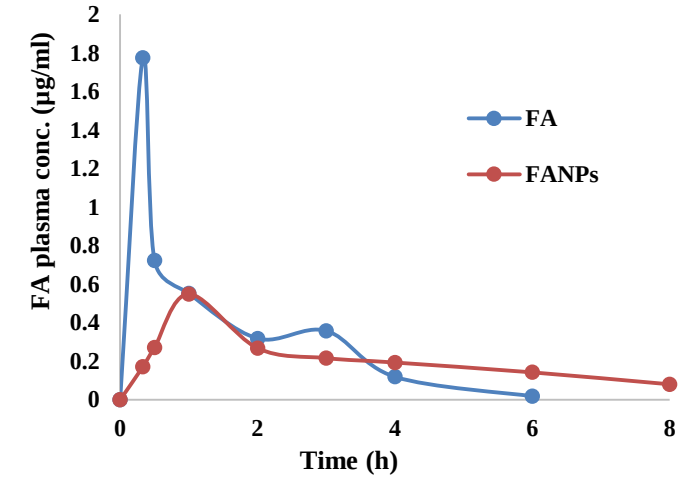

(A)

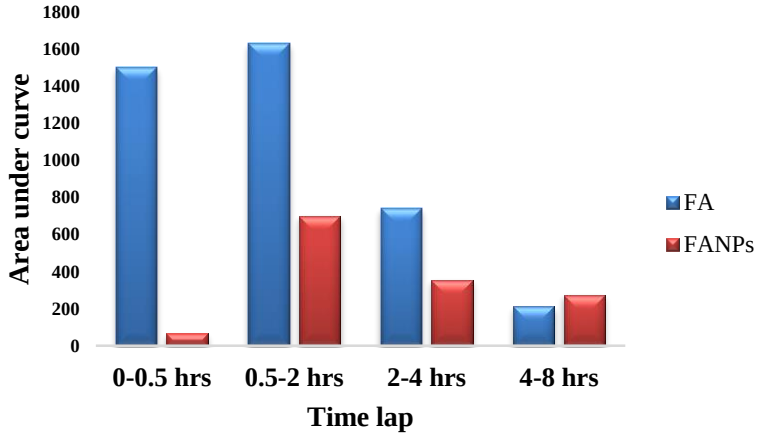

(B)

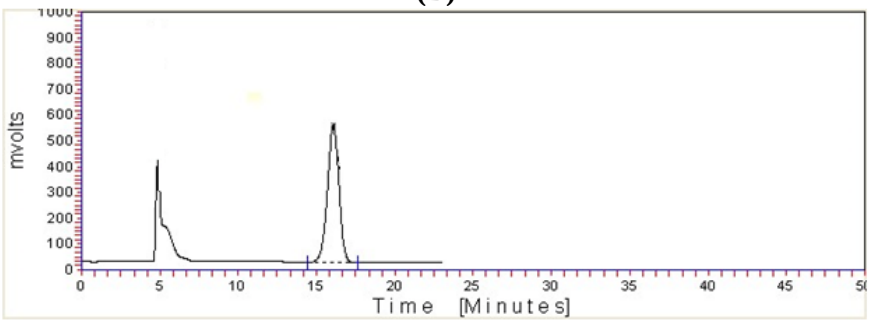

(C)

Figure 3.4: **(A)** Plasma conc. of free FA and FANPs at different time intervals post oral administration **(B)** Area under chromatographic curve for both formulations at different time intervals **(C)** HPLC chromatogram for free FA corresponding to its C_{max} (1.774243) and T_{max} (15 min)

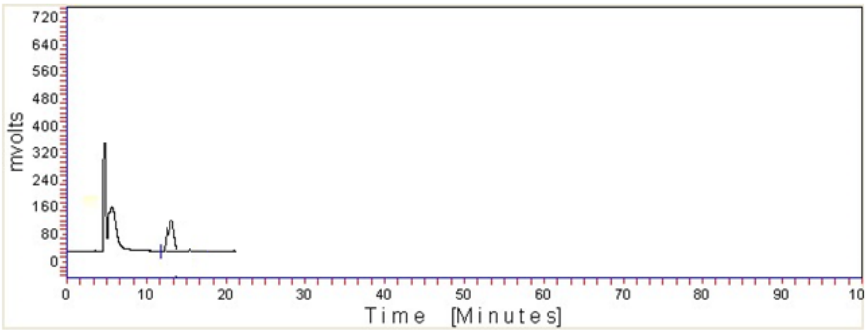

(A)

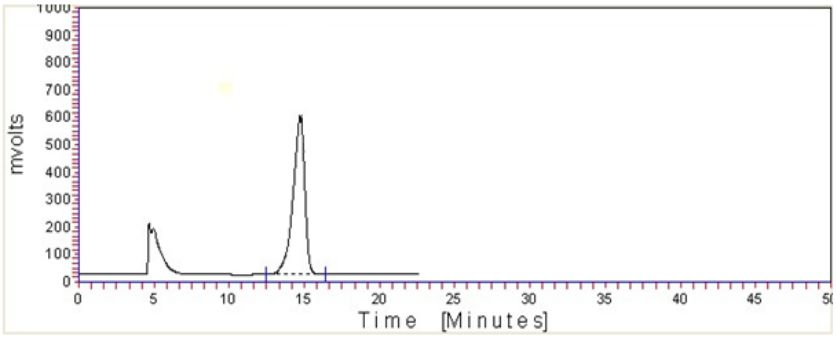

(B)

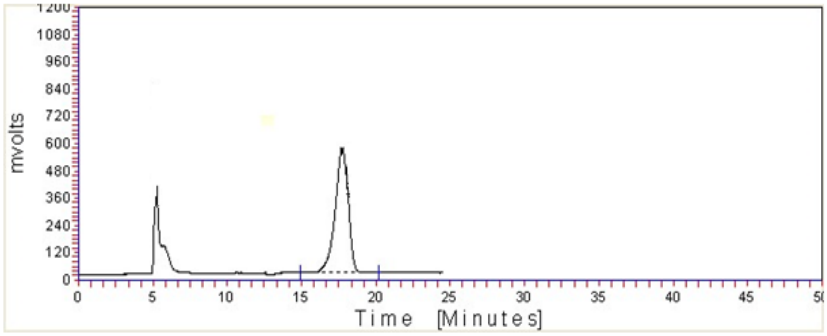

(C)

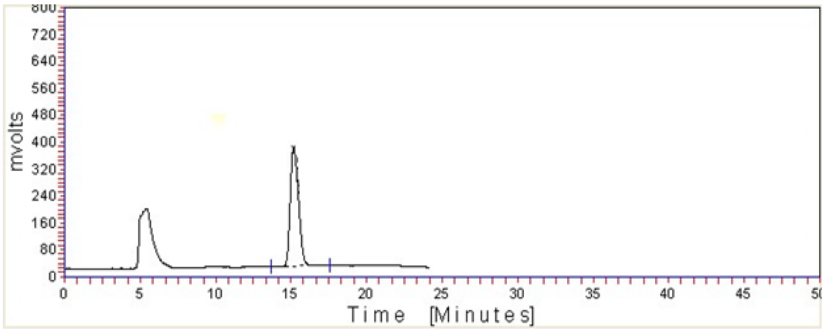

(D)

Figure 3.5: The HPLC chromatograms depicting FA release from rats treated with nanoformulation after **(A)** 0.5 h, **(B)** 1h, **(C)** 2h, **(D)** 6h

The bioavailability of FA is generally low due to its rapid conjugation in liver and high rate of free FA filtration through kidneys (Choudhury et al., 1999). Several mechanism, including an H^+ driven transport, monocarboxylic acid transporters and passive diffusion have been suggested for FA uptake and metabolism inside the biological systems (Poquet et al., 2008; Itagaki et al., 2005; Konishi et al., 2003).

The urinary excretion profile for free and encapsulated FA after oral ingestion of doses is displayed in Figure 3.6. Urinary excretion is the major route of FA (both free and conjugated form) elimination in rats, most of which generally occurs within 60-90 min of oral dose intake (Zhao et al., 2004). The similar trend was noticed in the present study for free FA, where most of the ingested FA (>80%) was excreted within first 2 h. Whereas in case of encapsulated FA, initial 2 h accounted for approximately 50% of its urinary excretion. A plateau of highest metabolic excretion was obtained at 4 h and the elimination was detected well beyond 8 h (Figure 3.4).

The variations in plasma level pharmacokinetics and urinary excretion profiles of free and encapsulated FA could be attributed to a sustained release action of CSNPs. Besides allowing controlled release, loading/encapsulation of a compound into CSNPs have a positive effect on its *in-vivo* stability as well as blood circulation time. Earlier studies conducted on curcumin, a plant phenol having structural similarity with FA showed markedly higher serum levels and plasma half- life of curcumin NPs in comparison to its free form (Anand et al., 2010).

Electrostatic interaction between negatively charged FA and the positive charges present on CSNPs could be responsible for the significantly slower release of FA from its nanoformulation. These interactions might be considered as stable since they prevented an initial burst release that was observed in case of free FA and brought about slower and extended release over a period of time. Once entering the cell's internal environment, polymeric nanoparticles are attacked by degrading enzymes and undergo sequential release of encapsulated bioactives (Figure 3.3). A similar pattern of drug release behavior has been observed for CS based nanocomposite carrier (Yuan et al., 2010).

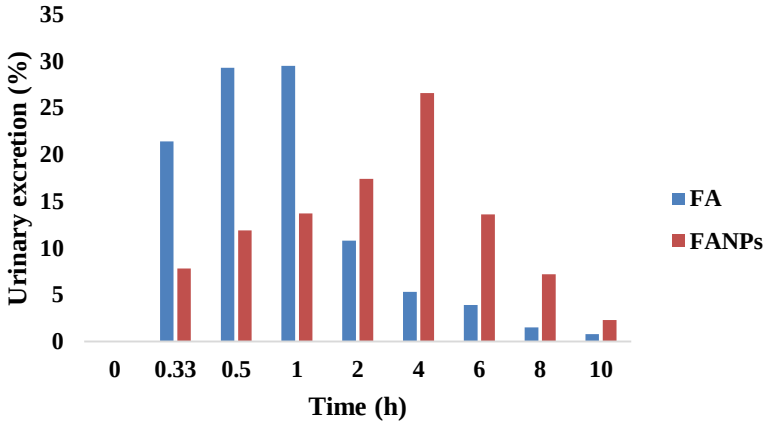

Figure 3.6: Urinary excretion profile of animals administered with free FA and FANPs

Inflammation is an element of body defense against various internal and external stimuli such as pathogens or to remove damaged cells and tissues. During acute inflammation, histamine, prostaglandins platelet activating factor and serotonin are released that tend to increase vascular permeability, resulting in tissue edema (Kumar et al., 2015). Chronic inflammations account for initiation of different diseases including arthritis, cardio-vascular problems, diabetes and cancers. Various medical researchers have reported a close relationship between inflammation and cancers by studying its role at all three stages (initiation, progression, and metastasis) of cancer (Grivennikov and Karin, 2010; Balkwill and Mantovani, 2010; Coussens and Werb, 2002). Steroidal and non-steroidal drugs currently available for treatment of chronic inflammations may lead to toxicity and other harmful health disorders such as gastric ulcers (Kumar et al., 2015). Hence, alternative plant derived therapeutics to formulate non-steroidal anti-inflammatory drugs becomes a prerequisite.

As discussed earlier (section 3.1), bioactive FA possess an anti-inflammatory potential, though its application is limited owing to its lower bioavailability. In our experiment we used carrageenan-induced hind paw edema Wistar albino rats to testify the inflammation healing potential of test compounds. Rat paw edema is the standard experimental model for acute inflammation and exhibits a high degree of reproducibility. Carrageenan is routinely used as a model phlogistic agent for the testing of anti-inflammatory drugs since it do not generate any immune response. The reduction in the volume induced paw edema with free FA and FANPs at 10 mg/kg was found 26.78% & 35.71% respectively, whereas the standard diclofenac sodium showed maximum reduction 37.52% (Table 3.1). Upon analyzing the data, it could be

established that the controlled release of FA from CSNPs led to the enhancement of its anti-inflammatory potential.

In various pharmacological studies, phyto-constituents and nano-formulated nutraceuticals having anti-inflammatory properties have been reported and used for the management of inflammatory diseases for example rheumatism is controlled through inhibition of synthesis of cellular prostanes (Just et al., 1998; Suleyman et al., 1991). In another study, Lorenzo et al. (1998) entrapped diclofenac sodium into CS core for its enhanced colonial delivery for 8-12 h. Researchers have also described intimate links between several inflammatory components (cytokines and chemokines) and tumor cells (Nair et al., 2010). Tumor-associated macrophages and pro-inflammatory cytokines including tumor necrosis factor-alpha and interleukin-6 directly regulates the recruitment of leukocytes towards neoplasm cells. Critically elevated levels of proliferation in any part of the body during inflammatory responses might be treated as biological markers indicating cancer development. For this reason, regulation of metabolic pathways associated with these sites represents natural target for chemoprevention. Modern days clinical trials emphasizes on targeting inflammatory machineries to combat the risk associated with or to destroy the neoplastic cells.

Table 3.1: Effect of native FA and FANPs on carrageenan induced paw edema rat groups, compared with standard diclofenac sodium. Values are mean ± standard error, where n=6, *p<0.05, **p<0.01 and ***p<0.001

Groups	Paw volume (mm) (Mean±SEM)					% Inhibition
	0 h	1 h	2 h	3 h	4 h	
I Control	0.28±0.01	0.46±0.02	0.56±0.03	0.63±0.03	0.56±0.02	-
II Diclofenac treated	0.31±0.01	0.36±0.03a*	0.4±0.02a**	0.36±0.03a***	0.35±0.02a***	37.52
III Native FA treated	0.31±0.01	0.41±0.01	0.48±0.03	0.45±0.02a**	0.41±0.01a***	26.78
IV FANPs treated	0.3±0.02	0.35±0.02a*	0.4±0.02a**	0.4±0.02a***	0.36±0.02a***	35.71

3.5. Conclusion

A plethora of studies have established FA as a strong antioxidant and anti-inflammatory agent, though its clinical applications remained limited due to low bioavailability. Absorption, metabolism and excretion are some of the important factors that determine *in-vivo* bioavailability of a compound. Free FA is quickly eliminated from circulation owing to its rapid and extensive metabolism and mostly excreted through urine. Nanoparticle encapsulation of bioactive compound for enhancement of their aqueous solubility and bioavailability has been extensively reported over the last decade. In the same context, pharmacokinetic and urinary excretion profile analysis were carried out for free and encapsulated FA (FANPs) using healthy Wistar albino rats. The encapsulated FA displayed extended plasma retention time and maximum plasma conc. was recorded at 60 min which implied four times enhancement of T_{max} compared to free FA. The elimination of compound from animal body also displayed a similar pattern where the peak urinary excretion of FA from nanoformulations was measured at 4 h contrary to 2 h in case of free FA. Animals with carrageenan-induced paw edema showed a better recovery when treated with FANPs, thus establishing this formulation as a highly promising and cost-effective nutraceutical with commendable safety profile.

Chapter 4

Evaluation of FANPs as an Anticancer Agent

4.1. Introduction

Nanotechnology has recently emerged as a promising arena in medical therapeutics where nanoparticles are frequently used for tissue delivery of drugs and bioactives having partial aqueous solubility and low bioavailability. In the previous chapters we have reported preparation and characterization of stable FANPs with extended plasma retention time in Wistar albino rats. Encapsulated FA displayed higher anti-inflammatory potential compared to its free counterpart, by virtue of controlled drug release ability of polymeric CSNPs. Close association between inflammation and different types of cancers has also been discussed previously (section 3.4). A vast array of chemotherapeutic drugs are available to counteract or reduce the risks associated with different carcinomas, however most of them are not free from undesirable side effect including toxicity towards normal/non-cancerous body cells.

Recently, polyphenols have emerged as a powerful and safe alternative to combat or prevent carcinogenesis, with low side effects (Domenico et al., 2012). FA is a dietary phytochemical that is known to possess antitumor activities against cervical, colon, gastric, breast and prostate cancers (Eroğlu et al., 2015; Janicke et al., 2011; Kampa et al., 2004; Kyoungho et al., 2001). Cervical carcinoma represents the second most leading cause of cancer mortality in women following breast cancer (Ellenson and Wu, 2004). Radiotherapy is the major therapeutic technique to minimize the effect of cervical cancer but due to its adverse effect on normal tissues, the role of alternative plant-derived therapeutic drugs are being tested (Seiwert et al., 2007). A large number of natural compounds have shown cytotoxic effects in different cancer models either alone or together with radiation (Garg et al., 2005). Subburayan et al. (2011) have reported a decrease in radiation surviving fraction of the cancer cells and increased lipid peroxidation indices on human cervical carcinoma ME-180 cells treated with FA.

Corresponding to cervical cancer, which is considered a major threat to women well-being, prostate cancer presents the second most common cause of death in men after lung cancer. Traditional chemopreventive strategies for prostate cancer are not much successful since the condition is aggravated due to late age of disease onset, slow progression and high incidences

along with limited sensitivity or selectivity of diagnostic tools (Eroğlu et al., 2015). In this regard, phenolic compounds having potential anti-cancerogenic properties may provide an exciting rationale to counteract initiation and progression of prostate cancer. A recent study conducted on prostate cancer cells reported the involvement of FA in bringing about cell cycle arrest in PC-3 cells lines *in-vitro* (Eroğlu et al., 2015). However the unfavorable pharmacokinetic and low bioavailability of FA necessitate its encapsulation into CS, the latter being a non-toxic, biocompatible polymer. Therapeutic efficacy of encapsulated drugs tend to improve in lieu of their increased biodistribution in different tissues and organs (Schroder et al., 2009). Strategies are currently being developed to overcome multidrug resistance in cancer through nanoparticles encapsulation of required drugs (Forrest et al., 2011). Janes et al. (2001) reported the ability of CSNPs to allow a minimal burst release of encapsulated doxorubicin relative to its free form while maintaining its cytostatic activity against human melanoma A375 and murine colorectal carcinoma C26 cells.

The focus in present chapter lies on the evaluation of anticancer potential of FANPs on ME-180 human cervical carcinomas and PC-3 human prostate cancer cell lines. Initially, the *in-vitro* release of FA from its nanoformulation was evaluated at different pH, followed by screening of both cell lines with different conc. of FANPs to estimate minimum conc. required for their 50% inhibition (IC_{50}). Subsequently, the effect of nanoformulation on cell proliferation were assessed via MTT assays and flowcytometry; morphological changes occurring within the formulation treated cells were visualized through FE-SEM and fluorescence microscopy. Finally, the cytocompatibility of corresponding formulations was checked on Human Embryonic Kidney (HEK-293) cell lines.

4.2. Materials and methods

Heat inactivated fetal calf serum (FBS), XTT (2,3,-bis(2-methoxy-4-nitro-5-sulfophenyl)-5-((phenylamino)-carbonyl)-2H-tetrazolium salt) assay kit, RPMI 1640 medium, glutamine, penicillin–streptomycin, EDTA, trypsin, annexin V-fluorescein 5(6)-isothiocyanate (FITC) and propidium iodide (PI) were obtained from Sigma-Aldrich (St. Louis, MO, USA). Cell culture-grade dimethyl sulfoxide (DMSO), acridine orange (AO), ethidium bromide (EtBr), 3-(4,5-dimethylthiazol-2-yl)-2,5-diphenyltetrazolium bromide (MTT) assay kit, phosphate buffered saline (PBS), fetal bovine serum (FBS), Dulbecco's modified Eagle medium (DMEM), gluteraldehyde and yeast peptone dextrose (YPD) other standard analytical chemicals were procured from Himedia (Himedia, India) and Merck (Merck Ltd, Mumbai, India). ME-180,

HEK-293 and PC-3 cell lines were procured from National Centre for Cell Science (NCCS), Pune, India.

Preparation of test formulations

CSNPs and FANPs for the current investigation were synthesized using earlier optimized protocol (section 2.2.2). Various dilution of FANPs and native FA viz. 10, 20, 40 and 80, 120 and 200 µM were prepared in 1% DMSO for cytotoxicity evaluation.

Maintenance of cell cultures

ME-180 and PC-3 cells were maintained in McCoy's modified medium and RPMI-1640 basal mediums respectively, supplemented with 10% FBS, 1% glutamine, 100 U ml^{-1} penicillin/ 100 µg/ ml streptomycin. HEK-293 cell lines used for the cytocompatibility evaluation of native FA, CSNPs and FANPs were propagated in DMEM medium augmented with 100 µg ml^{-1} streptomycin, 100 U ml^{-1} penicillin and 10% FBS. All cell lines were incubated for 24 h at 37°C with 95% humidified air and in 5% CO_2 atmosphere.

4.2.1. In- vitro release analysis

In vitro FA release profile of FANPs was studied by employing the method reported by Merlin et al. (2012). Concisely, 5 mg lyophilized FANPs sample was added to 30 ml PBS and kept in water bath shaker (120 rpm) at 37ºC. At predetermined time intervals 2 ml sample was retrieved from the dispersion medium which was replaced with same amount of fresh PBS. The absorbance value of each sample was recorded at 319 nm using UV spectrophotometer and the FA present in supernatant was quantified. FA release (%) was calculated by using the equation:

$$\text{FA release (\%)} = (FA_{initial}\text{-}FA_{supernatant})/\ FA_{initial}\times 100$$

4.2.2. Screening of formulations

The IC_{50} doses of FANPs were assessed in terms of changes in cell metabolic activities using MTT assay. After 24 h incubation of cells in their respective media, both ME-180 and PC-3 cells were seeded in 96 wells microtiter plates (1.0×10^4 cells/ml) and treated with 10 µL of each conc. of FANPs for 24, 48, and 72 h. Subsequently, the MTT solution (20 µl of 5 mg/ml stock) was added to each well containing sample and incubated at 37˚C for 6 h. The solution in the wells was then removed carefully and 200 µl of DMSO was added to dissolve the MTT

formazan crystals. Lastly, 100 µl of the dissolved formazan solution of each test sample was transferred to individual wells of 96 well plate to determine the absorbance at 540 nm using microplate reader (Fluostar optima, BMG labtech, Germany). Untreated cells growing in culture media were taken as control (Panwar et al., 2015). The cell viability was calculated as:

Cell viability (%) = OD_{540nm}(test samples) / OD_{540nm}(control)×100

4.2.3. Cytotoxicity analysis

The test formulations for cytotoxicity analysis refers to FANPs at their respective IC_{50}, native FA in equimolar conc. and CSNPs. To assess the effects of test formulations, MTT assay was carried out in both cancer cell using the protocol as stated above (section 4.2.2).

Visualization of apoptotic morphological changes

Cells treated with different test formulations along with control cells were incubated at 37 °C for 24, 48 and 72 h in a CO_2 incubator. The cells were washed thrice with PBS immediately after their incubation period to remove the unattached cells and observed using inverted phase contrast microscope (CarlZeiss, Axiovert 25, Germany). To carry out FESEM analysis, the above incubated cells were fixed onto a glass slide by immersing it for 4 h into 2.5 % glutaraldehyde PBS solution. The samples were then subjected to stepwise dehydration by ethanol (25, 50, 75, 90 and 100 %) and subsequently visualized (Vashisth et al., 2015). For fluorescence microscopic analysis, working solution of AO:EtBr was prepared by dissolving 10 µl each of AO (5 mg/ml in 95% ethanol) and EtBr (3 mg/ml in absolute ethanol) in PBS (10 ml). After 24 h incubation in 5% CO_2 atmosphere at 37°C, both type of cells were rinsed thrice with PBS and stained with equivalent mixture of AO:EtBr (10 µl). The cells were then observed under fluorescence microscope (Carl Zeiss, Axiovert 25, Germany).

Quantification of apoptotic cells through flow-cytometry

Impact of FANPs on apoptotic cells was determined by staining the cells with annexin V-FITC (AV-FITC) and propidium iodide (PI) for flow cytometric evaluation. Cells treated with test formulations were seeded in 24 well plates containing their respective media and incubated upto a confluency level of 80%. After 24 h, cells were stained with AV-FITC and PI using the procedure indicated by manufacturer and analyzed via fluorescence activated cell sorter equipped with CellQuest^{TM} Pro software (FACS Calibur, BD Biosciences, San Jose, CA). The excitation (λ_{ex})/emission (λ_{em}) wavelength used for AV-FITC and PI were 488/520 nm and

540/630 respectively. Untreated cells were taken as negative control (AV^-/PI^-), cells undergoing early apoptosis could take only AV strain (AV^+/PI^-) while late apoptotic and necrotic population were stained by both dyes (AV^+/PI^+).

4.2.4. Cytocompatibility evaluation

Cytocompatibility of different test formulations was tested on HEK-293 cells using MTT assay. The morphological changes in cells were visualized through FESEM and fluorescence microscopy. FANPs at 20, 40 and 80, 120 and 200 µM dilutions (NP_1-NP_5) and native FA at equimolar conc. (FA_1-FA_5) were tested along with CSNPs following the procedure described in sections 4.2.2 and 4.2.3.

4.3. Results and Discussion

4.3.1. In vitro FA release analysis

Endurance of FA encapsulated in CSNPs was investigated by monitoring its drug-release profile over a period of 5 days (120 h) in physiological condition at varying pH (Figure 4.1). Initial 12 h accounted for a slow release of FA, wherein 21.4% (pH 7.4) and 26.8% (pH 5) of total sample was detected in dispersion medium. Release rate was slightly increased between 12 to 24 h and, at the end of 24 h, more than 50% of encapsulated FA had dissipate into the release medium (pH 5). During the subsequent time period a continuous and sustained release of FA was observed and by at the end of 120 h (5 days), about 78% of the total FA was measured in dispersion medium at pH 5. The dispersion of FA was faster at pH 5 than at pH 7.4 as the amino groups of CS get protonated at acidic pH that leads to swelling of polymeric matrix, aiding in its enhanced release (Jayakumar et al., 2007). Controlled release profile observed for FA may be attributed to the slow and controlled dissipation or diffusion of compound that was entrapped within CS polymeric structure.

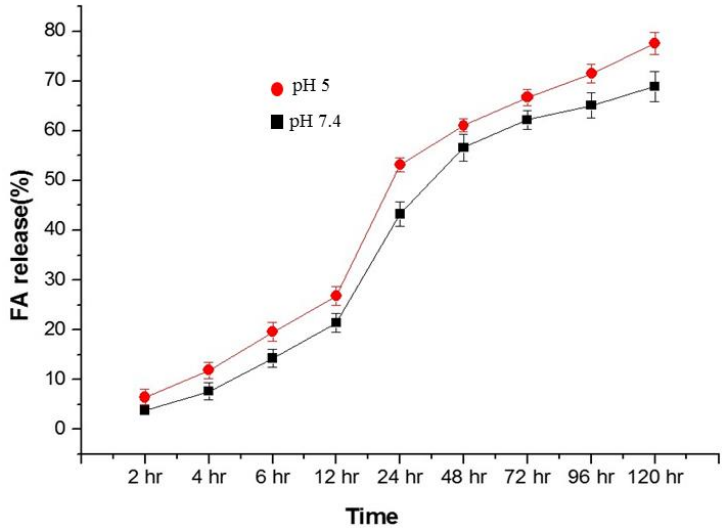

Figure 4.1: *In- vitro* release of FA from its nanoformulations over a period of 120 h in PBS at different pH values

4.3.2. Screening of FANPs effective conc.

The strong antioxidant character of FA is attributed to its unsaturated side chain and phenolic nucleus that spontaneously forms resonance stabilized structures, thus making it an effective antiproliferative agent. We hypothesized that FA encapsulated into CSNPs would show better anticancer/ antiproliferative activity *in-vitro*, pertaining to its controlled *in-vitro* drug release. In this context, FANPs prepared at different conc. were screened to testify their inhibition potential on ME-180 and PC-3 cancer cells. MTT assay revealed the cytotoxic effect of different FANPs conc. in terms of percentage decrease in metabolic activity of cells (Figure 4.2A and B). Variations in metabolic activity of a cell is a direct parameter indicating the changes occurring in its growth and proliferation. Phase contrast micrographs showing the effect of different conc. of FANPs on ME-180 and PC-3 cell lines are depicted in figure 4.3A-C and 4.4A-C respectively. The screening results indicated that 40 µM conc. of FANPs caused 54% inhibition of proliferation (IC_{50}) in ME-180 cervical cancer cell lines after 24 h. The similar degree of proliferation inhibition (52%) was achieved at an IC_{50} value of 80 µM for PC-3 prostate cancer cell lines after 48 h.

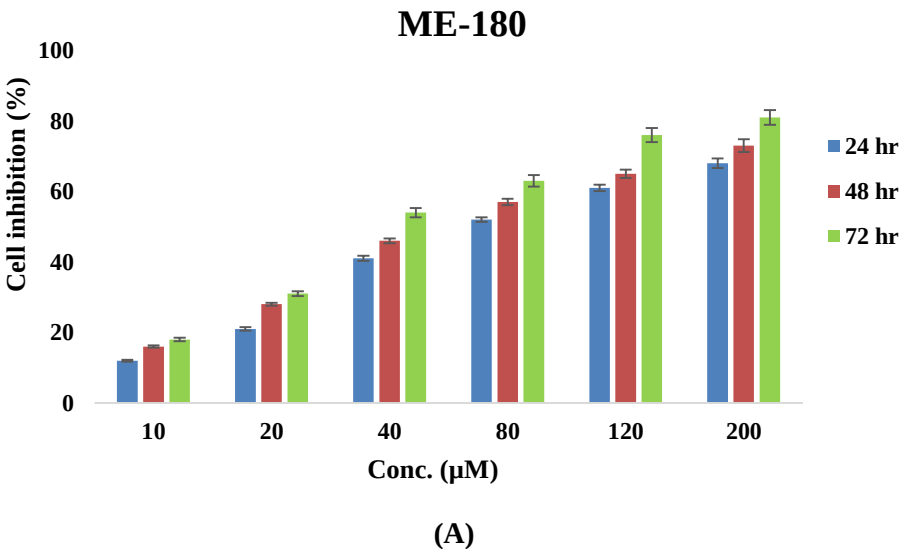

(A)

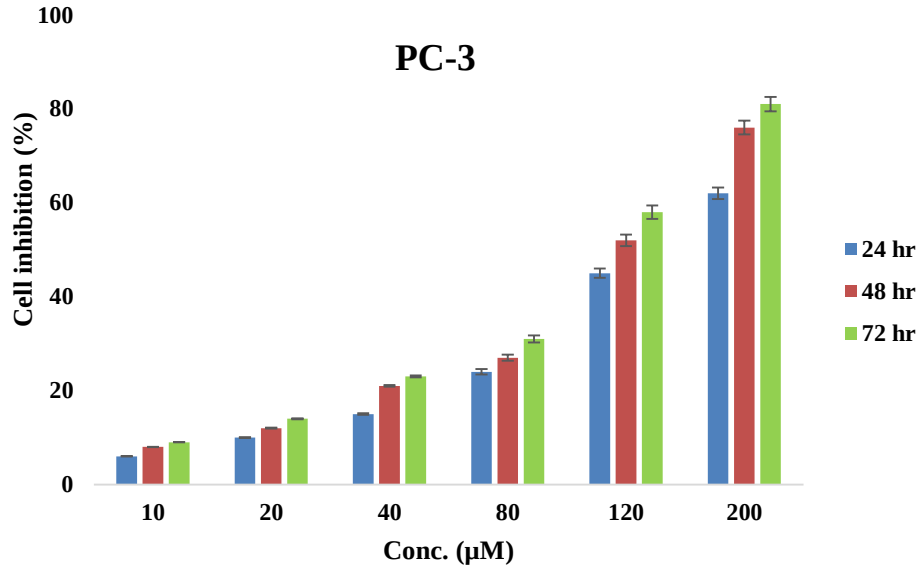

(B)

Figure 4.2: MTT metabolic activity assay for **A)** ME-180 **B)** PC-3 cells treated with different test formulations for 72 h. Error bars represent mean ± standard deviation for three independent experiments (n = 3)

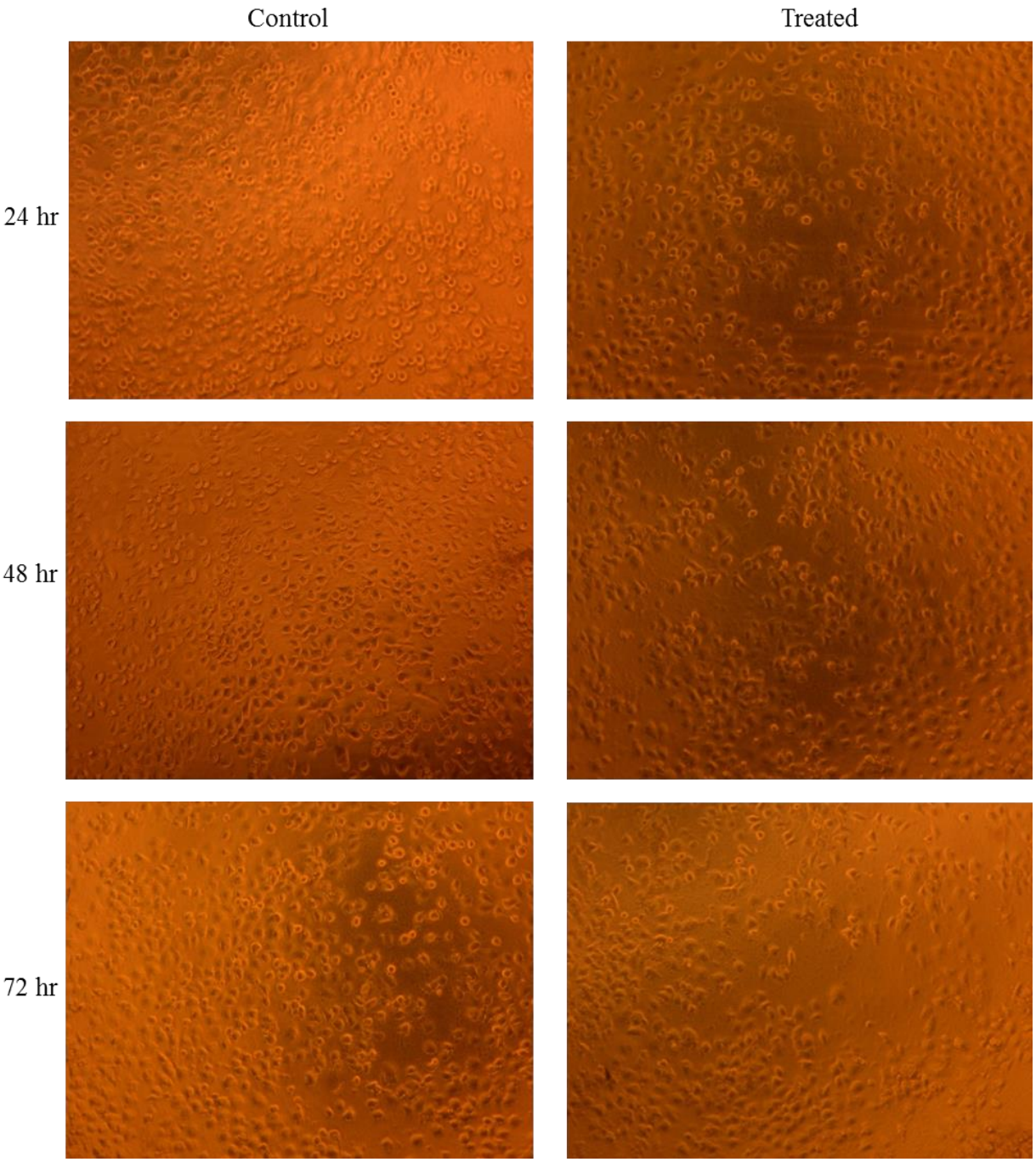

Figure 4.3 (A)

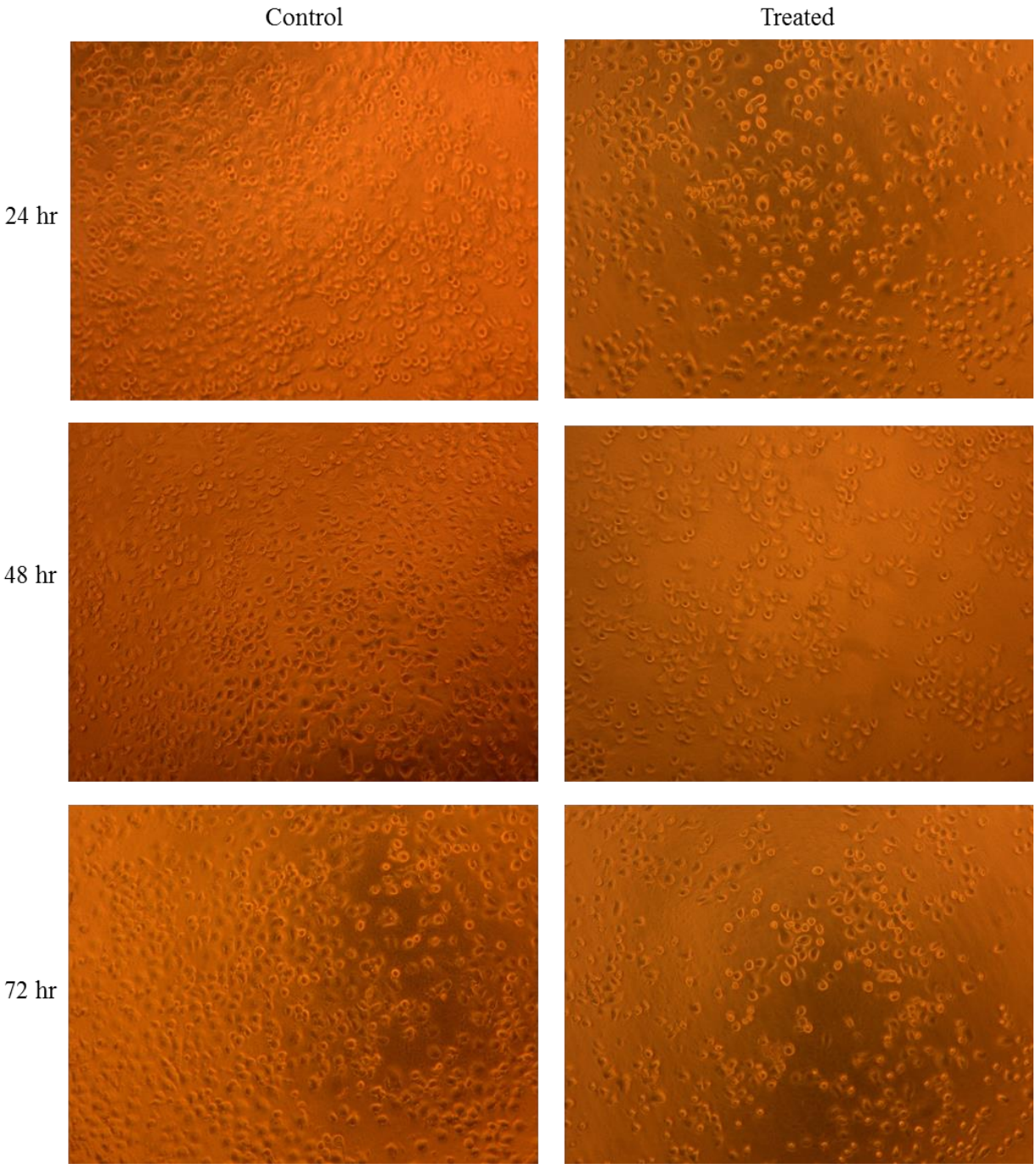

Figure 4.3 (B)

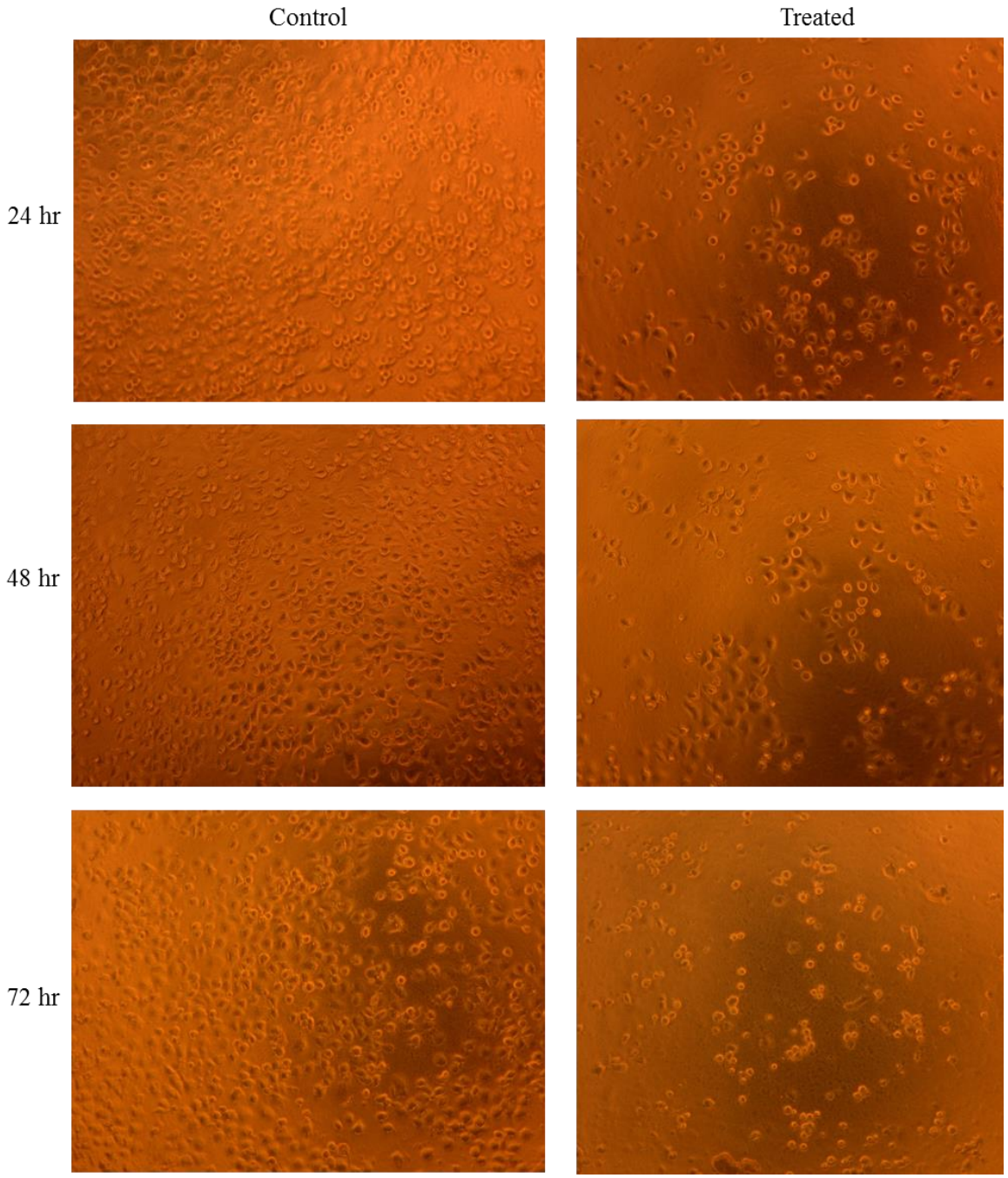

Figure 4.3 (C)

Figure 4.3: Phase contrast micrographs showing the effect FANPs on ME-180 cell lines **A)** 10 µM, **B)** 20 µM, **C)** 40 µM; (Scale bar 10 µm, microscopic magnification 50X)

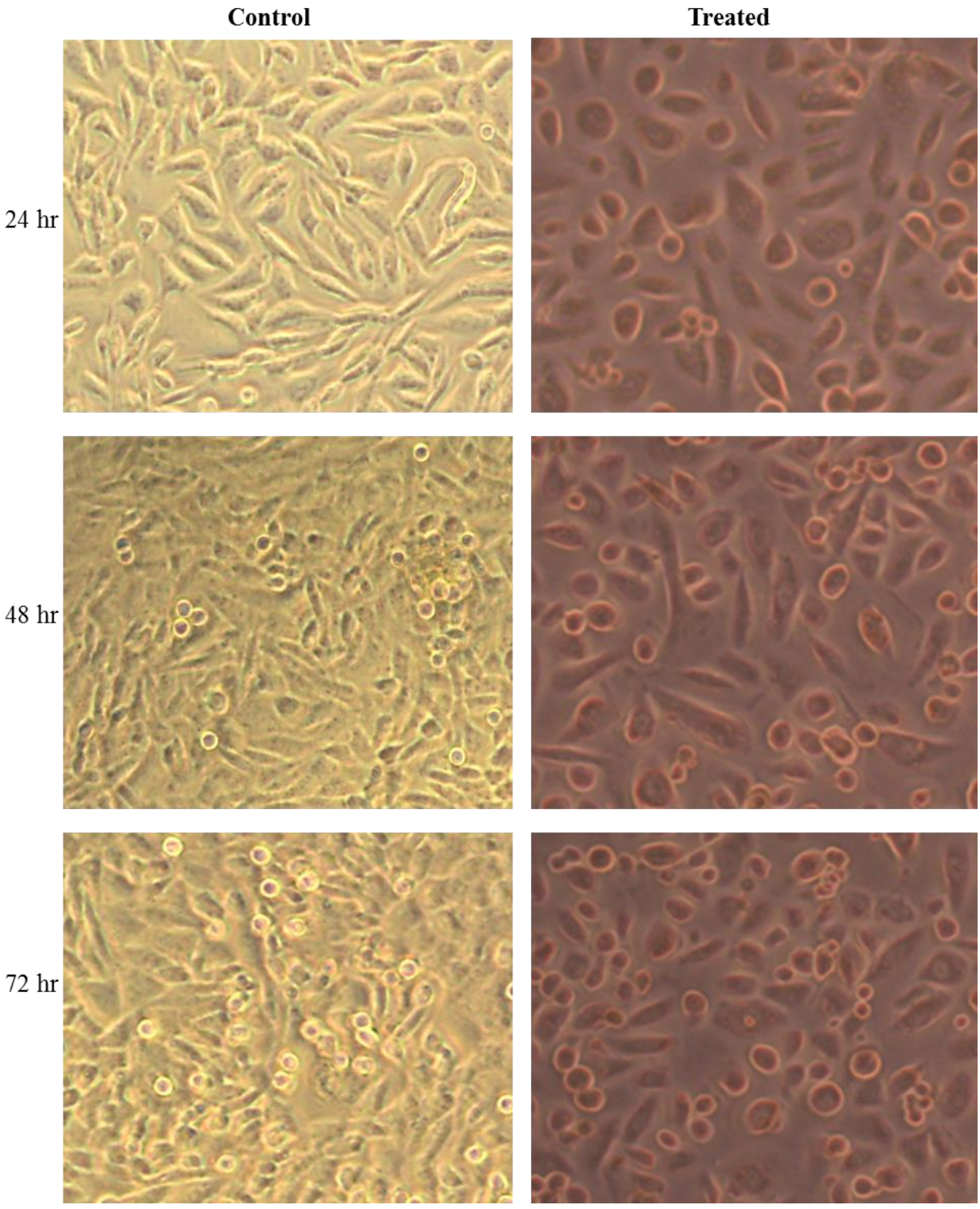

Figure 4.4 (A)

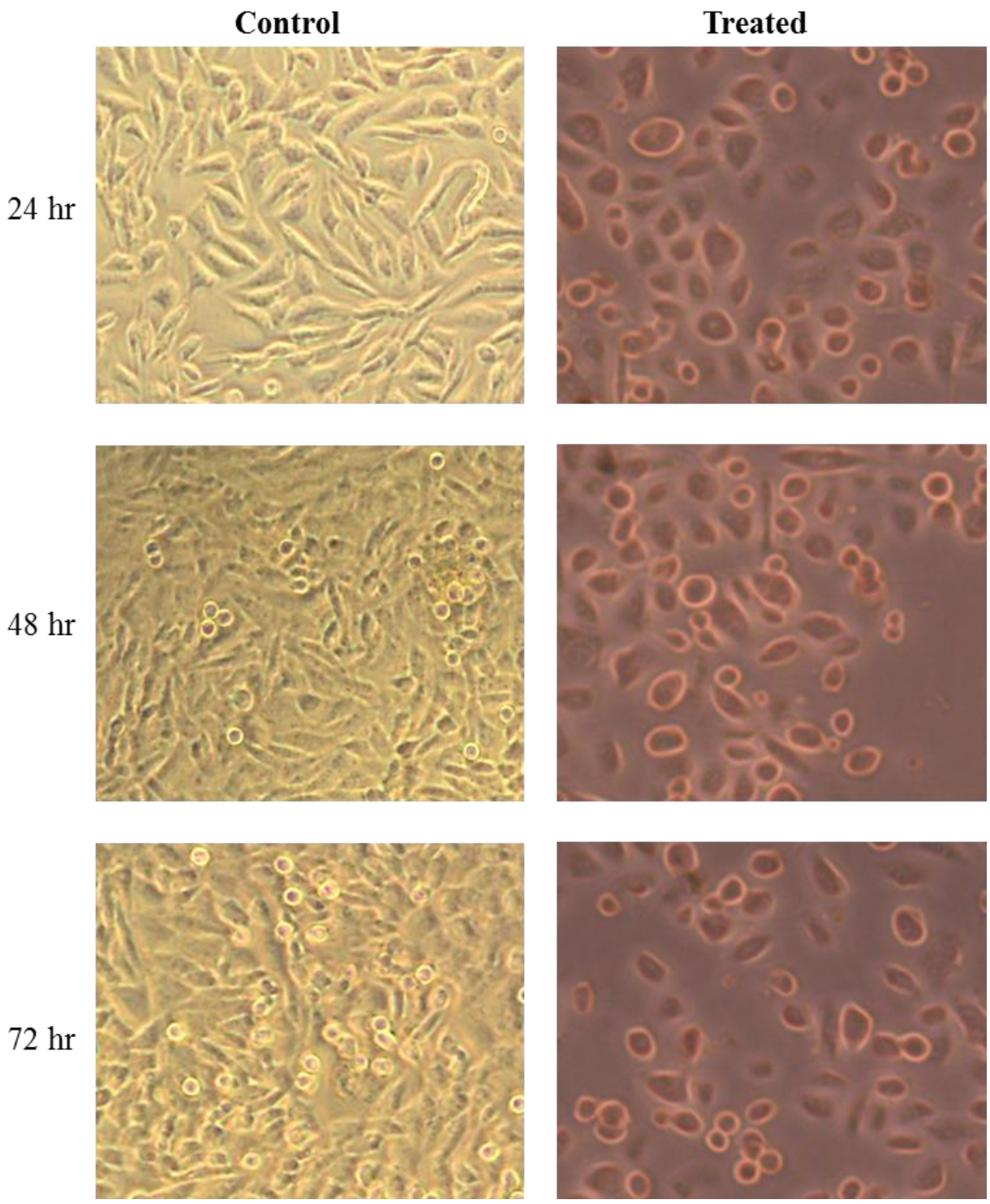

Figure 4.4 (B)

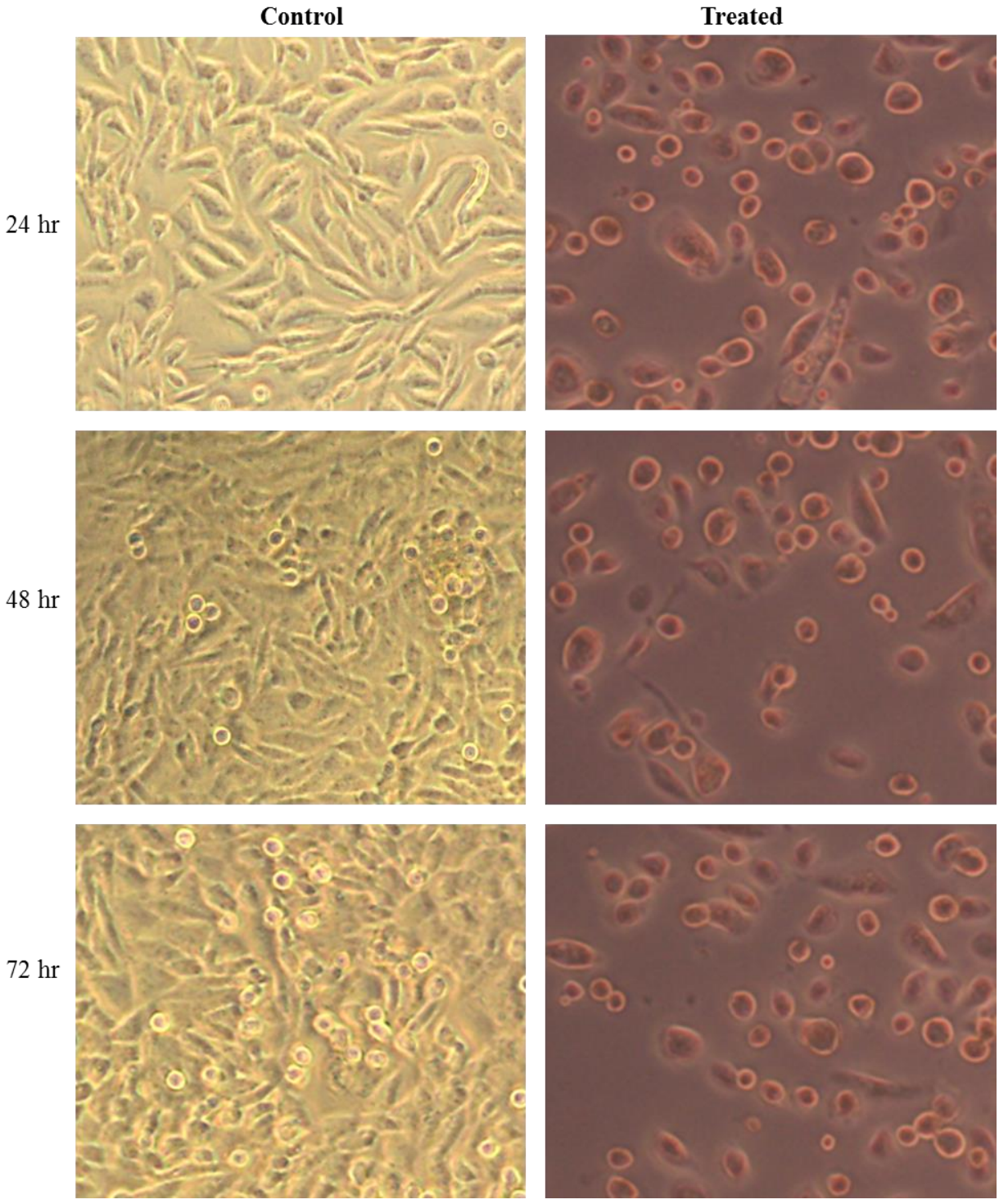

Figure 4.4 (C)

Figure 4.4: Phase contrast micrographs showing the effect FANPs on PC-3 cell lines **A)** 40 µM, **B)** 80 µM, **C)**120 µM; (Scale bar 10 µm, microscopic magnification 50X)

4.3.3. Cytotoxicity evaluation

FANPs at their respective IC_{50} with native FA at equimolar conc. and CSNPs were examine for their effect on cell metabolic activity and in turn, proliferation (Figure 4.5A and B). Data inferred that FANPs at conc. 40 µM (ME-180, 24 h) and 80 µM (PC-3, 48 h) caused maximum inhibition of cancer cells proliferation compared to native FA and CSNPs.

Previous studies on FA treated ME-180 cervical cancer cell lines have indicated an increased intracellular ROS levels along with inhibition of cell growth, increased lipid peroxidation and profound induction of cell apoptosis, in combination with gamma radiations (Subburayan et al., 2011). Eroğlu et al. (2015) have reported the cytotoxicity of FA in prostate cancer PC-3 cell lines with an IC_{50} dose of 300 µM after 48 h. Higher cytotoxicity of FANPs could be ascribed to the prolonged and controlled *in-vitro* release of FA from CSNPs. Literature reports that CSNPs, owing to their positive surface charges adsorbs with a high affinity onto the negatively charged tumor cell membranes, are internalized and bring about decrease in mitochondrial membrane proteins (Qi et al., 2005a).

CSNPs also displayed a high predisposition to accumulate at tumor sites and resulted in leakage of tumor vasculature (Nagpal et al., 2010). Zhou et al. (2007) reported the 27% inhibition of HeLa cervical cancer cell lines when treated with 500 mg/l chitosan nanoparticles (Zhou et al., 2007). In the present perspective, FANPs are believed to adhere to the tumor cell membrane via electron interactions, entering the cell through endocytosis and releasing the encapsulated FA slowly into the cytosol (Figure 4.6). As a result of increased bioavailability in cellular environment, FA exhibit its antitumor effect by influencing the mitochondrial activity and antioxidant status of the cell, disrupting the cell organelle which would eventually lead to cell death.

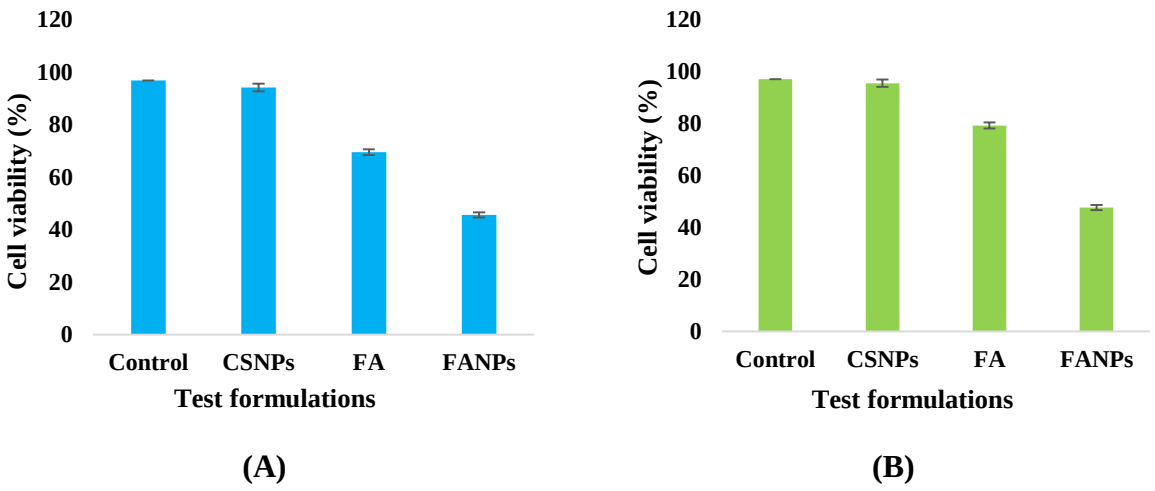

Figure 4.5: Graphs representing viability of cancer cells treated with different test formulation **A)** ME-180 **B)** PC-3

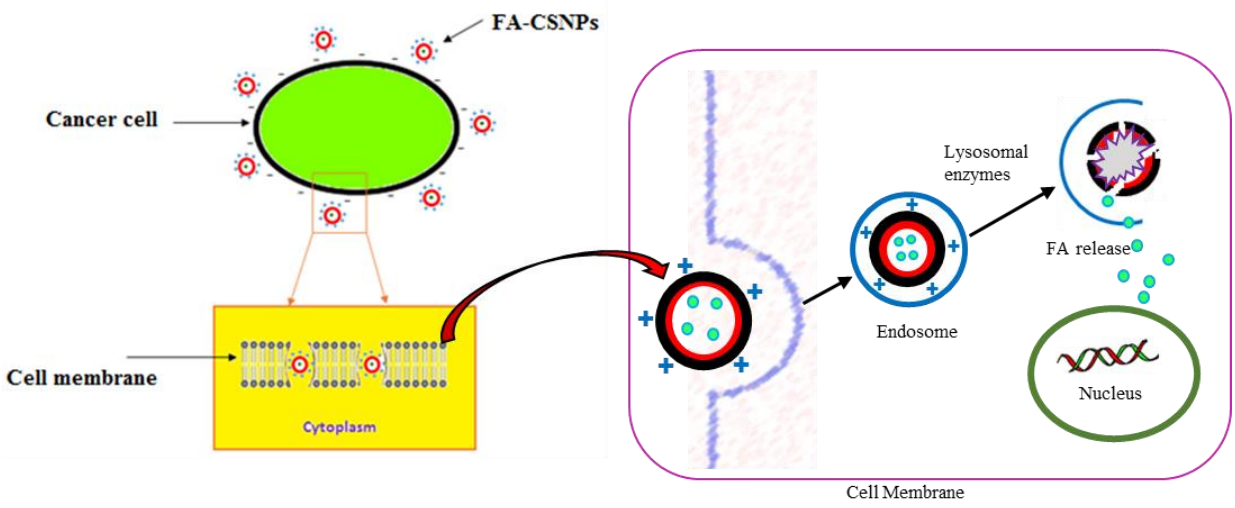

Figure 4.6: A possible mechanism of interaction of FANPs with tumor cells: FANPs might bind to the tumor cell membrane via electron interactions, entered the cell through endocytosis and release the encapsulated FA slowly into the cytosol

Apoptotic morphological changes

The morphological characteristics presented for ME-180 and PC-3 cell lines in figure 4.3C and 4.4C respectively displayed higher cell shrinkage, cytoplasmic condensation, and irregularity in shape upon treatment with FANPs at their corresponding IC_{50} values. The changes occurring in morphologies of cells treated with different formulations were visualized through FE-SEM and fluorescence microscopy.

Significant reduction in cancer cell number/growth was observed through FESEM micrographs in both cell lines when cultured on FANPs at their corresponding IC_{50} (Figure 4.7A and B). To further confirm the induction of apoptosis, formulation treated cells were visualized by fluorescence microscopy following treatment with 1:1 ratio of AO/EtBr, which allow differentiation of dead and viable cells by staining DNA (Figure 4.8 and 4.9). Cells with intact membranes fluoresce green due to AO staining while EtBr stains cells with damaged membranes which exhibit orange fluorescence due to DNA intercalation of both stains. Cells treated with CSNPs alone did not show any retardation of cell proliferation, with staining pattern analogous to control cells. On the other hand, considerable damage was shown in cells treated with native FA and FANPs for both cell lines. Morphological signs such as chromatin condensation and damaged wrinkled cells in the micrographs indicated FANPs induced apoptosis inhibiting the cancer cells. Earlier, literature reported the antitumor and antiproliferative nature of FA encapsulated in biocompatible polymers against different cell lines (Vashisth et al., 2105; Panwar et al., 2015). Researchers have also reported that CSNPs possess the capacity to induce cancer cells apoptosis in a dose-dependent manner, subsequently leading to cell death (Qi et al., 2005b). Our results suggested the role of CSNPs in guiding the encapsulated FA more precisely towards a physiological target hence complementing to generate stronger and more efficient antiproliferative action of FANPs as compared to native FA.

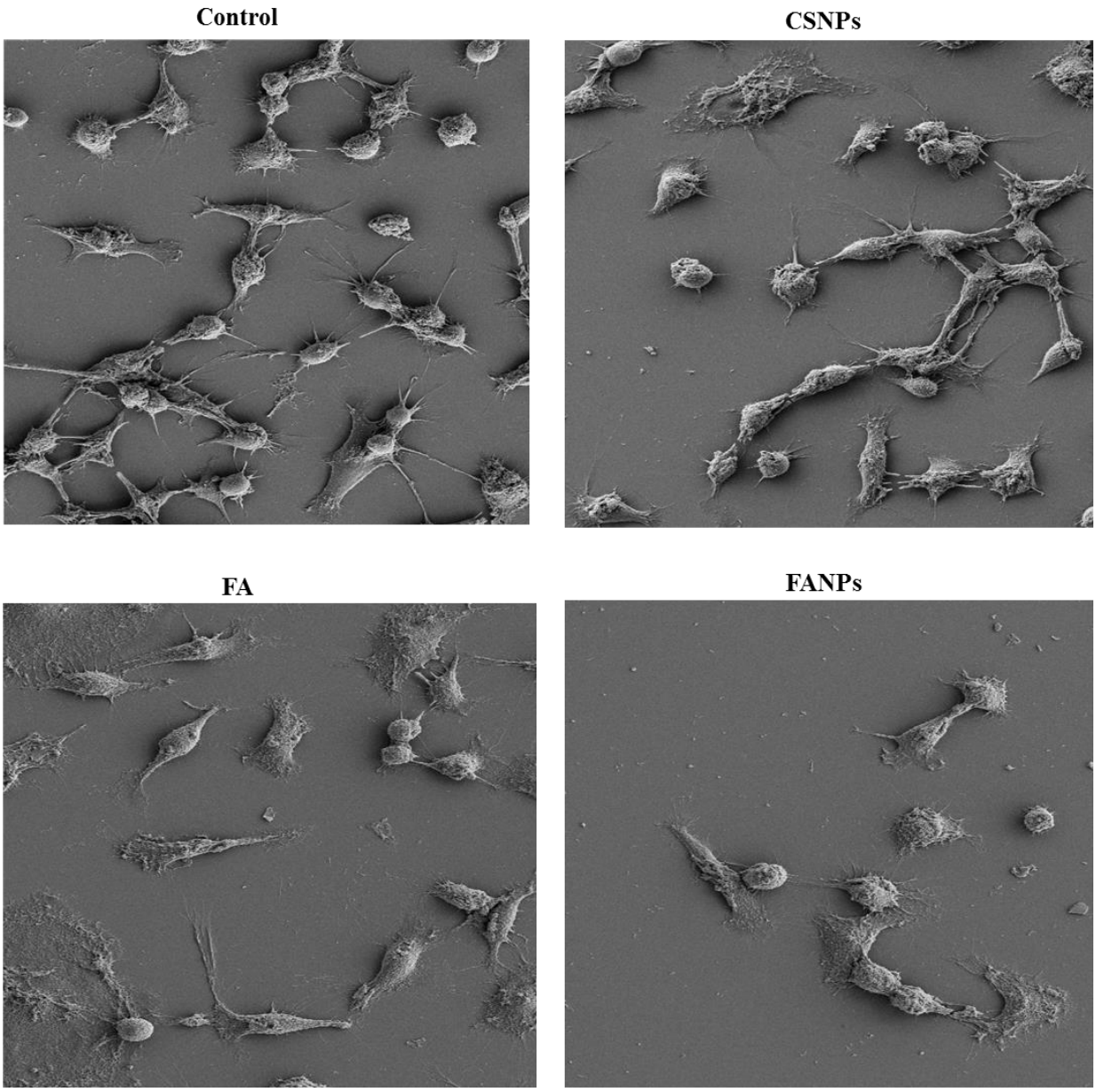

Figure 4.7 (A)

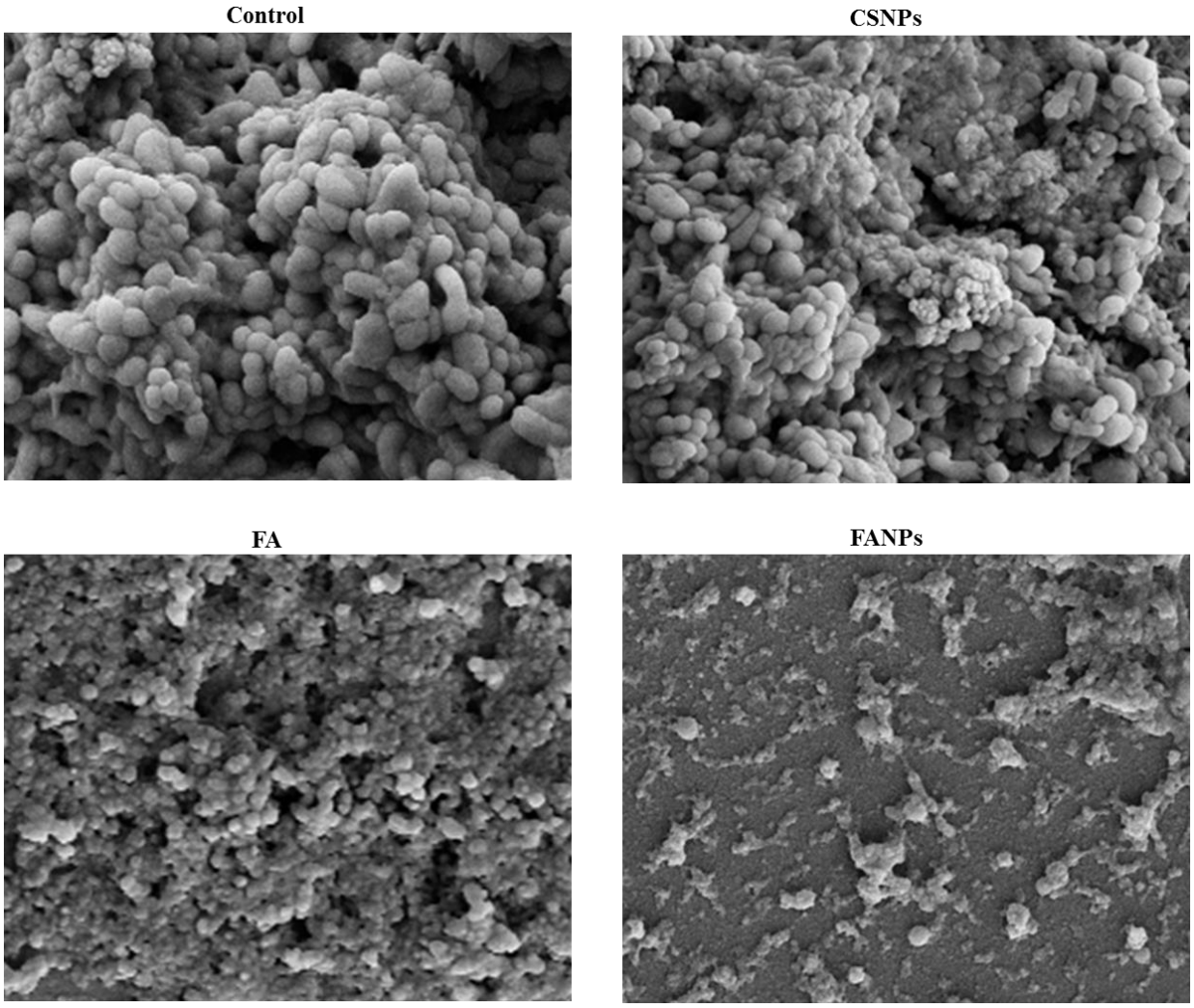

Figure 4.7 (B)

Figure 4.7: FE-SEM micrographs of cells cultured in presence of FANPs at corresponding IC50, showing reduction in cell numbers **A)** ME-180 cells **B)** PC-3 cells; (Scale bar 10 µm, microscopic magnification 10 KX)

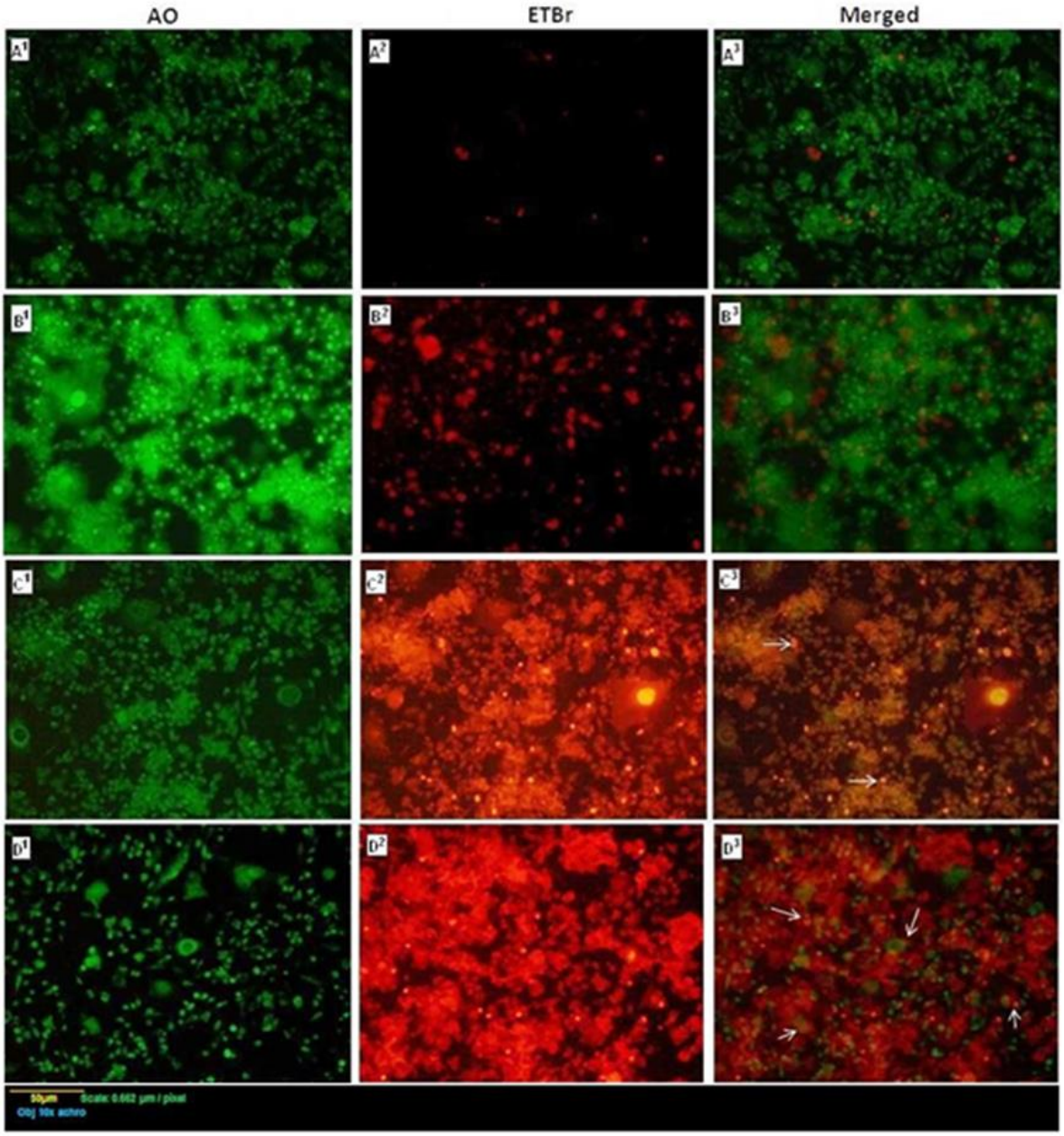

Figure 4.8: Fluorescent micrographs of AO:EtBr stained ME-180 cells treated with different test formulations **(A^1-A^3)** control cells, **(B^1-B^3)** CSNPs treated, **(C^1-C^3)** 40µM native FA treated and **(D^1-D^3)** 40µM FANPs treated cells after 24 h incubation. Morphological changes such as chromatin condensation and damaged wrinkled cells are marked with white arrows; (Microscopic magnification 100KX)

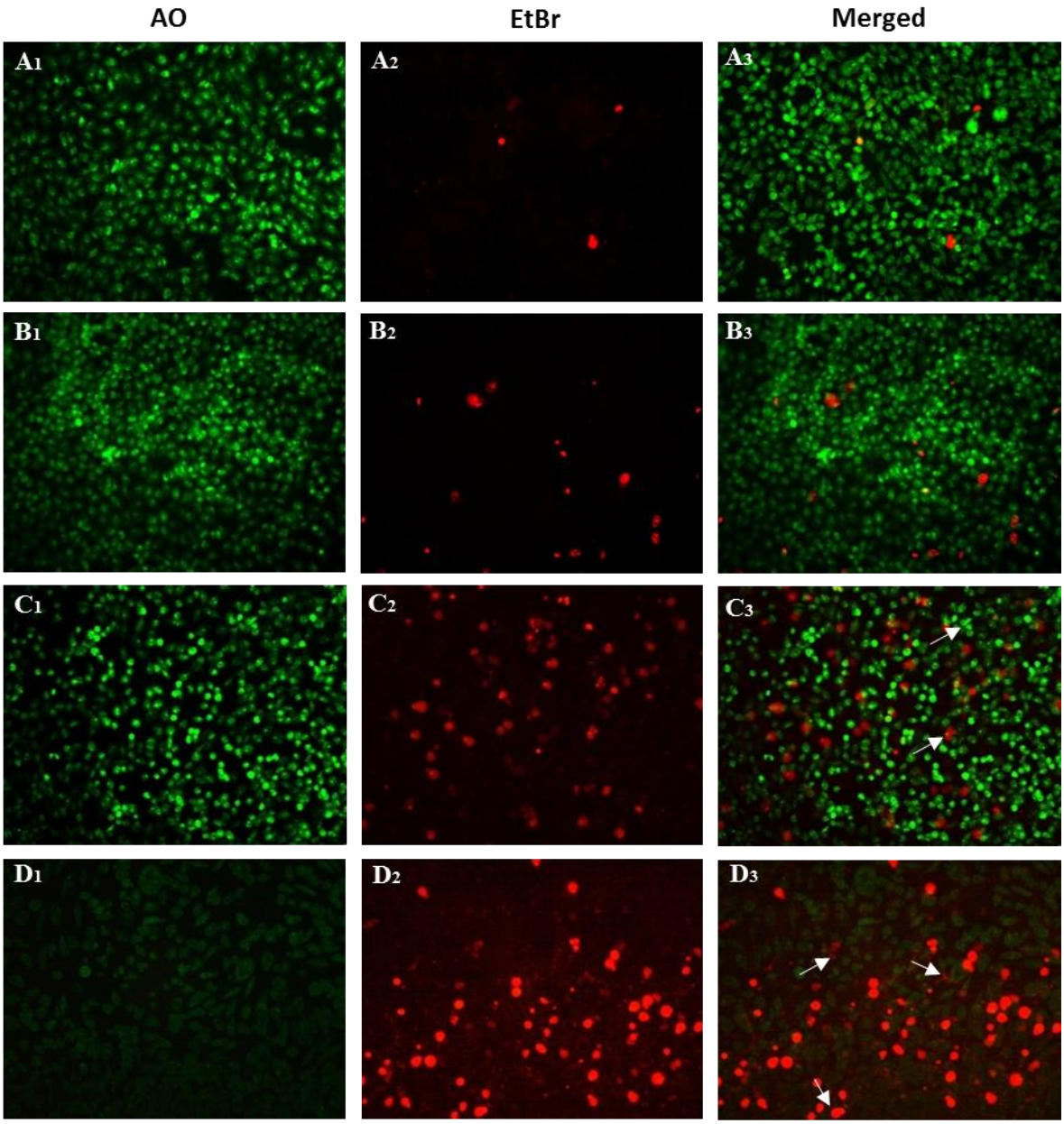

Figure 4.9: Fluorescent micrographs of AO:EtBr stained PC-3 cells treated with different test formulations **(A_1-A_3)** control cells **(B_1-B_3)** CSNPs treated **(C_1-C_3)** 80µM native FA **(D_1-D_3)** FANPs at 80µM conc. after 48 h incubation. Morphological changes such as chromatin condensation and damaged wrinkled cells are marked with white arrows; (Microscopic magnification 100KX)

Quantification of apoptosis

Formulation treated cancer cell lines were dual stained with AV-FITC/PI and subjected to fluorescence activated cell sorter analysis. AV binds to phosphatidylserine, a phospholipid of plasma membrane that generally extrude into the outer leaflet of membranes in cells undergoing apoptosis. This dye is usually conjugated to a fluorophore, which provide signal that are absent in healthy/control cells.

The graphs generated through flow cytometer represented normal healthy cells in quadrant 2, Q2; early apoptotic cells in quadrant 3, Q3; late apoptotic cells in quadrant 4, Q4; dead or necrotic cells in quadrant 1, Q1 (Figure 4.10 and 4.11). Highest population of late apoptotic (Q4) as well as necrotic cells (Q1) was observed for cells treated with FANPs in both cell lines. It is interesting to note that a large population underwent the transition from healthy to early apoptotic stage upon treatment with native FA in ME-180 (19.5%) and PC-3 (21.7%) cell lines. However, most of the necrotic/dead cells indicative of actual and irreversible cell death was noticed in population treated with FANPs in Q1 (Figure 4.10 and 4.11). For ME-180 cells, the percentage change in population density undergoing late apoptosis from untreated control (0.1%) to FANPs treated cells (61.7%) in Q4 was substantially higher in comparison of other formulations treated populations (Figure 4.10). Similar trend was noticed for PC-3 cell lines, where the apoptotic cell numbers were increased from 3% in control to 56.7% in FANPs treated cells (Figure 4.11). Results obtained for flow cytometric monitoring were in consistency with the findings of MTT assay and suggested that the reduction in viability of cancer cells was due to apoptosis. It could therefore be inferred that FANPs prepared under the given conditions and parameters possess a high anti-neoplastic capacity *in-vitro* and lead to inhibition of tumor cells.

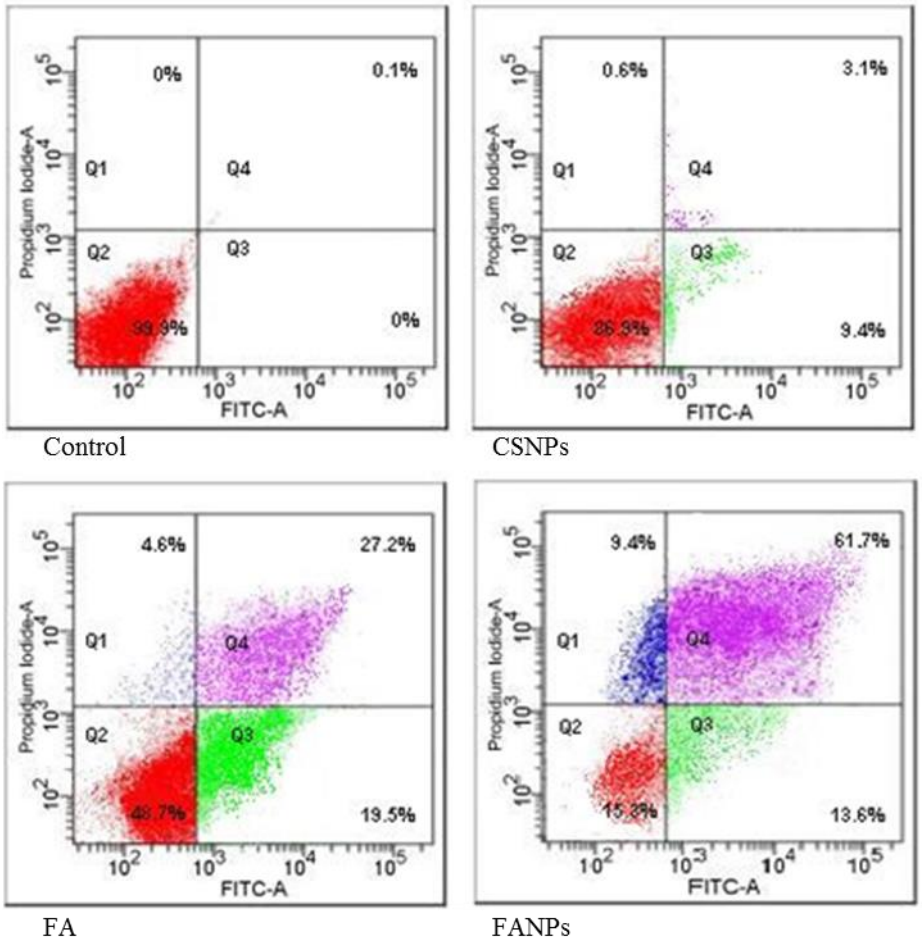

(A)

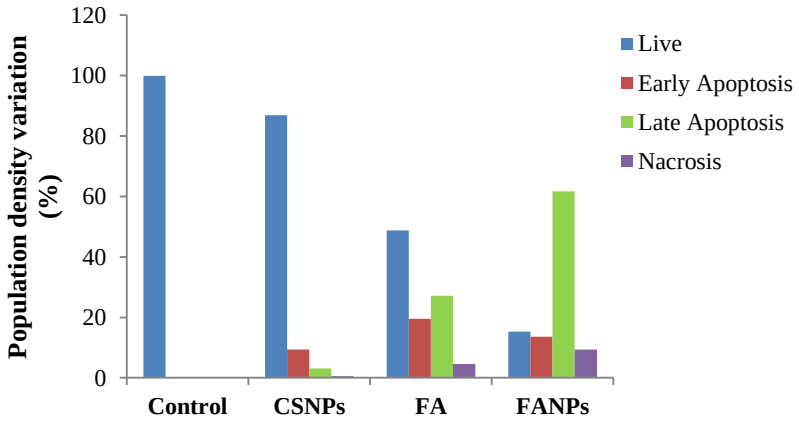

(B)

Figure 4.10: **A)** Flow-cytometric graphs showing induction and progression of apoptosis at varying stages for ME-180 cell lines treated with different formulations **B)** Graph showing percentage variations in cells density upon treatment with different formulations

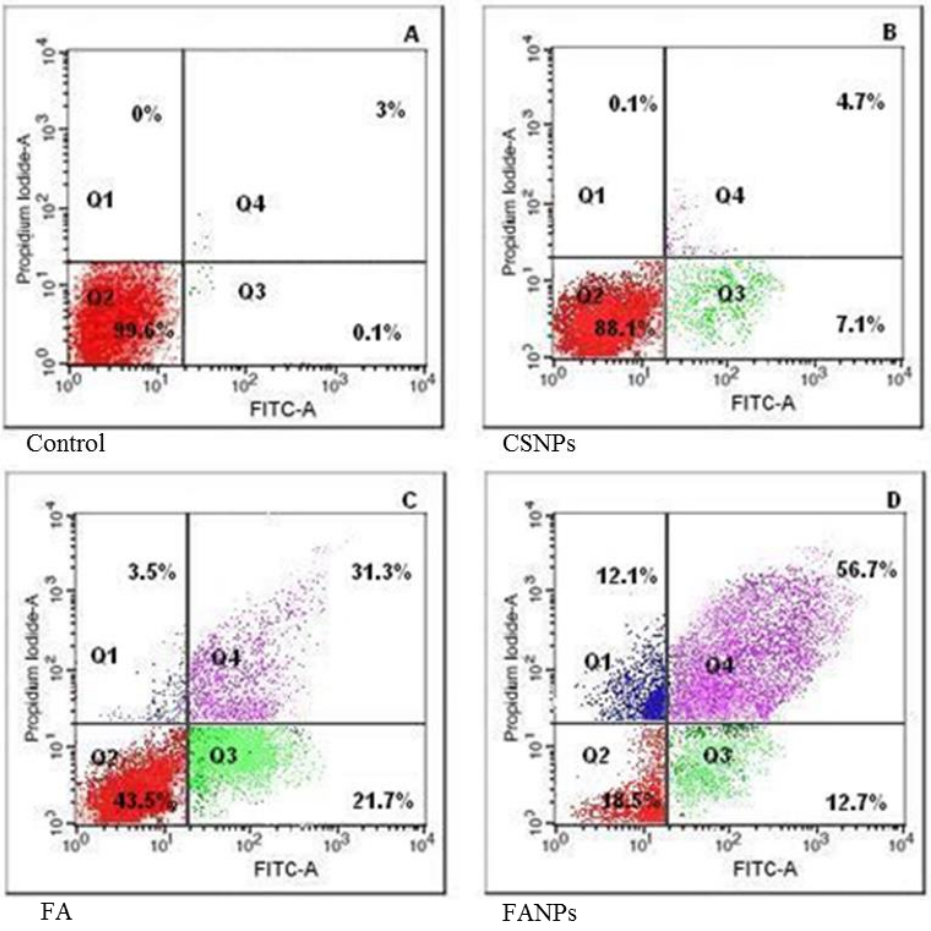

(A)

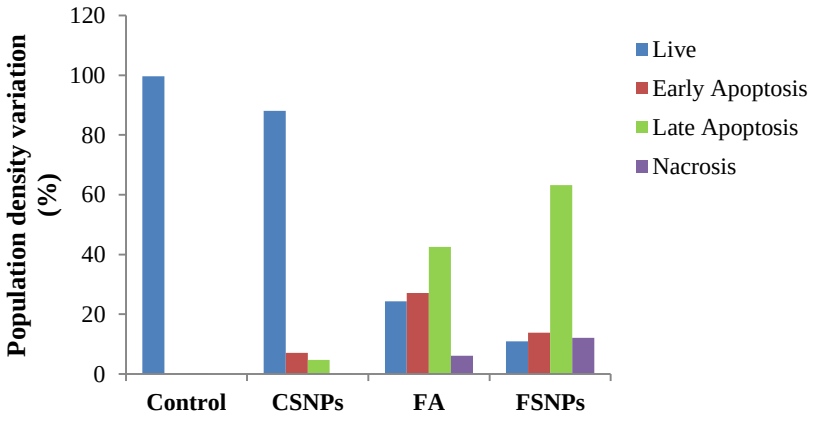

(B)

Figure 4.11: **A)** Flow-cytometric graphs showing induction and progression of apoptosis at varying stages for PC-3 cell lines treated with different formulations **B)** Graph showing percentage variations in cells density upon treatment with different formulations

4.3.4. Cytocompatibility evaluation

Cell viability and FESEM analysis

Cytocompatibility of different test formulations on HEK-293 cell lines was evaluated using MTT assay (Figure. 4.12). Cell viability graph indicated that HEK cells were negligibly affected upon treatment with CSNPs, NP_1, NP_2, and NP_3 compared to control cell ($p<0.05$). However, the viability of cells treated with NP_4 and NP_5 were reduced upto 72.83% and 70.05% respectively. Interestingly, native FA at conc. of FA_4 and FA_5 also reduced HEK cells viability upto 39.54% and 31.42% respectively.

FA is a potent antioxidant with free radical scavenging activity, though at higher conc. it can also act as a prooxidant generating reactive oxygen and reactive nitrogen species to oxidative damage of cellular components (Galati and O'Brien, 2004; Heim et al., 2002). Substantial reduction in metabolic activity of HEK-293 cells at higher conc. (FA_2-FA_5) of native FA could be due to the response of cells towards these ROS and RNS while CSNPs were found to be highly cytocompatible, similar to those reported earlier (Qi et al., 2004). Changes in morphology of HEK-293 cells in presence of different formulations were visualized by FESEM (Figure. 4.13). In comparison to control HEK-293 cells, the morphology remain unaltered in NP_2 treated cells (Figure. 4.13A and B), whereas certain changes in cellular morphology could be visualized upon treatment with NP_5 (Figure. 4.13C). Noticeable morphological alterations proportional with increasing FA conc. were recorded in the cells treated with native FA (Figure. 4.13D-F). At FA_1, cells with distorted morphology were visualized (Figure. 4.13D), with further damage to structural integrity by FA_2 (Figure. 4.13E) followed by complete damage of cells when treated with FA_5 (Figure. 4.13F). This sequence of events could partially be attributed to prooxidant nature of FA which at higher conc. interacts with transition metal ions found in biological systems and lead to oxidative damage of normal cellular components (Maurya and Devasagayam, 2010; Heim et al., 2002).

There are literature studies reporting phenolic compound acting indiscriminately towards diseased as well as healthy cells following their systemic administration and causing undesirable side effects (Park et al., 2010). Nanoencapsulation of these compounds in polymers such as CS allow them to accumulate passively at the specific target sites and thereby preventing the normal tissue from deleterious effects.

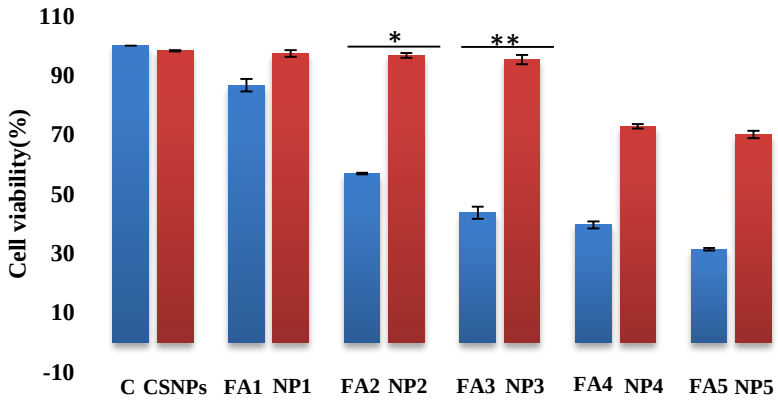

Figure 4.12: Cytocompatibility evaluation of test formulations on HEK-293 cell lines after 24 h incubation by MTT assay. Error bars represent mean ± standard deviation for three independent experiments (n = 3); *p< 0.02; **p< 0.05

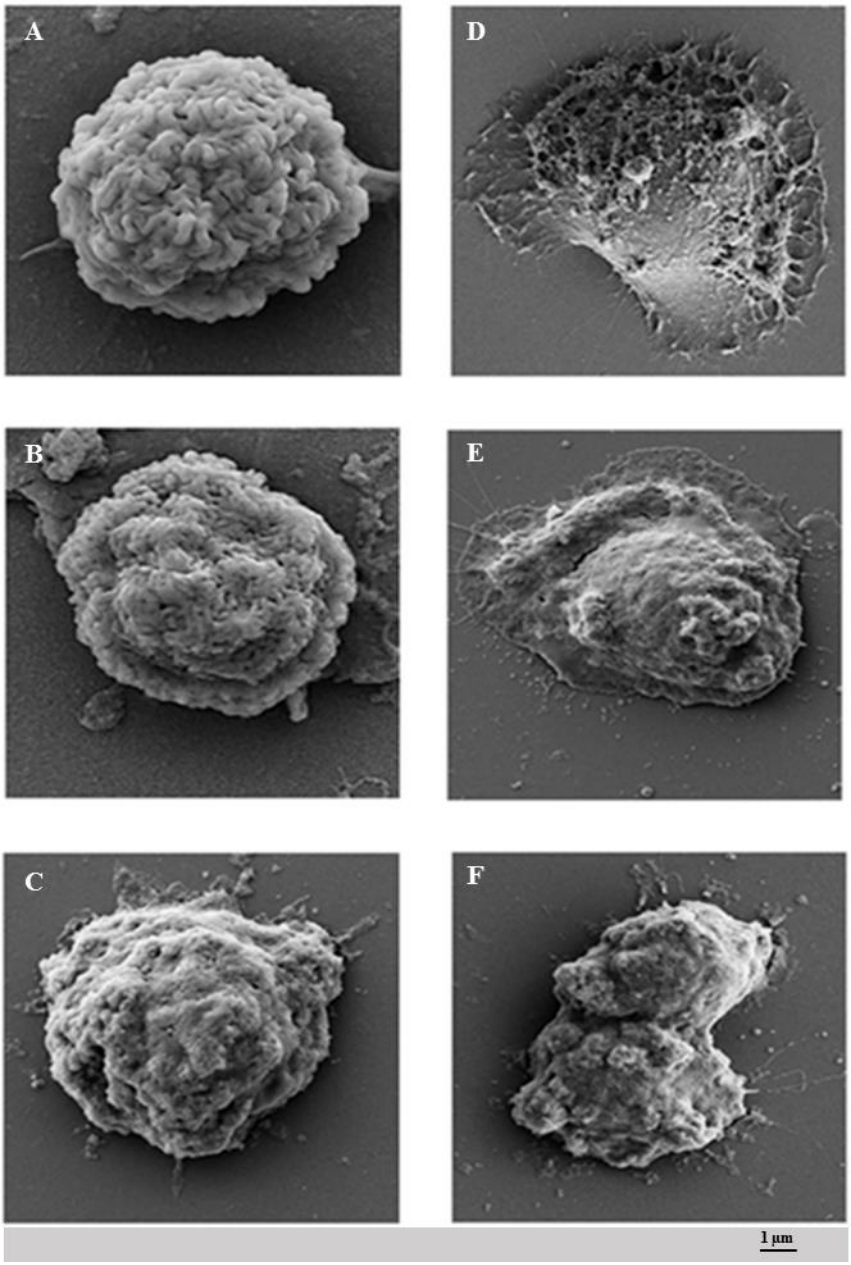

Figure 4.13: Scanning electron micrograph of HEK-293 cell lines. **A)** untreated control cells, **B)** cells treated with NF_2, **C)** cells treated with NF5, **D)** cells treated with FA_1, **E)** cells treated with FA_2, **F)** cells treated with FA_5; (Scale bar 1µm, Magnification 50KX)

Cell death analysis by fluorescence microscopy

Differentiation of dead and viable HEK-293 cells was done by staining them with AO:EtBr 1:1 mixture for fluorescence microscopic evaluation (Figure 4.14). Negligible growth inhibition was noticed for cells treated with NP_2 and NP_3 compared to control cells (Figure 4.14A3, B3, and C3), while maximum reduction was observed with NP_5 nanoformulation. As evident, data

obtained by fluorescence microscopy complies with the observations of MTT assay as well as FESEM analysis. Results validated that under given experimental parameters, FANPs upto to a conc. 80 µM showed maximum cytocompatibility among the tested formulations.

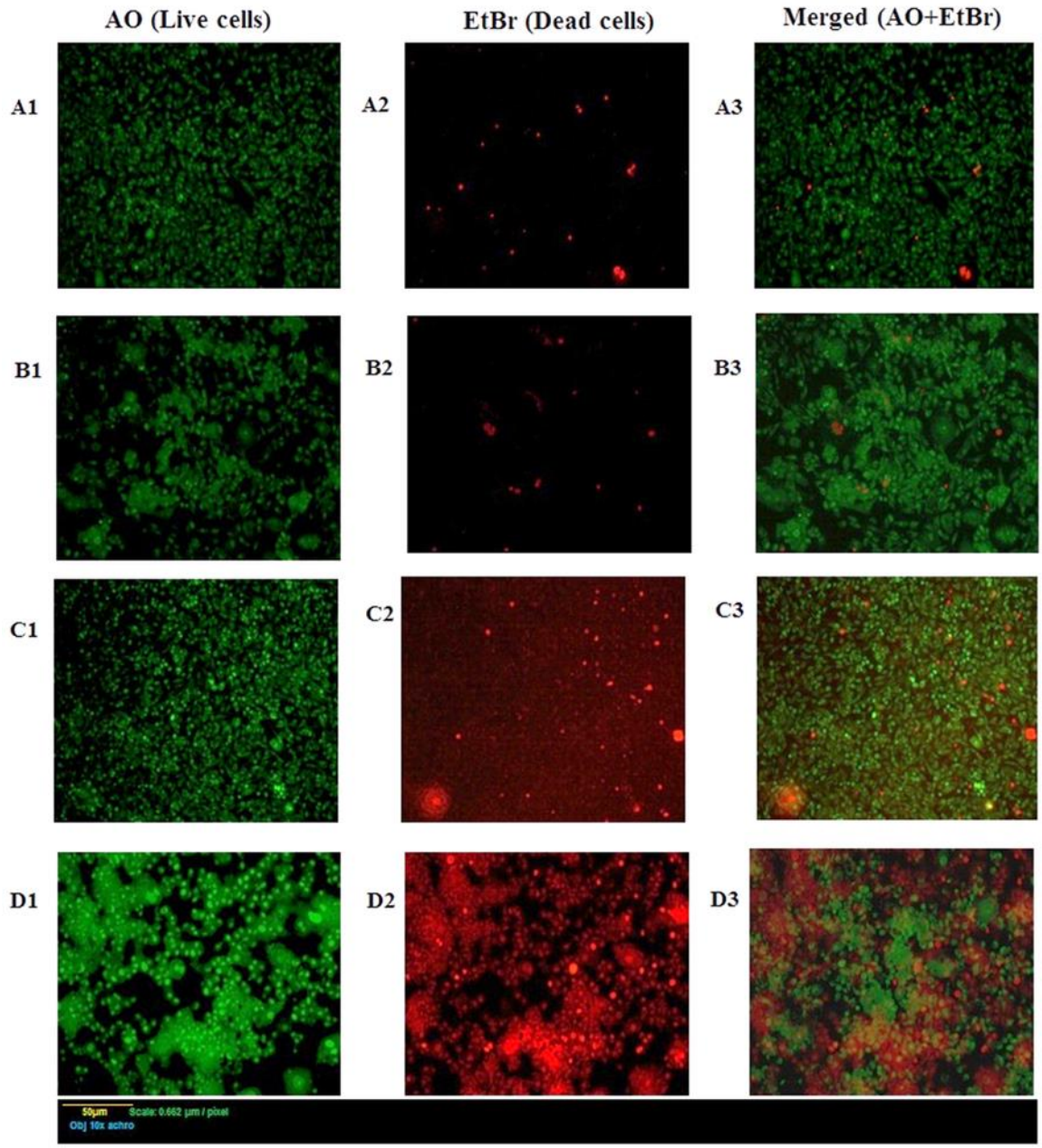

Figure 4.14: Fluorescent micrographs of AO:EtBr stained HEK-293 cells. **A1-A3)** control cells, **B1-B3**) cells treated with NF_2, **C1-C3**) cells treated with NF_3, **D1-D3**) cells treated with NF_5 after 24 h incubation; (Scale bar 50µm, Magnification 10KX)

4.4. Conclusion

In the present study, cytotoxicity evaluation of FANPs established them as strong antiproliferative agents against ME-180 human cervical and PC-3 human prostate cancer cell lines. Reduction in cell population density was tested through monitoring the changes in metabolic activity of cells treated with different formulations and further validated by quantification of apoptosis through flow cytometry. The morphological changes taking place in cancer cells were visualized using FE-SEM and fluorescence microscopies. Finally, FANPs were also found to be cytocompatible with HEK-293 cell lines upto a conc. of 80 µM. The results suggested that encapsulation of FA into CSNPs may enhance its anticancer potential against ME-180 and PC-3 cell lines without any potential toxicity to normal healthy cells, thereby presenting it as a potent therapeutic agent for medicine and clinical usage.

Chapter 5

FANPs as Potent Antibiofilm Agents

5.1. Introduction

Candida species are one of leading causes of hospital acquired systemic infections, displaying striking ability to form drug-resistant biofilms on surgical implants such as an intravascular or urinary catheter, prosthetic heart valves, cardiac pacemakers and joint replacements (Kojic and Darouiche, 2004; Lane and Matthay, 2002). Biofilms are microbial communities that are often embedded in a matrix of slimy extracellular polymers. They are significantly less susceptible to antifungal drugs, becoming the foremost cause of virulence associated with *Candida* species (Flemming and Wingender, 2010).

Within entire *Candida* genus, *Candida albicans* is the major multidrug tolerant species, causing life-threatening infections among immunocompromised individuals and patients relying on various kinds of implants and cytotoxic chemotherapies (Ortega et al., 2011; LaFleur et al., 2006; Kumamoto et al., 2002). *C. albicans* represents second highest colonization-to-infection rate with overall highest crude mortality and its virulence in large, could be attributed to its ability to propagate in more than one morphological form (Kumamoto and Vinces, 2005; Crump and Collignon, 2000). *C. albicans* biofilms are reported to be 4000 times more resistant to antifungal drug fluconazole when compared to planktonic or free-floating counterparts (Ramage et al., 2001). As a result, biofilm community survives, disseminating candidemia and lead to device removal in some cases (Zhang and Camp, 2007; Kojic and Darouiche, 2004). Hence, there is an urgent need to search alternatives to the conventional drugs so as to combat *C. albicans* biofilms.

Natural biological molecules are currently being evaluated for their antibiofilm activities so as to develop alternative preventive or therapeutic rationale (Pauli, 2006). One such alternative is provided by plant derived polyphenols which interacts with nucleophilic groups present in *Candida* cell membrane and causes its disruption (Pauli, 2006). Among other phenolic compounds, FA and its derivatives have been screened recently for their antibiofilm potential against *C. albicans* (Alavarce et al., 2015; Raut et al., 2014). As compared to conventional synthetic antifungal drugs that have become unyielding towards the biofilm matrix, there is a

less likelihood of the development of resistance by biofilm cells against naturally occurring FA (Ramage et al., 2005). However, as discussed previously, applicability of FA is limited owing to its low permeability, instability and bioavailability which could be circumvented by FA nano-encapsulation into CSNPs. Earlier, studies have also reported the antifungal activity of CSNPs against *C. albicans* (Wimardani et al., 2012; Ing et al., 2012). CS based zinc oxide nanoformulations have been synthesized and evaluated for antimicrobial and antibiofilm potential against various microbial strains including *C. albicans* (Dhillon et al., 2014). In the present study, it was hypothesized that FANPs could easily penetrate the biofilm cells and matrix owing to their high surface area to volume ratio and disrupt or alter the permeability of fungal cell plasma membrane, as well as reduce the cell population.

5.2. Material and methods

XTT (2,3,-bis(2-methoxy-4-nitro-5-sulfophenyl)-5-((phenylamino)-carbonyl)-2H-tetrazolium salt), RPMI 1640 medium, gluteraldehyde, yeast peptone dextrose (YPD) and other standard analytical chemicals/reagents were purchased from Himedia (Himedia, India).

Preparation of test formulations

FANPs at conc. 20 (NF_1), 40 (NF_2) and 80 µM (NF_3), native FA at equimolar conc. (FA_1, FA_2 FA_3) and CSNPs were used as test formulations to assess their efficiency against *C. albicans* biofilm cells. All test formulations were prepared according to procedure as described in (section 2.2.2).

Effect of formulations on *C. albicans* biofilm formation

Strain and biofilm growth conditions

The *C. albicans* MTCC 227 culture broth grown for 24 h on YPD broth medium (37°C) was centrifuged at 5000g (4°C) for 15 min (Singh et al., 2013). The pellet was washed twice with sterile PBS (pH 7.2) and diluted to standard suspension of 1×10^7 cells ml^{-1} in RPMI 1640-MOPS medium. *C. albicans* biofilms assay was performed using sterile, polystyrene 96-well microtitre plates (MTP). Standard suspension of *C. albicans* in RPMI 1640-MOPS medium was added to wells and incubated at 37°C for 90 min (adhesion phase). The wells were then washed with sterilized PBS to remove unbound cells and RPMI 1640-MOPS medium was added. Different test formulations were added to the MTP wells, incubated at 37°C for 24 h and the effect of test formulations on biofilm formation was quantified by using the XTT assay.

XTT assay

In this assay, the measurement of metabolic activity of *C. albicans* cells was based on the reduction of XTT to formazan product by mitochondrial dehydrogenase of active cells in the presence of menadione, an electron-coupling agent (Roehm et al., 1991). After 24 h of incubation, medium was aspirated from each well and rinsed twice with sterile PBS. XTT (1 mg/ml in PBS) -menadione (0.4 mM in acetone) solution was then added to each well and incubated at 37°C for 2 h in dark. The absorbance of XTT formazan product was measured at 492 nm using a microplate reader (Spectra Max M2). Percentage cells viability of *C. albicans* was calculated by the equation given below:

Cell viability (%) = OD_{492nm}(test samples) / OD_{492nm}(control)×100

FE-SEM analysis

Effect of nanoformulations on *C. albicans* morphology and biofilm structural integrity in comparison to control was visualized by FE-SEM analysis. After 24 h of incubation in presence of nanoformulations, *C. albicans* biofilm cells were fixed onto a glass slide with 2.5 % (v/v) glutaraldehyde in sterile PBS for 2 h at room temperature. The samples were then washed, dehydrated stepwise with ethanol (30, 50, 70, 90 and 100 %) and dried to critical point by a Polaron critical point drier. Subsequently, glass slide were sputter coated with gold and imaged.

Statistical analysis

All experiments were carried out in triplicate and the results represented are mean value ± Standard deviation of individual experiment. Significant difference between the mean values of different data sets was obtained by performing t-test and the $p<0.05$ was considered statistically significant value.

5.3. Results and discussion

Effect of FA-CSNPs on C. albicans biofilm formation

XTT assay

The choice of FANPs conc. was based upon their impact on non-cancerous HEK-293 cell lines (section 4.2.4). A possible mechanism through which FANPs owing to their positive surface charges (zeta potential) would bind to and penetrate the negatively charged *C. albicans* cell

membranes is represented in Figure 5.1. It was believed that this binding would lead to an increase in permeability of plasma membrane and leakage of intracellular constituents followed by fungal cell death. Similar mechanisms were reported for CS mediated damage of bacterial cell membrane (Liu et al., 2004).

The metabolic activity of *C. albicans* sessile cells treated with different test formulations was measured using XTT assay (Figure 5.2). CSNPs and NF_1 displayed 11.2% and 27.5% reduction in metabolic activity of *C. albicans* biofilm cells respectively ($p<0.0002$). Native FA and FANPs reduced the metabolic activity (%) in a dose-dependent manner but the decline was higher for FANPs. Each of the three nanoformulations (NF_1-NF_3) displayed antibiofilm activity, however, NF_3 reduced the metabolic activity significantly up to 21.4% thus inhibited biofilm formation ($p < 0.00001$). Fluconazole (0.625 µg/ml - 512 µg/ml) taken as positive control was ineffective in biofilm growth inhibition upto the conc. of 128 µg/ml. Modulations in population density of *C. albicans* biofilm cells treated with test formulations were observed using FESEM (Figure 5.3- Figure 5.7).

The exact mechanism of antibiofilm effect of FANPs is yet to be decipher. CSNPs have reported to interact effectively with negatively charged plasma membrane of fungal cells owing to their small and compact particle size as well as high surface charges (Tan et al., 2013; Qi et al., 2004). It has been proposed earlier that the exopolymeric matrix of candida biofilm may protect it from the effects of antifungal agents (Kumamoto and Vinces, 2005). Upon entering the fungal plasma membrane, FANPs could either inhibit *C. albicans* biofilm formation or destroy its structural integrity. Alternatively, CS would bind to the trace elements and make the essential nutrients unavailable inhibiting the normal fungal growth (Roller and Covill, 1999).

The inhibition of oxidative phosphorylation and respiratory chain functions in *C. albicans* upon treatment with FA may be attributed to the presence of resonating phenolic hydroxyl radical in FA structure (Pauli, 2006). A recent study illustrated that FA inhibited drug resistant *C. albicans* biofilm growth through degradation of cell membrane and disruption of biofilm cellular network at FA conc. greater than 4 mg/ml (Raut et al., 2014), while in our investigation FANPs (at NF_3) displayed substantial reduction in *C. albicans* cell density at a much lower conc. The antibiofilm potential of FANPs may be attributed to the synergistic effects of FA and CSNPs which offered compact particle size and enhanced surface area to volume ratio.

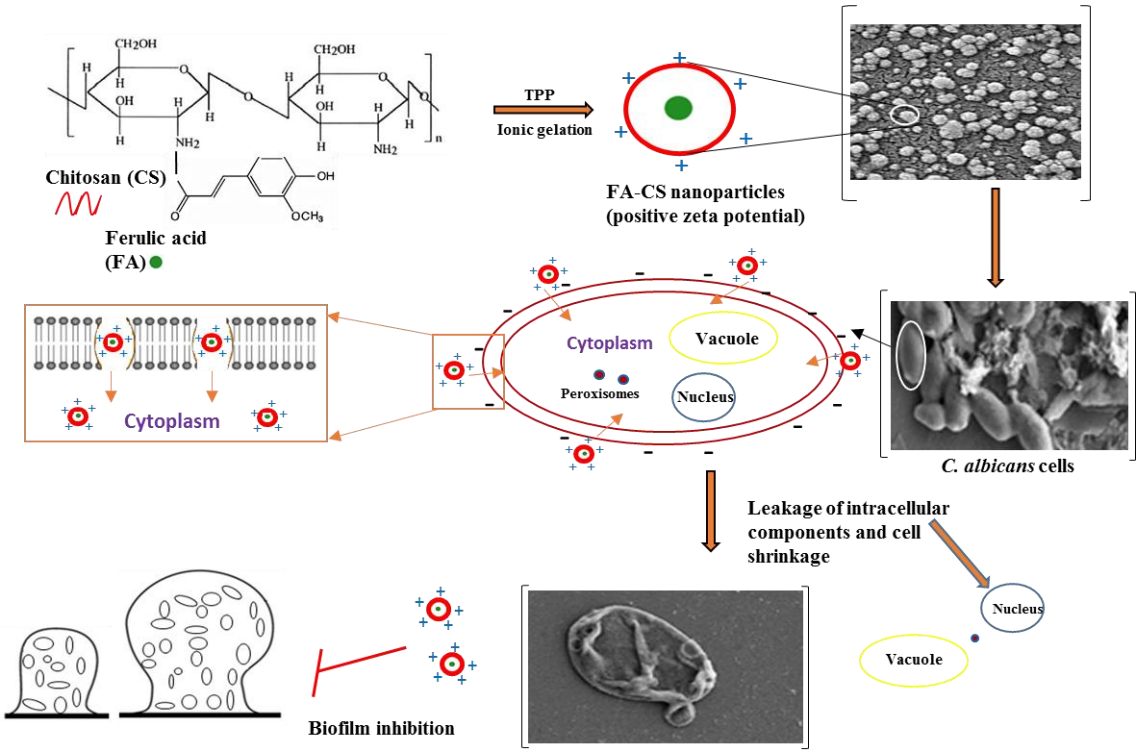

Figure 5.1: Proposed mechanism displaying binding of positively charged FANPs to negatively charged *C. albicans* cell membranes

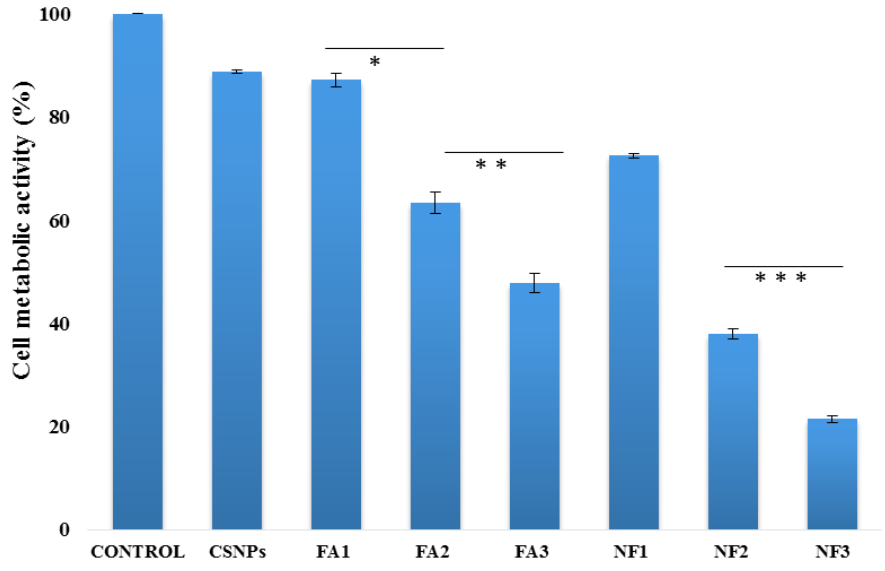

Figure 5.2: XTT assay representing changes in *C. albicans* cell metabolic activity (%) after 24 h incubation with different test formulation. Error bars represent mean ± standard deviation for three independent experiments (n = 3), *p< 0.0005, **p< 0.002, ***p < 0.00001

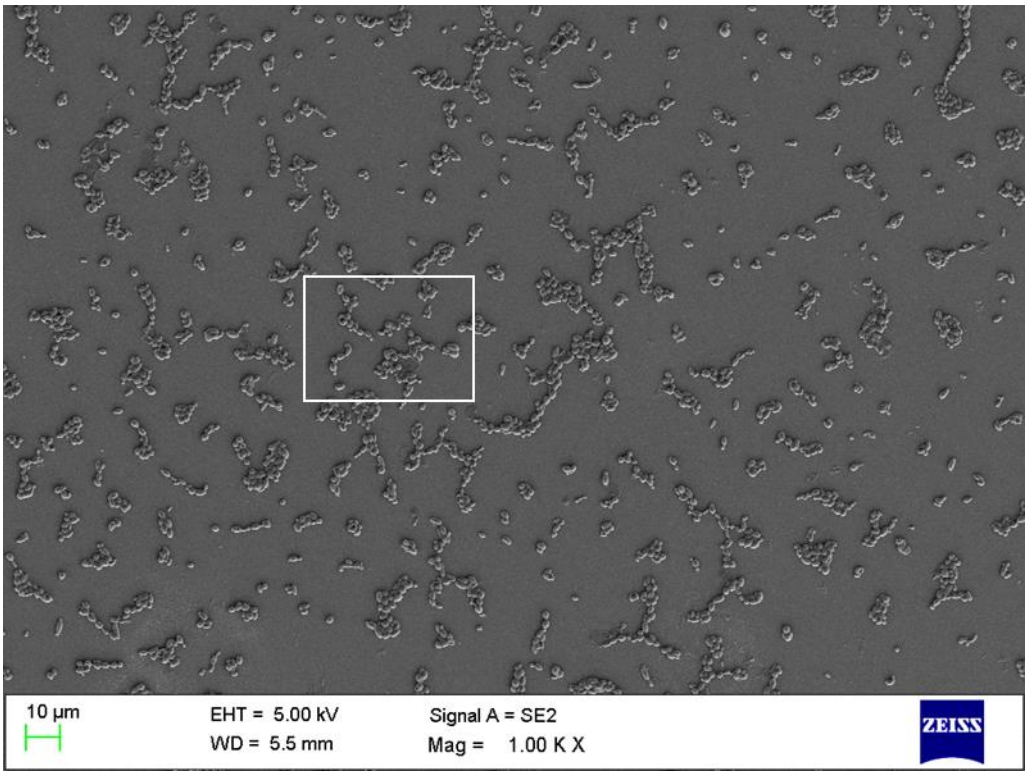

(A)

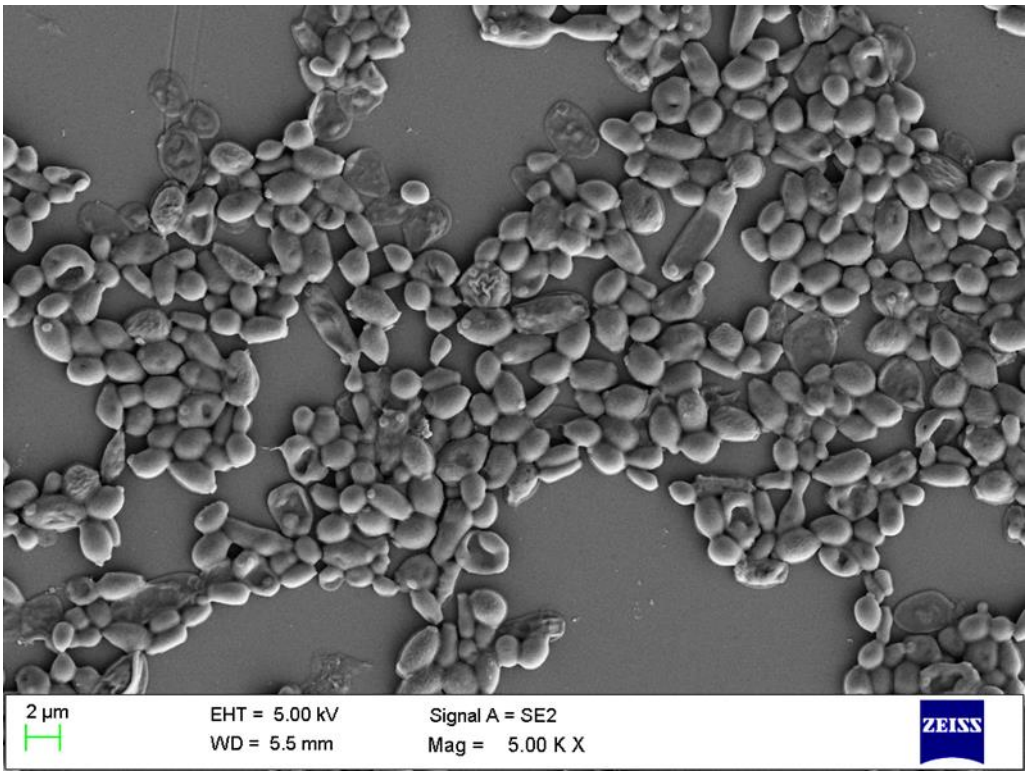

(B)

Figure 5.3: FE-SEM images of Control *C. albicans* biofilm cells at different magnifications **A)** 10 µm, 1KX, **B)** 2 µm, 5KX

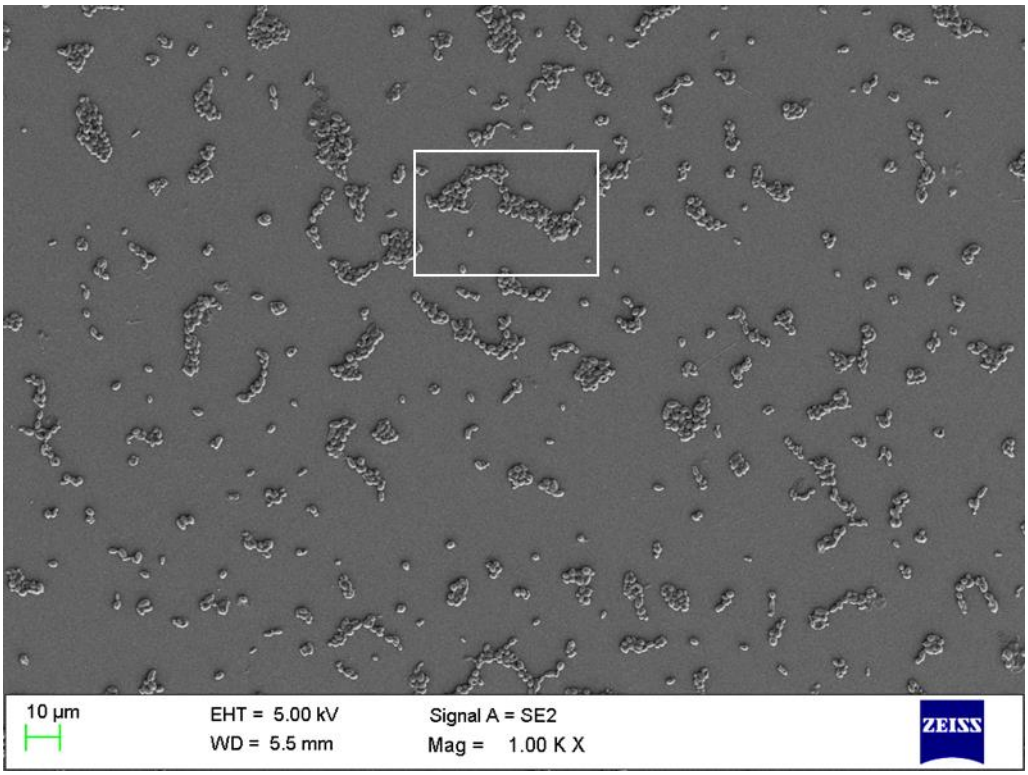

(A)

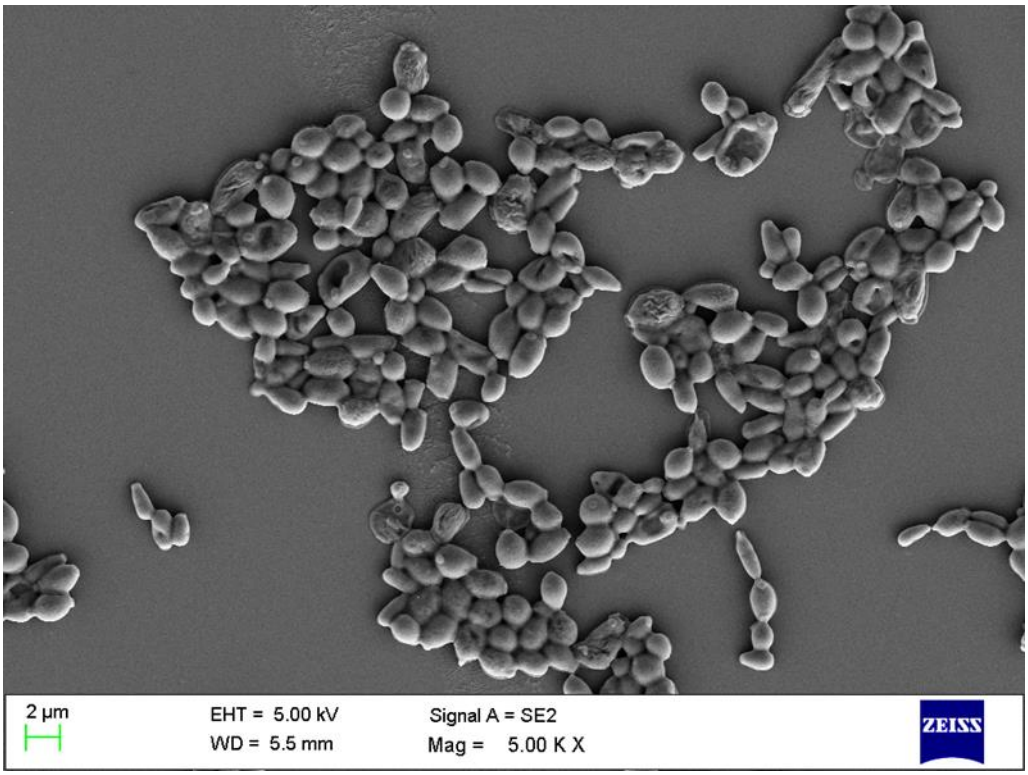

(B)

Figure 5.4: FE-SEM images of variation in cell density of *C. albicans* treated with CSNPs at different magnifications. **A)** 10 µm, 1KX, **B)** 2 µm, 5KX

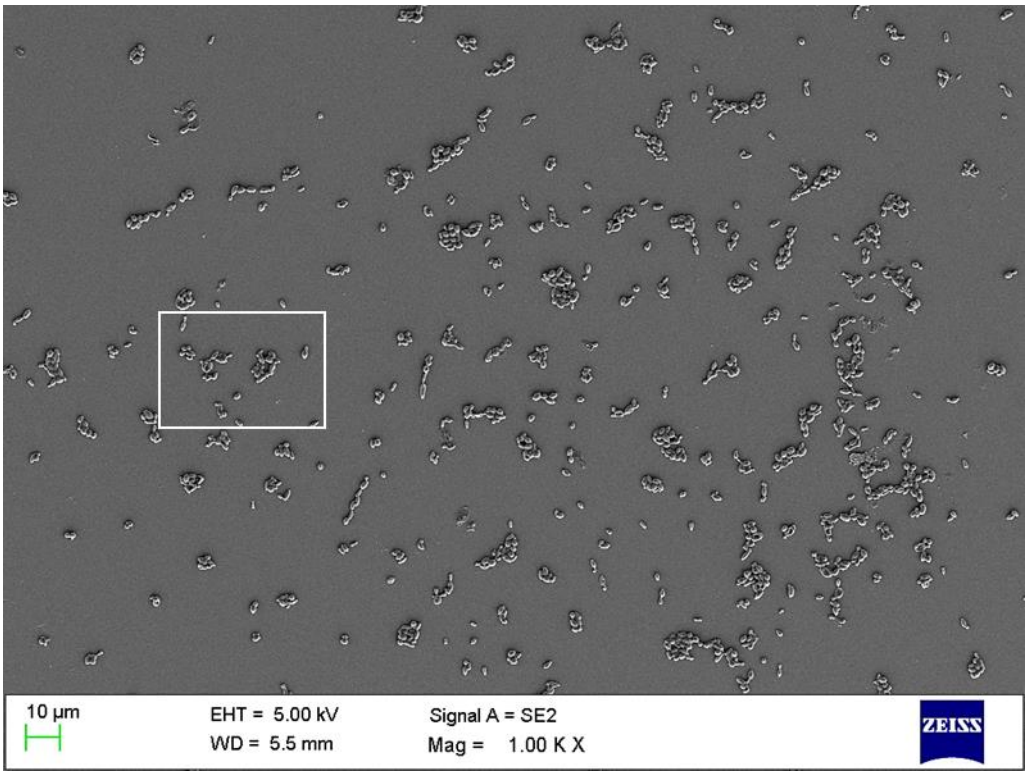

(A)

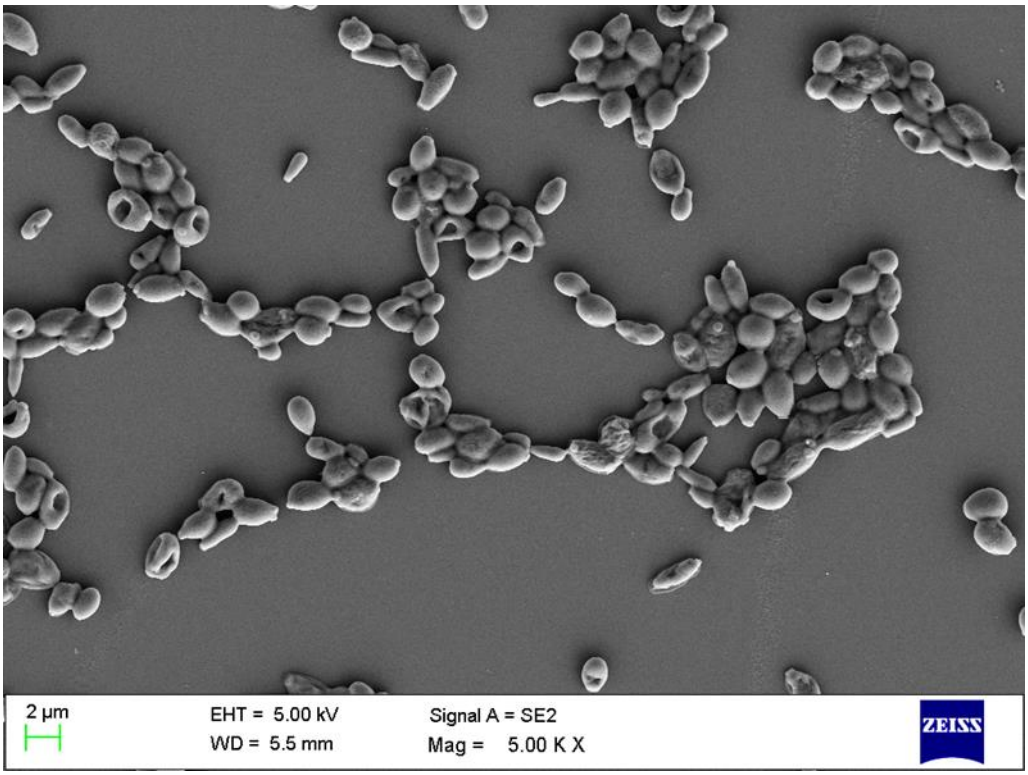

(B)

Figure 5.5: FE-SEM images of variation in cell density of *C. albicans* treated with FANPs (NF_1) at different magnifications. **A)** 10 µm, 1KX **B)** 2 µm, 5KX

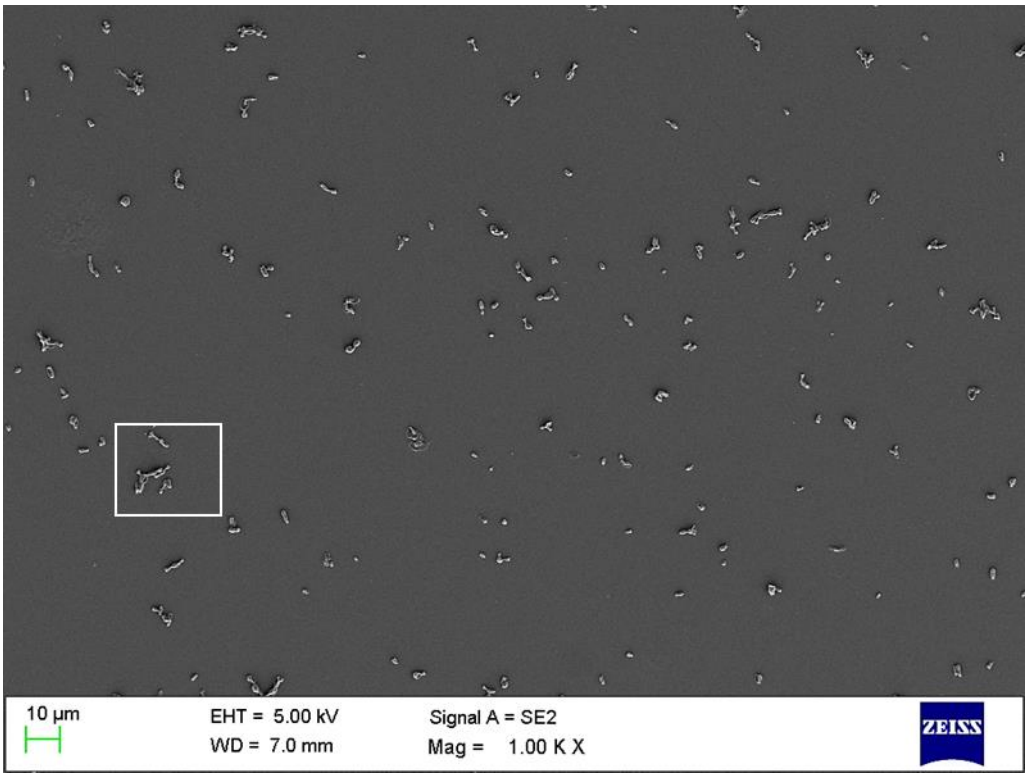

(A)

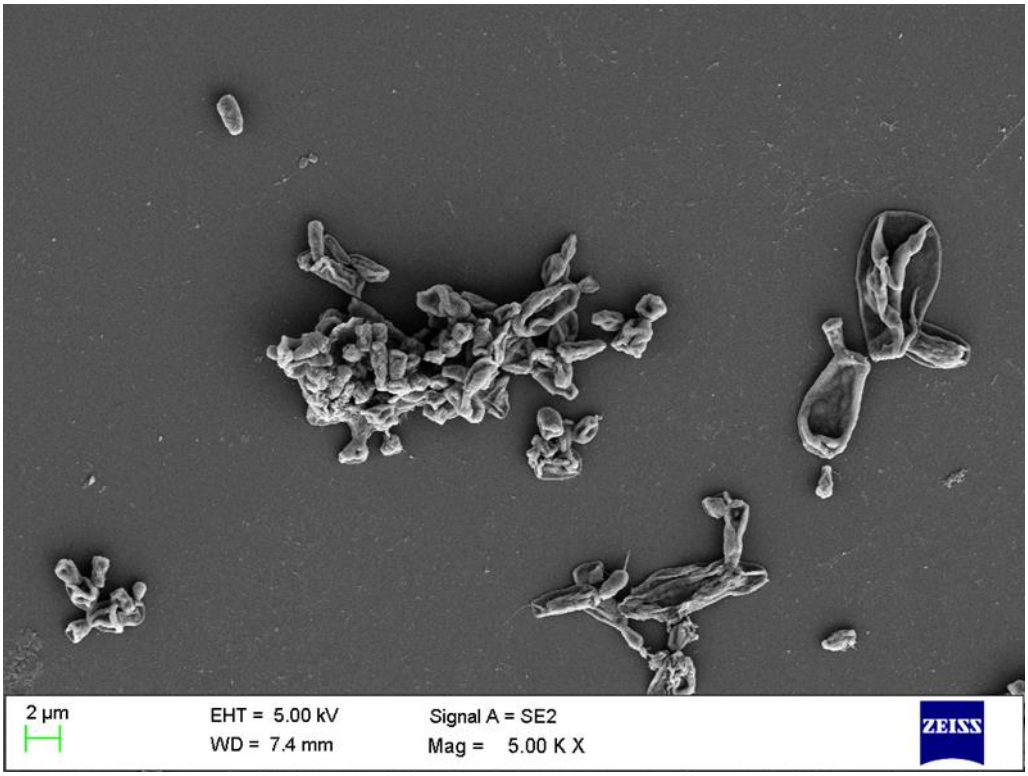

(B)

Figure 5.6: FE-SEM images of variation in cell density of *C. albicans* treated with FANPs (NF_2) at different magnifications. **A)** 10 µm, 1KX **B)** 2 µm, 5KX

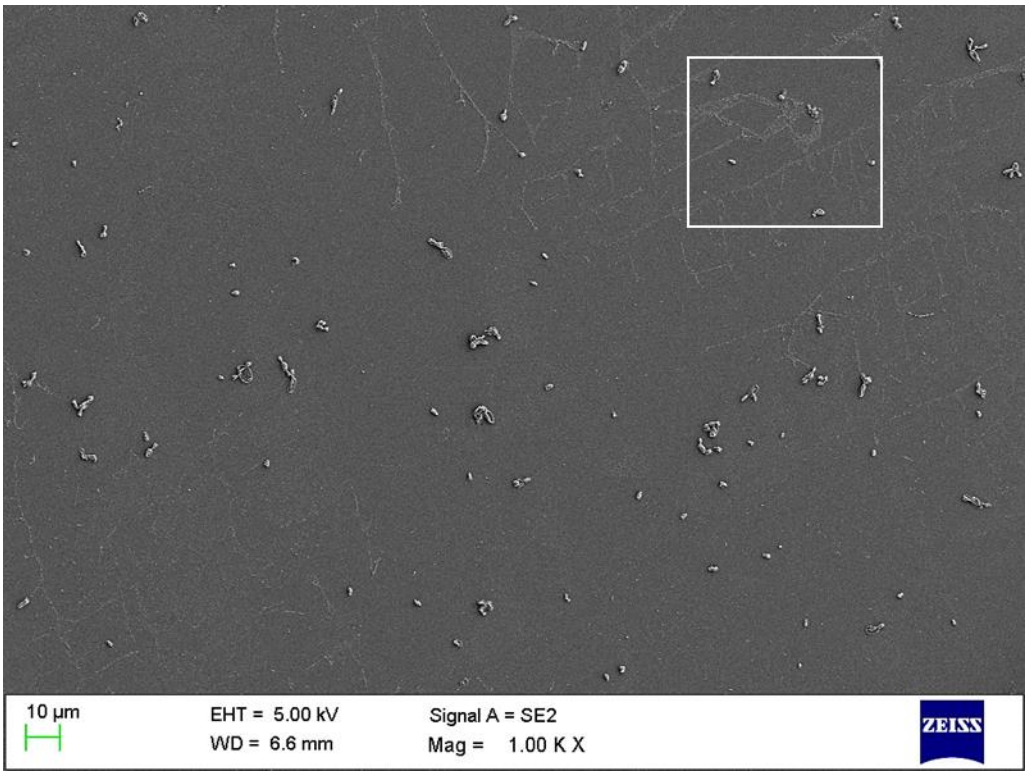

(A)

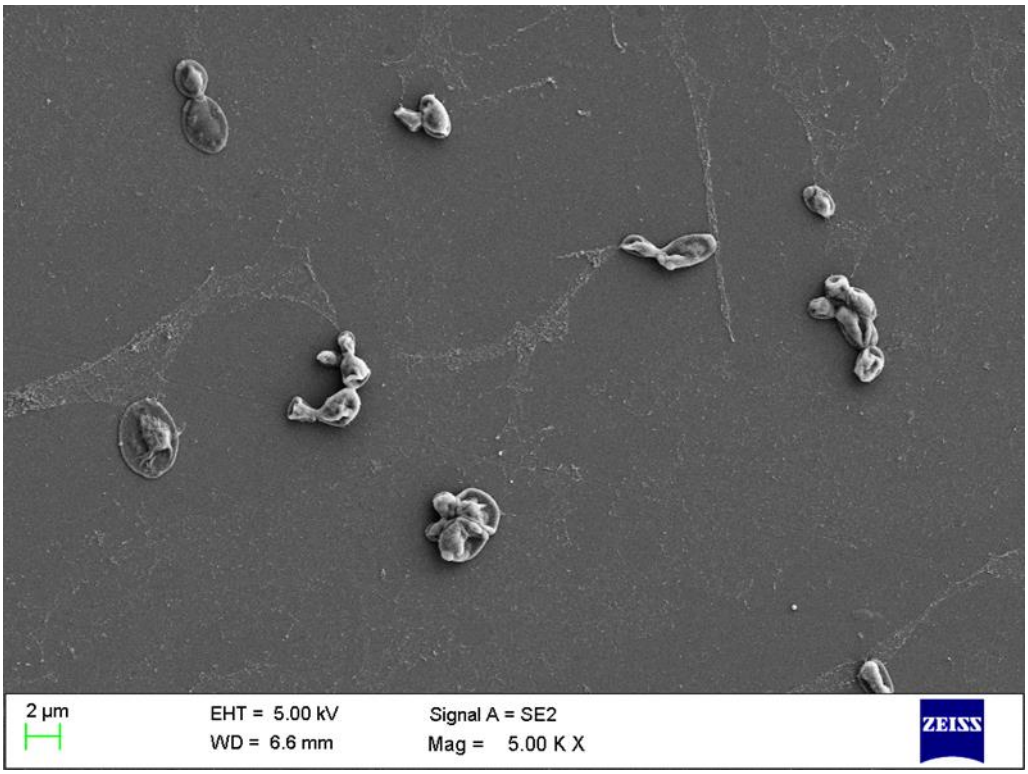

(B)

Figure 5.7: Variation in cell density of *C. albicans* treated with FANPs (NF_3) at different magnifications **A)** 10 µm, 1KX **B)** 2 µm, 5KX

FE-SEM evaluation of biofilm cells morphology

The inhibition of *C. albicans* biofilm and disruption of cellular morphology in presence of test formulations (CSNPs, NF_2, and NF_3) was observed by FESEM (Figure 5.8). The architectural integrity of *C. albicans* biofilm cells under the impact of CSNPs showed a slightly altered morphology with cells aggregation in comparison to control cells (Figure 5.8A and B). Distortion in morphology owing to cell shrinkage was visualized in NF_2 treated cells (Figure 5.8C). Damage of cell membranes along with leakage of intracellular constituents as a result of plasmolysis was significantly observed in *C. albicans* cells grown on NF_3 (Figure 5.8D). The data infers that larger surface area of CSNPs adsorb more tightly on to the fungal cell walls and aid in disruption of membrane integrity. Negatively charged plasma membrane is considered as main target site of action for different polycations therefore positively charged FANPs might have interacted more efficiently with the fungal membrane, diffused into intracellular matrix and consequently brought about the biofilm inhibition (Singh et al., 2008). Outcome of our investigation is in line with previous study by Ing et al. (2012) wherein CSNPs synthesized with CS conc. of 1 mg/ml were established as an effective antifungal agent against *C. albicans*. The results could also be correlated with the recent studies on antimicrobial and insecticidal activities of polyphenols and different nanoparticles (Salunke et al., 2014; Kumar et al., 2014; Pemmaraju et al., 2013; Hemaiswarya and Doble, 2010). Recently, CS-hydroxycinnamic acids conjugates including ferulic, caffeic and sinapic acid have also been synthesized to enhance the antimicrobial properties of chitosan (Lee et al., 2014). From the above discussion, it is clearly evident that the complementary effect of FA and CSNPs (NF_2, NF_3) caused alteration of cell permeability and membrane fluidity resulting in biofilm inhibition.

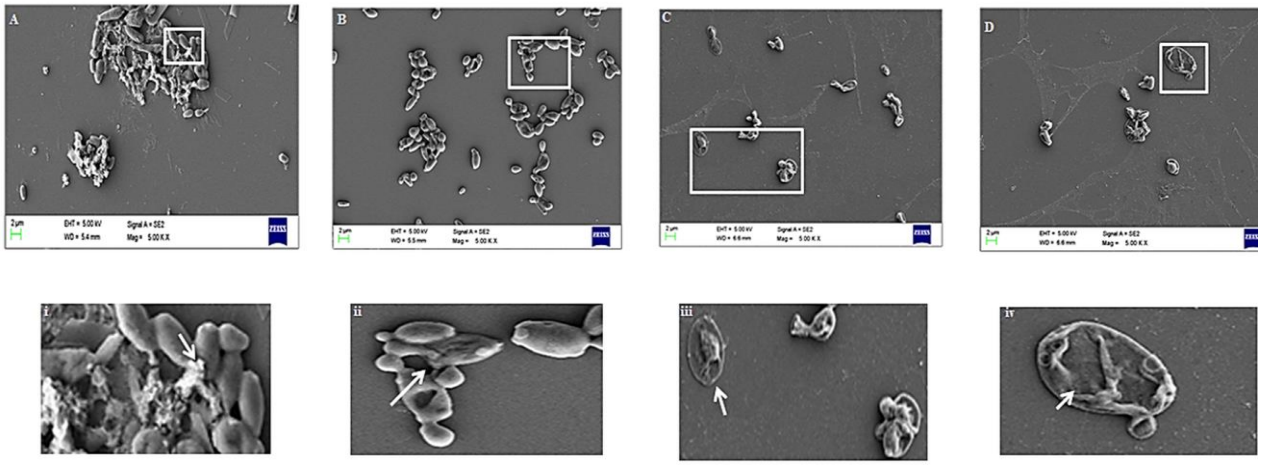

Figure 5.8: Scanning electron microscopic images of *C. albicans* **A)** Control biofilm cells embedded in exopolymeric substances (i, inset) indicated by white arrow, **B)** Biofilm formed in presence of unloaded CSNPs and white arrow indicates the rough cell wall (ii, inset), note that no exopolymeric matrix was observed, **C)** Inhibition of biofilm formation by NF_2, arrow (iii, inset) signify the cell membrane shrinkage, **D)** NF_3 treated cells showing distortion (iv, inset) due to leakage of cell contents by plasmolysis; (Scale bar 2 µM, Microscopic magnification 5KX)

5.4. Conclusion

Present investigation highlighted the antibiofilm activity of FANPs against *C. albicans*. Cytocompatible FANPs at conc. 40 and 80µM inhibited *C. albicans* biofilm cell upto 30% and 21.4% respectively, thus establishing them as a safe and powerful antifungal agent. Positive zeta potential of FANPs was suggested to be a crucial factor facilitating their binding with negatively charged membrane of fungal cell thus disrupting its integrity which eventually leads to leakage of intracellular material and biofilm inhibition. The intriguing synergistic effect of FANPs on prevention of *C. albicans* biofilm might offer a new hope in the management of *C. albicans* biofilm infections.

Chapter 6

FANPs as Anti-diabetic Agents: *In-vivo* Studies

6.1. Introduction

A large number of lifestyle diseases have emerged in the last few decades as a result of changes in human food habits, behavior and exercise regime. Among these diseases, diabetes mellitus (DM) is the most common endocrine disorder and would likely be affecting more than 200 million people by 2030 (Prabhakar et al., 2013; Boyle et al., 2001). DM is a condition which is characterized by various pathological disorders, all or most of which are integrated with chronic hyperglycemia. Hyperglycemic condition is generally associated with absolute or relative deficiencies in insulin secretion by pancreas or due to inefficiency of produced insulin to utilize the available glucose. It leads to lesser availability of glucose to body cells and tissues while increased glucose accumulation in liver. The hyperglycemic disorders are very likely to cause overproduction of free radicals, giving rise to an oxidative stress inside the body tissues. Many literature reports have established a strong intimacy between DM and oxidative stress, which is characterized by formation of free radicals as well as reduction in the activities of antioxidant enzymes (Ohnishi et al., 2004; Noumura et al., 2003).

Oxidative stresses in diabetes is known to exert deleterious effects by either disturbing the default signaling pathways or damaging the cellular DNA/proteins (Blasiak et al., 2003). Necessarily, the preventive strategies to combat the complications associated with DM must target to prevent hyperglycemia and consecutive oxidative stresses. In this regard, many synthetic drugs such as sulphonylureas and biguanides are available, accompanied by their parallel side effects including gastrointestinal, liver and kidney infections (Balasubashini et al., 2004). In order to overcome this troublesome disease, the emphasis is presently being laid upon the ingestion of fresh fruits and vegetables containing natural polyphenolic antioxidants. Many bioactive constituents present in medicinal plants are reported to successfully manage the oxidative stress or diabetes linked conditions hence provide an alternative, natural anti-diabetic approach (Prabhakar and Doble, 2008; Mukherjee et al., 2006).

Among various other plant constituents, FA displayed a strong anti-diabetic behavior by regulating a large number of biochemical as well as physiological pathways involved in

hyperglycemia. It is found to stimulate insulin secretion by pancreatic β-cells while inhibit lipid peroxidation in diabetic mice resulting in the improvement of hyperglycemia (Ohnishi et al., 2004; Noumura et al., 2003). Administration of FA in diabetic rats is associated with the increased activities of antioxidant enzymes such as SOD/CAT, higher insulin levels and increased body weight. On the other hand, decrease in blood sugar levels, total cholesterol and low density lipoprotein cholesterol in type-2 diabetic mice administered with FA revealed its potent anti- hyperglycemic effect (Fujita et al., 2008; Jung et al., 2007). Notwithstanding the fact that has previously been discussed, FA was encapsulated in CSNPs to achieve higher availability in biological systems and in turn enhance its pharmacological value. In the present chapter, we have evaluated and compared the anti-diabetic activity of native FA and FANPs in STZ induced diabetic Wistar albino rats.

6.2. Materials and methods

Glucose, STZ, hemotoxylin, eosin, ketamine and other standard analytical chemicals were purchased from Hi-media (Hi-media, Mumbai, India). Glibenclamide was provided as a gift from Sapience Bio-analytical Research Lab, Bhopal (India). Autospan diagnostics kits for estimation of cholesterol and triglyceride were obtained from Span diagnostics (Span diagnostics India Ltd, Aurangabad, India). LINCO rat/mouse ELISA kits to detect rat plasma insulin were procured from Merck (Merck Ltd, Mumbai, India).

Preparations of solutions

All required solutions and buffers were prepared freshly before each experiment. The working conc. of reagents were set according to the instructions mentioned in their respective diagnostic kits.

Animal care and habituation

The experiment was carried out on Wistar albino rats of 4 months, of both sexes, weighing between 110 to 190 g. The conditions for animal housing and prerequisites for blood collections were similar to those described earlier (chapter 3). Experimental protocol was approved as per CPCSEA guidelines by the Institutional Ethics Committee with an approval no. 1413/PO/a/11/CPCSEA.

6.2.1. Experimentations

Oral glucose tolerance test (OGTT)

Grouping and dosing: For OGTT, Animals were divided into five groups containing six animals each.

Group	Dosing and treatment
I	Control: saline only (1ml/100g)
II	Diabetic control: Glucose (2g/kg p.o.)
III	Reference drug: Glibenclamide (5 mg/kg) + Glucose (2g/kg p.o.)
IV	Native FA (10mg/kg p.o.)+ Glucose (2g/kg p.o.)
V	FANPs (10mg/kg p.o.)+ Glucose (2g/kg p.o.)

OGTT was performed by feeding glucose orally to the animals treated (singly) with different formulations in Groups II to V. After 1.5 h of glucose administration, blood samples were collected from tail vein at 0, 60, 120 and 180 min.

STZ induced diabetes:

After 14 day of OGTT, diabetes was induced in rats by a single intraperitoneal injection of a freshly prepared STZ. The rats were divided into following five groups of six animals each:

Group	Dosing and treatment
I	Control: saline only (1ml/100g)
II	Diabetic control: STZ only
III	Reference drug: Glibenclamide (5 mg/kg) + STZ
IV	Native FA (10mg/kg p.o.) + STZ
V	FANPs (10mg/kg p.o.) + STZ

STZ solution of 10 mg/ml was prepared in ice-cold citrate buffer (0.1 M, pH 4.5) and was administered at a dose of 50 mg/kg animal's body weight on day one. Different test formulations viz. reference drug, native FA and FANPs were administered orally after diabetes induction (day 3) for 14 days, once daily, preferably on same times. Animal's glucose level were measured on 3rd, 7th and 14th day while body weight measurement were recorded on 7th and 14th day.

6.2.2. Biochemical studies

Samples collection and storage

After 14 days, animals were anaesthetized with intraperitoneal injection of Ketamine (50 mg/kg) and blood was collected through retro-orbital puncture (section 3.2.3) in different tubes to obtain serum and plasma. A single drop of blood from each animal was immediately spread onto the marked end of gluco-strip and the displayed blood glucose levels were recorded. Serum and plasma were obtained by centrifugation of tubes at 3000g for 15 min. Animals were then sacrificed and pancreas were collected in 10% formalin for histopathology. All biological samples were store at −20 ºC until further analyzed.

Serum analysis for lipid profile

Autospan diagnostics kits were used for estimation and detection of total-cholesterol (TC), cholesterol-high density lipoproteins (HDL) and triglyceride (TG) through automated analyzer (Figure 6.1A and B).

(A) **(B)**

Figure 6.1: **(A)** Lipid profiling of rat serum **(B)** Automated analyzer

Estimation of Total-Cholesterol

Principle

In principle, cholesterol esters are first hydrolyzed by cholesterol esterase (CE) to give free cholesterol and fatty acids. In subsequent reaction, cholesterol oxidase (CHOD) oxidizes 3-OH group of free cholesterol to liberate cholest-4-en-3-one and hydrogen peroxide (H_2O_2). Under the presence of peroxidase (POD), H_2O_2 couples with 4-aminoantipyrine (4-AAP) and phenol to produce red quinoneimine dye. Absorbance of colored dye is measured at 505 nm and is proportional to the amount of TC conc. in the sample. The reaction could be summarized as follows:

Cholesterol ester $\xrightarrow{CE}$ Cholesterol + Fatty Acids

Cholesterol + O_2 $\xrightarrow{CHOD}$ Cholest-4-en-one + H_2O_2

$2H_2O_2$ + Phenol + 4-AAP $\xrightarrow{POD}$ Quinoneimine dye + H_2O

Procedure

All the reagents were ready to use and stable at 2-8 °C until the expiry date mentioned on the container label. Fresh clear serum without hemolysis was used for cholesterol estimation as per the instructions given in assay kit manual.

Reaction Parameters:

Wavelength	:	490-510 nm
Flow cell temperature	:	37 °C
Incubation	:	10 min
Sample volume	:	10 µl
Reagent volume	:	1 ml
Zero setting with	:	Reagent blank
Light path	:	1 cm

Estimation of HDL-Cholesterol

Reagent composition and working solutions

The kit contains 4 Reagents:

(a) Enzyme Reagents
(b) Diluent buffer
(c) Precipitating reagents PEG-6000
(d) Standard

Working reagent solution was prepared by dissolving enzyme reagent with 25 ml of diluents buffer 10 min prior to its use. Low density lipoprotein (LDL) cholesterol, very low-density lipoprotein (VLDL) cholesterol and chylomicron fraction were precipitated by addition of PEG 6000 to the sample. After centrifugation at 1000 rpm for 10 min, the HDL fraction was recovered in the supernatant and determined with CHOD-POD principle using span diagnostics kit. The absorbance of reference and test samples were measured and calculated as per given formula:

HDL-cholesterol conc. (mg/dl) = Abs of test/Abs of standard ×50 × 2*

Abs- absorbance, 2* dilution factor, (as sample was diluted 1:1)

Estimation of TG

TG were estimated using accurate triglycerides kit (Span Diagnostics). The kits were formulated using glycerol 3-phosphate oxidase (GPO) and peroxide for quantitative estimation of serum triglycerides.

Principle

TG are hydrolyzed by lipoproteins lipase (LPL) to produce glycerol and free fatty acids (FFA). In presence of glycerol kinase (GK) and ATP, glycerol is converted to glycerol 3-phosphate, which is further oxidized to dihydroxyacetone phosphate (DAP) and H_2O_2. In presence of peroxidase, H_2O_2 couples with 4-AAP and 4-cholorophenol to produce red quinoneimine dye. Absorbance of colored dye is measured at 505 nm and is proportional to triglycerides conc. in the sample.

Triglycerides $\xrightarrow{\text{LPL}}$ Glycerol + FFA

Glycerol + ATP $\xrightarrow{\text{GK}}$ Glycerol 3-phosphate + ADP

Glycero 3- phosphate + O_2 $\xrightarrow{\text{GPO}}$ DAP+H_2O_2

$2H_2O_2$ + 4-AAP Chorophenol $\xrightarrow{\text{POD}}$ Quinoneimine dye + $4H_2O$

Reagent composition and working solutions

The kit contained three components:

(a) Enzyme reagents
(b) Diluent buffer
(c) Standard

The contents of enzyme reagent were dissolved in 10 ml of diluent buffer, resulting working solution was stable for 4 - 6 week at 2 – 8 ºC. For TG estimation, fresh clear serum was used and procedure given in assay kit manual was followed.

Wavelength	:	490-550 nm
Flow cell temperature	:	37 °C
Incubation	:	10 min
Sample volume	:	10 µl
Reagent volume	:	1 ml
Zero setting with	:	Reagent blank

An indirect approach was employed for the calculation of low and very low density lipoproteins cholesterols (Prabhakar et al., 2013). Since the ratio of TG to cholesterol in VLDL is 5%, its value was calculated as TG/5 for individual animal. The value of LDL cholesterol was ascertain from the given equation:

LDL cholesterol (mg/dl) = Total cholesterol (mg/dl) − HDL cholesterol (mg/dl) − (TG/5) (mg/dl)

Estimation of plasma insulin

Quantitative estimation of insulin in rat plasma was carried out by following the detailed procedure outlined in rat insulin ELISA kits (LINCO ELISA). The kit was supplied with all the necessary reagents, which could be stored up to 2 weeks at 2-8 $^{\circ}$C. It works on an enzyme immunoassay in which two monoclonal antibodies are sandwiched between two separate antigenic determinants on the insulin molecule. In this solid phase two sites assay, the insulin present in the sample reacts with peroxidase-conjugated anti-insulin antibodies during incubation. The unbound enzyme loaded antibodies were washed away at the end of assay and the reaction was terminated by acid addition. Bound conjugates were detected spectrophotometrically at 450 nm, upon reaction with 3, 3', 5, 5'-tetramethylbenzidine (Padiya et al., 2011).

Histopathological studies:

Pancreas for histopathological studies were excised quickly after rat's sacrifice and the samples were fixed in 10% formalin (Figure 6.2.A and B). Organs were then stained with hemotoxylin and eosin to be observed under light microscope.

(A) **(B)**

Figure 6.2: (A) Excision of rat pancreas, **(B)** Pancreas kept in 10% formalin

Statistical analysis

The data are expressed as mean ± standard error, results were analyzed statistically by "graphpad instat 3" software using ANOVA followed by *Tukey's* multiple comparison test. The minimum level of significance was fixed at $p<0.05$.

6.3. Results and discussion

STZ induced diabetes in rodents is a universally applied model for the preliminary screening of compound having anti-diabetic activities. It acts as a potent DNA methylating agent and work by damaging pancreatic β cells through nitric oxide induction and free radicals (Spinas, 1999). In this study, STZ induced diabetic rats were administered with oral doses of reference drug (glibenclamide), native FA and FANPs in same amount (10 mg/kg) to assess and compare their effect on diabetes related symptoms. The variation in different parameters viz. blood glucose level, body weight, serum lipid profile and pancreatic islets of animals treated with different formulations were measured and visualized.

OGTT was conducted to observe the effect of oral administration of glucose on healthy rats following their treatment with different test formulations. The blood glucose level was significantly reduced in animals treated with reference drug glibenclamide, native FA and FANPs ($p<0.01$; group 3, 4 and 5 respectively) compared to diabetic control (group 2). All the more, animals treated with FANPs showed a marked reduction ($p<0.01$) in glucose level compared to diabetic control as well as glibenclamide treated animals (Figure 6.3). The oral feeding of glucose to test animals helps examine the body's ability to use glucose as a main source of energy. OGTT measure the fasting plasma glucose conc., thus offer an initial diagnostic basis to simplify and facilitate the diagnosis of diabetes (Sornalakshmi et al., 2016). Glucose lowering effects of FANPs in non-diabetic healthy animals provided an exciting rationale to proceed further into analysing the protective effects of FANPs in diabetes induced animal models.

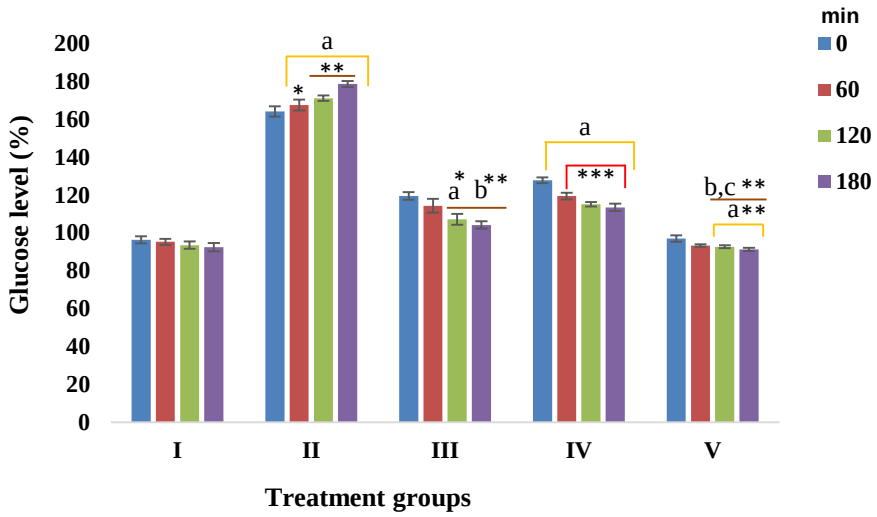

Figure 6.3: Effect of test formulations on blood glucose levels in glucose loaded normal rats. Values are mean ± standard error, where n=6, *p<0.05, **p<0.01 and ***p<0.001. a- Significance difference as compare to control group, b- significance difference as compare to diabetic control group, c-significance difference as compare to reference drug treated group

Variations in body weight of diabetic animals belonging to different test groups during the study period of 14 days is shown in figure 6.4. No change in the body weight of control animals were observed during 14 days, whereas diabetic control rats showed maximum percentage reduction in body weight (7.43%). On the other hand, smaller variation in weight was observed for animal groups treated with native FA (2.82%) and FANPs (2.05%) compared to diabetic control.

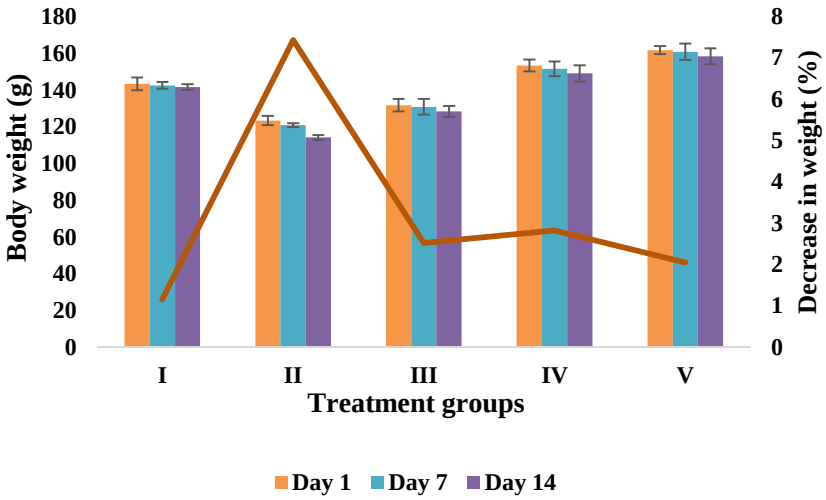

Figure 6.4: Variations in body weight of STZ induced diabetic rats treated with different formulations over 14 days along with percent decrease in body weight

Changes in blood glucose and insulin level in STZ induced diabetic rats treated with different test formulations is depicted in figure 6.5A and B. Control rats did not show any noticeable variation in blood glucose whereas animals injected with STZ underwent a two-fold increase in glucose level, while significant reduction in blood insulin after 14 days of injection ($p<0.05$, group 2). The elevation in blood glucose level must have been brought about by STZ induced oxidative stress in pancreatic cells which sequentially hampered insulin secretion, resulting in the decreased utilization of glucose by body tissues (Omamoto et al., 1981). Conversely, group 4 and 5 treated with native FA and FANPs exhibited a marked reduction in blood glucose, at the same time, insulin levels did not display any pronounced decline. More exciting results were obtained in case of rats treated with FANPs, where a significant reduction in blood glucose level was observed during the entire study period in comparison to both diabetic control group (group 2; $p<0.01$) as well as glibenclamide treated rats (group 3; $p<0.01$).

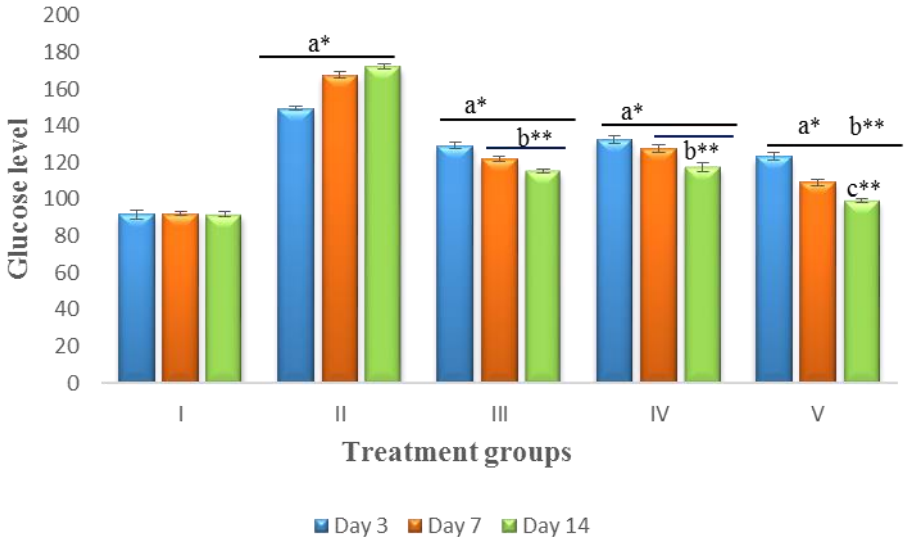

(A)

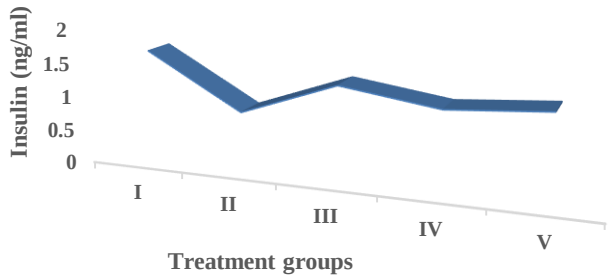

(**B**)

Figure 6.5: Impact of different test formulations in STZ induced diabetic rats on **A)** blood glucose level, **B)** blood insulin level. Values are mean ± standard error, where n=6, *p<0.05, **p<0.01; a- Significance difference as compare to control group, b-significance difference as compare to diabetic control group, c-significance difference as compare to native FA

Serum lipid profile analysis of different treatment groups of rat showed a significant enhancement (p<0.001) in TC, TG, LDL and VLDL while a significant reduction (p<0.001) in HDL cholesterol compared to normal control group (Table 6.1). Significant reduction in TC was observed in rats treated with FANPs (group 5), in comparison to diabetic control group (p<0.05; group 2). Similarly, significant decline was observed in TG and LDL levels for same group of animals when compared with both diabetic control group (p<0.01) as well as native FA treated group (p<0.05).

Table 6.1: Serum lipid profile of animal groups treated with different test formulations. Values are mean ± standard error, where n=6, *p<0.05, **p<0.01 and***p<0.001. a-Significance difference compared to control group, b-significance difference compared to diabetic control group, c-significance difference compared to native FA treated group

Groups	Treatment	Lipid Profile				
		CHL (mg/dl)	HDL (mg/dl)	TG (mg/dl)	LDL (mg/dl)	VLDL (mg/dl)
I	Control	139.1±1.5	68.0±1.23	126.5±2.0	45.8±1.9	25.3±0.4
II	Diabetic control	172.5±1.2 a***	43.0±2.72 a***	163.0±1.4 a***	96.1±1.4 a***	34.6±0.2 a***
III	Standard (Glibenclamide 5 mg/kg)	152.5±1.2 a***,b**	56.33±2.07 a*,b***	141.8±3.1 a***,b***	74.8±3.2a***, b***	27.36±0.6 a***,b***
IV	Native FA (10 mg/kg)	149.6±2.4 a*	45.16±2.44 a***	153.66±2.0 a**	89.4±4.0 a***	30.7±0.4 a*
V	FANPs (10 mg/kg)	144.3±1.4 a*, b**	53.16±1.72 a***, c*	143.1±3.2 a**,b**, c*	79.5±2.6 a***,b**, c*	27.6±0.6 a***,b**

Defects in insulin production or impaired functioning of this hormone is one of the major cause of chronic hyperglycemia which ultimately leads to diabetes. During the past years, medicinal plants or their polyphenolic extracts have been extensively testified to nullify the damaging effects of reactive oxygen species produced during hyperglycemia, in STZ induced diabetes and other oxidative stress conditions (Sharma et al., 2013; Orsolic et al., 2011; Ugochukwu and Babady, 2003). FA has been reported to reduce the toxicity generated by free radicals in pancreatic cells of STZ induced diabetic rats. Resultantly, more insulin was secreted by proliferation of β cells, which helped in utilization of glucose by hepatic tissues thus lowering overall glucose level in the body (Ohnishi et al., 2004). In addition to that, CSNPs were reported to enhance the intestinal absorption of insulin in simulated GI model, along with lowering of blood glucose level *in-vivo* in diabetic rat models (Mukhopadhyay et al., 2013). Oral controlled delivery of CSNPs encapsulated insulin was able to reduce the diabetic glucose level over a period of more than 15 h, by virtue of its extended pharmacological bioavailability in induced diabetic rats Pan et al. (2002).

During diabetes, a highly active lipase enzyme tends to increase the conc. of free fatty acids (FFA) in blood circulations, which in turn increases the β oxidation of fatty acids resulting in higher levels of cholesterols. Under normal conditions, insulin inhibits the activity of lipase, thereby limiting the conc. of FFA in healthy non-diabetic animals. Approximately 50% decline in insulin conc. in diabetic rats (group 2), compared to non-diabetic healthy animals (group 1) could be one of the reasons for potentially higher levels of TC in these animals (Figure 5.5B). Apart from the regulation of FFA, insulin is also required for receptor-mediated removal of LDL-cholesterol and TG, both of which were present in higher amounts in diabetic control group of rats as compared to control group (Table 5.1). Besides well-documented cholesterol lowering effect, FA also helps to prevent the oxidation of LDL, thus accelerating the uptake and degradation of cholesterol by liver (Scavariello and Ardlano, 1998; Bourne and Rice, 1997). Animal fed with FA and FANPs exhibited low levels of TC, LDL and TG in treated groups, hence these formulations are believed to reduce the diabetes associated complications. More pronounced impacts on animals were obtained with FANPs, which may be attributed to a slow and controlled release of encapsulated FA at conc. similar to free form. In the same context, CSNPs were found to enhance insulin retention at high gastric pH, for a sustained period of time (Mukhopadhyay et al., 2013). It was observed that the biological activity of insulin loaded in nanoparticles remained un-compromised, post oral administration in diabetic mice.

Pancreatic histopathology of control rats represented well developed islet of Langerhans within normal pancreatic acini (Figure 6.6A). On the contrary, diabetic rat's pancreas displayed shrunken and ruptured acini with damaged islets of Langerhans (Figure 6.6B). However, normal islets and pancreatic acini were observed in the pancreas of animal groups treated with reference drug glibenclamide and FANPs (Figure 6.6C and D). Histopathological studies revealed that FANPs have the capacity to stabilize the islet cells mass, as well as to avoid shrinkage and destruction caused due to STZ injection, that was visible in diabetic control group. As discussed earlier, increased β-cell would increase the secretion of insulin, which would necessarily prompt the hepatic tissues to utilize more glucose, lowering its overall body conc. From data it could be inferred that reduction in blood glucose level accompanied by increase in body weight in rats treated with FANPs was brought about by synergistic action of native FA and CSNPs. The interaction of both components to minimize the toxicity associated with hyperglycemia, may provide a natural alternative for synthetic drugs being used to cure diabetes.

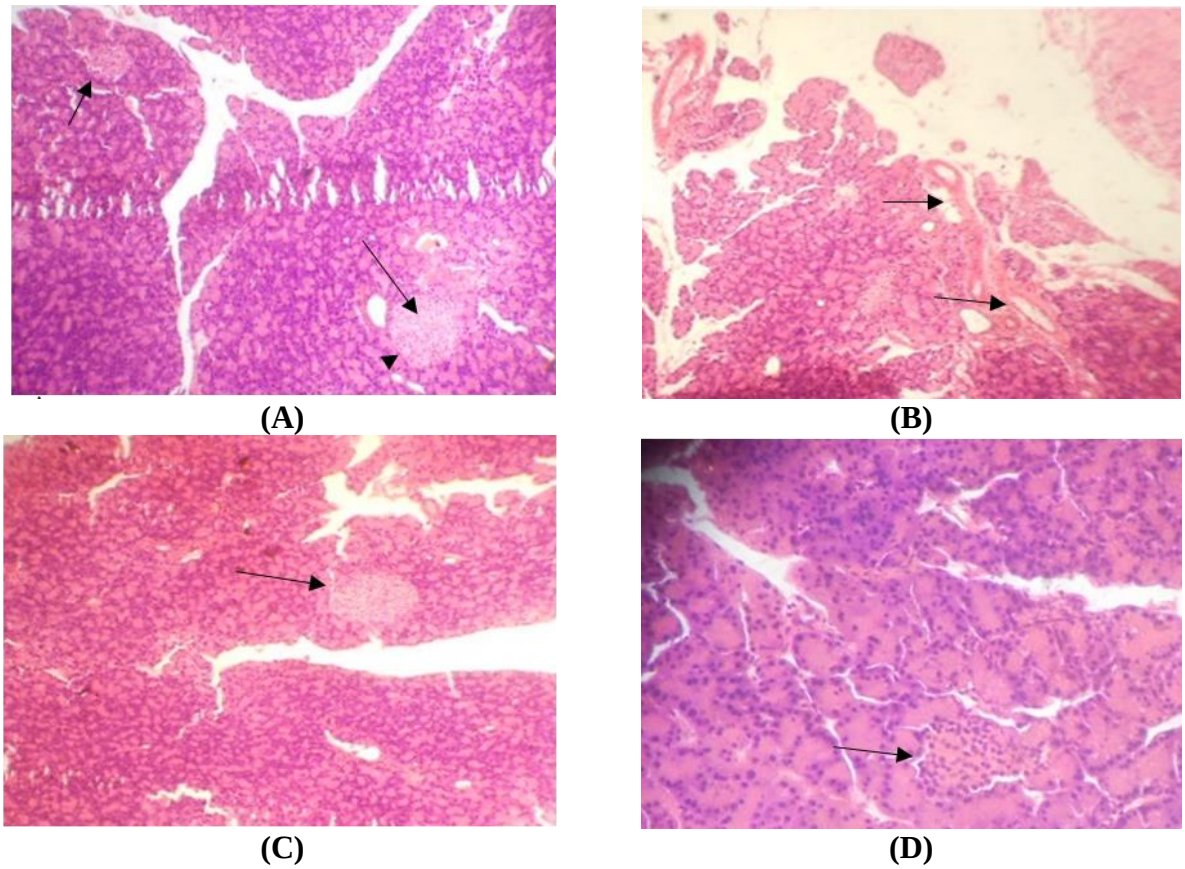

Figure 6.6: Histopathological representation of pancreas treated with hemotoxylin and Eosin **A)** control group; pancreas with normal islets of Langerhans (arrow) within normal pancreatic acini (arrow head), **B)** diabetic group; pancreas showing shrunken islets with deformed acini, **C)** groups treated with standard glibenclamide showing normal islets and acini, **D)** groups treated with FANPs showing recovered islets of Langerhans with higher cells mass. (Microscopic magnification 100X)

6.4. Conclusion

Here, we evaluated the effect of FANPs on STZ induced diabetic Wistar albino rats. These nanoparticle's formulations exhibited a positive effects on diabetes associated symptoms such as lowering of blood glucose levels, enhancement in body weight along with reduction in TC, LDL and TG conc. in diabetic animals. FANPs also resisted a sharp decline in insulin level, which allowed further regulation of cholesterol, TG and overall lipid profile in induced diabetes. Positive impact of FANPs in improving the hyperglycemic condition prevalent in diabetic rats might provide new avenues for the treatment of diabetes mellitus and help avoid the secondary complications associated with synthetic drugs.

Summary and Future Scope

Role of naturally occurring plant polyphenolic compound in fighting against diverse kind of diseases has been extensively assessed during last two-three decades. Ferulic acid, major compound of hydroxycinnamic acids subclass of plant phenolic acids has displayed its healing potential in various clinical conditions. A wide spectrum of therapeutic activities have been reported for FA, most important of them being antioxidant, anti-inflammatory, antidiabetic and anticancer among others. In spite of having noted healing properties against different chronic disorders, its applicability as a clinical drug is potentially limited as a result of its small plasma retention time, hence low bioavailability. This limitation could be circumvented by encapsulation of FA into polymeric chitosan nanoparticles. These FANPs were found to retain their antioxidant activity along with potential increase in plasma retention time compared to free FA. Anticancer activities of FANPs against human cervical cancer ME-180 and prostate cancer PC-3 cell lines were also higher in comparison with the fee form of compound. FANPs were found to reduce the cell viability through induction of apoptotic cell death in tested cancer cells. Similarly, a noticeable inhibition potential of FANPs was visualized against *Candida albicans* biofilm cells. A significant reduction in blood glucose level; blood TC, TG and LDL was also observed in hyperglycemic induced diabetes rats treated with FA nanoformulations.

Several hypotheses have been proposed by different researchers describing the mechanisms involved in FA interaction with tumor or microbial cells and the influence it exerts in associated biological disorders. For example, FA role has been discussed in modulation of the expression of genes responsible for cell proliferation as well as signaling pathway proteins in cancer cells. Its role in Alzheimer's disease as an inhibitor (both *in-vivo*, *in-vitro*) of neurotoxic Aβ-aggregation through programmed cell death has also been reported. However, till date no validated theory has been offered to describe the role of FA-CS conjugates or FANPs in microbial or tumor cells. In conjunction with the objectives of present investigation, it becomes worthwhile to identify the genes involved in neoplasm initiation, progression and microbial pathogenesis. The study of molecular genetic pathways would aid in ascertaining the impact of nanoparticles on the development of neoplasm or microbial infection and would help to develop target based therapeutic strategies. New FA derivatives linked with CS could also be fabricated and tested for their pharmacological prospects.

References

Adam, A., Crespy, V., Levrat-Verny, M. A., Leenhardt, F., Leuillet, M., Demigne, C., Remesy, C. (2002). The bioavailability of ferulic acid is governed primarily by the food matrix rather than its metabolism in intestine and liver in rats. *J Nutr*. 132, 1962-1968.

Adisakwattana, S., Chantarasinlapin, P., Thammarat, H., Yibchok-Anun, S. (2009). A series of cinnamic acid derivatives and their inhibitory activity on intestinal alpha-glucosidase. *J Enzyme Inhib Med Chem*. 24, 1194-1200.

Adluri, R. S., Nagarajan, D., Periyaswamy, V., Venugopal, P. M. (2008). Dose-response effect of ferulic acid against nicotine-induced tissue damage and altered lipid levels in experimental rats: a pathohistological evaluation. *Fundam Clin Pharmacol*. 22, 557-567.

Ai, H., Wang, F., Xia, Y., Chen, X., Lei, C. (2012). Antioxidant, antifungal and antiviral activities of chitosan from the larvae of housefly *Musca domestica* L. *Food Chem*. 132, 493-498.

Akihisa,T., Yasukawa, K., Yamaura, M., Ukiya, M., Kimura, Y., Shimizu, N., Arai, K. (2000). Triterpene alcohol and sterol ferulates from rice bran and their anti-inflammatory effects. *J Agric Food Chem*. 48, 2313-2319.

Alavarce, R. A. S., Saldanha, L. L., Almeida, N. L. M., Porto, V. C., Dokkedal, A. L., Lara, V. S. (2015). The beneficial effect of Equisetum giganteum L. against candida biofilm formation: new approaches to denture stomatitis, J. *Evid Based Complementary Altern Med*. 1-9. DOI: http://dx.doi.org/10.1155/2015/939625

Alias, L. M., Manoharan, S., Vellaichamy, L., Balakrishnan, S., Ramachandran, C. R. (2009). Protective effect of ferulic acid on 7, 12-dimethylbenz (a) anthraceneinduced skin carcinogenesis in Swiss albino mice. *Exp Toxicol Pathol*. 61(3), 205-214.

Allan, C. R., Hadwiger, L. A. (1979). The fungicidal effect of chitosan on fungi of varying cell wall composition. *Exp Mycol*. 3, 285-287.

Anand, P., Nair, H. B., Sung, B., Kunnumakkara, A. B., Yadav, V. R., Tekmal, R. R. (2010). Design of curcumin-loaded PLGA nanoparticles formulation with enhanced cellular

uptake, and increased bioactivity in vitro and superior bioavailability in vivo. *Biochem Pharmacol*. 79, 330-338.

Anandan, R., Ganesan, B., Obulesu, T., Mathew, S., Asha, K. K. (2013). Antiaging effect of dietary chitosan supplementation on glutathione-dependent antioxidant system in young and aged rats. *Cell Stress Chaperones*. 18, 121-125.

Andreasen, M. F., Landbo, A. K., Christensen, L. P., Hansen, A., Meyer, A. S. (2001). Antioxidant effects of phenolic rye (Secalecereale L.) extracts, monomeric hydroxycinnamates, and ferulic acid dehydrodimers on human low-density lipoproteins. *J Agric Food Chem*. 49, 4090-4096.

Anselmi, C., Centini, M., Maggiore, M., Gaggelli, N., Andreassi, M., Buonocore, A. (2008). Non-covalent inclusion of ferulic acid with α-cyclodextrin improves photostability and delivery: NMR and modeling studies. *J Pharm Biomed Anal*. 46 (4), 645-652.

Artursson, P., Lindmark, T. (1994). Effect of chitosan on the permeability of monolayers of intestinal epithelial cells (Caco-2). *Pharm. Res.* 11 (9), 1358–1361.

Asanoma, M., Takahashi, K., Miyabe, M., Yamamoto, K., Yoshimi, N., Mori, H., Kawazoe, Y. (1994). Inhibitory effect of topical application of polymerized ferulic acid, a synthetic lignin, on tumor promotion in mouse skin two-stage tumorigenesis. *Carcinogenesis*. 15, 2069-2071

Badawy, D., El-Bassossy, H. M., Fahmy, A., Azhar, A. (2013). Aldose reductase inhibitors zopolrestat and ferulic acid alleviate hypertension associated with diabetes: effect on vascular reactivity. *Can J Physiol Pharmacol*. 91, 101-107.

Balasubashini, M. S., Rukkumani, R., Menon, V. P. (2003). Protective effects of ferulic acid on hyperlipidemic diabetic rats. *Acta Diabetologica*. 40, 118-122.

Balasubashini, M. S., Rukkumani, R., Viswanathan, P., Menon V. P. (2004). Ferulic acid alleviates lipid peroxidation in diabetic rats. *Phytother Res*. 18(4), 310-314.

Balkwill, F., Mantovani, A. (2010). Cancer and inflammation: implications for pharmacology and therapeutics. *Clin Pharmacol Ther*. 87, 401-406.

Bandugula, V.R., Prasad, N. R. (2013). 2-Deoxy-D-glucose and ferulic acid modulates radiation response signaling in non-small cell lung cancer cells. *Tumour Biol*. 34, 251-259.

Bansal, V., Kumar, M., Dalela, M., Brahmne, H.G., Singh H. (2014). Evaluation of synergistic effect of biodegradable polymeric nanoparticles and aluminum based adjuvant for improving vaccine efficacy. *Int J Pharm.* 471, 377–384.

Baskaran, N., Manoharan, S., Balakrishnan, S., Pugalendhi, P. (2010). Chemopreventive potential of ferulic acid in 7, 12- dimethylbenz (a) anthracene-induced mammary carcinogenesis in Sprague-Dawley rats. *Eur J Pharmacol*. 637(1-3), 22-29.

Benfer, M., Kissel, T. (2012). Cellular uptake mechanism and knockdown activity of siRNA-loaded biodegradable DEAPA-PVA-g-PLGA nanoparticles. *Eur J Pharm Biopharm.* 80(2), 247-256.

Benzie, I. F. (2000). Evolution of antioxidant defence mechanisms. *Eur J Nutr*. 39, 53-61.

Bhattarai, N., Edmondson, D., Veiseh, O., Frederick, A., Zhang, M. (2005). Electrospun chitosan-based nanofibers and their cellular compatibility. *Biomaterials*. 26, 6176-6184.

Bhattarai, N., Gunn, J., Zhang, M. (2010). Chitosan-based hydrogels for controlled, localized drug delivery. *Adv Drug Deliv Rev.* 62, 83-99.

Blasiak, J., Sikora, A., Czechowska, A., Drzewoski, J. (2003). Free radical scavengers can modulate the DNA-damaging action of alloxan. *Acta Biochim Pol*. 50, 205-210.

Bourne, L. C., Rice-Evans, C. A. (1997). The effect of the phenolic antioxidant ferulic acid on the oxidation of low-density lipoprotein depends on the pro-oxidant used. *Free Radic Res*. 27(3), 337-344.

Boyle, J. P., Honeycutt, A. A., Narayan, K. M. V., Hoerger, T. J., Geiss, L. S., Chen, H., Thompson, T. J. (2001). Projection of diabetes burden through 2050: Impact of changing demography and disease prevalence in the U.S. *Diabetes Care*. 24, 1936-1940.

Bravo, L. (1998). Polyphenols: chemistry, dietary sources, metabolism, and nutritional significance. *Nutr Rev.* 56, 317-333.

Buanafina, M. M. (2009). Feruloylation in grasses: current and future perspectives. *Mol plant*. 2(5), 861-872.

Buranov, A. U., Mazza, G. (2008). Lignin in straw of herbaceous crops: A review. *Ind Crops Prod*. 28, 237-259.

Buranov, A.U., Mazza, G. (2009). Extraction and purification of ferulic acid from flax shives, wheat and corn bran by alkaline hydrolysis and pressurised solvents. *Food Chem*. 115, 1542-1548.

Cai, Y., Luo, Q., Sun, M., Corke, H. (2004). Antioxidant activity and phenolic compounds of 112 traditional chinese medicinal plants associated with anticancer. *Life Sci*. 74(17), 2157-2184.

Chan, M., Rocha, S., Lehman, M., White, S., Santana, I., Nip, J. (2004). Clinical and in vitro investigation of the effects of ferulic acid on human skin pigmentation. *J Invest Dermatol*. 122, A157-A157.

Chaudhury, A., Das, S. (2011). Recent advancement of chitosan-based nanoparticles for oral controlled delivery of insulin and other therapeutic agents. *AAPS PharmSciTech*. 12(1).

Cho, J. Y., Kim, H. S., Kim, D. H., Jan, J. J., Suh, H. W., Song, D. K. (2005). Inhibitory effects of long-term administration of ferulic acid on astrocyte activation induced by intra cerebroventricular injection of beta-amyloid peptide (1–42) in mice. *Prog Neuropsychopharmacol Biol Psychiatry*. 29, 901-907.

Choi, R., Kim, B. H., Naowaboot, J., Lee, M. Y., Hyun, M. R., Cho, E. J., Lee, E. S., Lee, E. Y., Yang, Y. C., Chung, C. H. (2011). Effects of ferulic acid on diabetic nephropathy in a rat model of type 2 diabetes. *Exp Mol Med*. 43, 676-683.

Choudhury, R., Srai, S. K., Debnam, E., Rice-Evans, C. A. (1999). Urinary excretion of hydroxyl cinnamates and flavonoids after oral and intravenous administration. *Free Radic Biol Med*. 27, 278-286

Coussens, L. M., Werb, Z. (2002). Inflammation and cancer. *Nature*. 420, 860-867.

Couvreur, P. (1988). Polyalkylcyanoacrylates as colloidal drug carriers. *Crit Rev Ther Drug Carr Syst*. 5, 1-20.

Crump, J. A., Collignon, P. J. (2000). Intravascular catheter-associated infections. *Eur J Clin Microbiol Infect Dis*. 19, 1-8.

Dhillon, G. S., Kaur, S., Brar, S. K. (2014). Facile fabrication and characterization of chitosan-based zinc oxide nanoparticles and evaluation of their antimicrobial and antibiofilm activity. *Int Nano Lett*. 4**,** 107-118.

Di Domenico, F., Foppoli, C., Coccia, R., Perluigi. M. (2012). Antioxidants in cervical cancer: Chemopreventive and chemotherapeutic effects of polyphenols. *Biochimica et Biophysica Acta*. 1822, 737-747.

Duan, J., Zhang, Y., Han, S., Chen, Y., Li, B., Liao, M. (2010). Synthesis and in vitro/in vivo anti-cancer evaluation of curcumin-loaded chitosan/poly(butyl cyanoacrylate) nanoparticles. *Int J Pharm.* 400(1-2), 211-220.

Dutt, S. (1925). General synthesis of a-unsaturated acids from malonic acid. *J Chem Soc.* 1, 297-301.

Elgadir, M. A., Uddin, M. S., Ferdosh, S., Adam, A., Chowdhury, A. K., Sarker, M. I. (2015). Impact of chitosan composites and chitosan nanoparticle composites on various drug delivery systems: a review. *J Food Drug Anal*. 23, 619-629.

Ellenson, L. H., Wu, T. C. (2004). Focus on endometrial and cervical cancer. *Cancer Cell*. 5, 533,-538.

Eroğlu, C., Seçme, M., Bağci G., Dodurga, Y. (2015). Assessment of the anticancer mechanism of ferulic acid via cell cycle and apoptotic pathways in human prostate cancer cell lines. *Tumor Biol*. 36, 9437-9446.

Fazary, A. E., Ju, Y. H. (2007). Feruloylesterases as biotechnological tools: current and future perspectives. *Acta Biochim Biophys Sinica*. 39, 811-828.

Fernández, M. A., Sáenz, M. T., García, M. D. (1998). Natural products: anti-inflammatory activity in rats and mice of phenolic acids isolated from scrophulariafrutescens. *J Pharm Pharmacol.* 50(10), 1183-1186.

Fetoni, A. R., Mancuso, C., Eramo, S. L., Ralli, M., Piacentini, R., Barone, E., Paludetti, G., Troiani, D. (2010). In vivo protective effect of ferulic acid against noise-induced hearing loss in the guinea-pig. *Neuroscience*. 169, 1575-1588.

Flemming, H. C., Wingender, J. (2010). The biofilm matrix. *Nature Rev Microbiol*. 8, 623-633.

Forrest, M. K., Wang, F. Y., Fang, C., Mok, H., Wang, K., John, R., Silber, R. G., Ellenbogen, Zhang, M. (2011). Doxorubicin loaded iron oxide nanoparticles overcome multidrug resistance in cancer in vitro. *J Control Release*. 152, 76-83.

Fujita, A., Sasaki, H., Doi, A., Okamoto, K., Matsuno, S., Furuta, H., Nishi, M., Nakao, T., Tsuno, T., Taniguchi, H., Nanjo, K. (2008). Ferulic acid prevents pathological and functional abnormalities of the kidney in Otsuka Long-Evans Tokushima Fatty diabetic rats. *Diabetes Res Clin Pract*. 79, 11-17.

Galati, G., O'Brien, P. J. (2004). Potential toxicity of flavonoids and other dietary phenolics: significance for their chemo preventive and anticancer properties. *Free Radical Biol Med*. 37, 287-303.

Garg, A. K., Buchholz, T. A., Aggarwal, B. B. (2005). Chemo sensitization and radio sensitization of tumors by plant polyphenols. *Antioxid Redox Signal*. 7, 1630-1647.

Ghosh, S., Patil, S., Ahire, M., Kitture, R., Gurav, D. D., Jabgunde, A. M., Cameotra, S., Bellare, J., Jabgunde, A., Chopade, B. A. (2012). Gnidiaglauca flower extract mediated synthesis of gold nanoparticles and evaluation of its chemocatalytic potential. *J Nanobiotechnology*. 10:17.

Gopalakrishnan, L., Ramana, L. N., Sethuraman, S., Krishnan, U. M. (2014). Ellagic acid encapsulated chitosan nanoparticles as anti-hemorrhagic agent. *Carbohydr Polym.* 111, 215-221.

Gorewit, R.C. (1983). Pituitary and thyroid hormone responses of heifers after ferulic acid administration. *J. Dairy Sci*. 66, 624-633.

Graf, E. (1992). Antioxidant potential of ferulic acid. *Free Radic Biol. Med*. 3, 435-513.

Grivennikov, S. I., Karin, M. (2010). Inflammation and oncogenesis: a vicious connection. *Curr Opin Genet Dev*. 20, 65-71.

Hartley, R. D., Ford, C. W. (1989). Phenolic constituents of plant cell walls and wall biodegradability. *Acs Symposium Series*. 399,137-145.

Heim, K. E., Tagliaferro, A. R., Bobilya, D. J. (2002). Flavonoid antioxidants: chemistry, metabolism and structure-activity relationships. *J. Nutr. Biochem*.13, 572-584.

Hemaiswarya, S., Doble, M. (2013). Combination of phenylpropanoids with 5-fluorouracil as anti-cancer agents against human cervical cancer (HeLa) cell line. *Phytomedicine*. 20, 151-158.

Hemaiswarya, S., Doble, M. J. (2010). Synergistic interaction of phenylpropanoids with antibiotics against bacteria. *Med Microbiol*. 59, 1469-1476.

Hertog, M. G., Feskens, E. J., Hollman, P. C., Katan, M. B., Kromhout, D. (1993). Dietary antioxidant flavonoids and risk of coronary heart disease: the zutphen elderly study. *Lancet*. 342, 1007-1011.

Hirabayashi, T., Ochiai, H., Sakai, S., Nakajima, K., Terasawa, K. (1995). Inhibitory effect of ferulic acid and isoferulic acid on murine interleukin-8 production in response to influenza virus infections *in-vitro* and *in-vivo*. *Planta Med*. 61(3), 221-226.

Hiramatsu, K., Tani, T., Kimura, Y., Izumi, S., Nakane, P. K. (1990). Effect of gamma-oryzanol on atheroma formation in hypercholesterolemic rabbits. *Takai J Exp Clin Med*. 15, 299-305.

Hirosi, M., Takahashi, S., Ogawa, K., Futakuchi, M., Shirai, T. (1999). Phenolics: blocking agents for heterocyclic amine-induced carcinogenesis. *Food Chem Toxicol*. 37(9-10), 985-992.

Hosoda, A., Ozaki, Y., Kashiwada, A., Mutoh, M., Wakabayashi, K., Mizuno, K., Nomuraa, E., Taniguchi, H. (2002). Syntheses of ferulic acid derivatives and their suppressive effects on cyclooxygenase-2 promoter activity. *Bioorg Med Chem.* 10, 1189-1196.

Hu, B., Pan, C., Sun, Y., Hou, Z., Ye, H., Hu, B., Zeng, X. (2008). Optimization of fabrication parameters to produce chitosan-tripolyphosphate nanoparticles for delivery of tea catechins. *J Agric Food Chem.* 56, 7451-7458.

Hua, D., Ma, C., Song, L., Lin, S., Zhang, Z., Deng, Z., Xu, P. (2007). Enhanced vanillin production from ferulic acid using adsorbent resin. *Appl Microbiol Biotechnol.* 74, 783-790.

Huang, R. H., Mendis, E., Rajapakse, N., Kim, S. K. (2006). Strong electronic charge as an important factor for anticancer activity of chitooligosaccharides (COS). *Life Sci.* 78(20), 2399-2408.

Hui, Y., Huang, N., Ebbert, L., Bina, H., Chiang, A., Maples, C., Pritt, M., Kern, T., Patel, N. (2007). Pharmacokinetic comparisons of tail-bleeding with cannula- or retro-orbital bleeding techniques in rats using six marketed drugs. *J Pharmacol Toxicol Methods*. 56, 256-264.

Ing, L. Y., Zin, N. M., Sarwar, A., Katas, H. (2012). Antifungal Activity of chitosan nanoparticles and correlation with their physical properties. *Int J Biomater.* 1-9.

Itagaki, S., Kobayashi, Y., Otsuka, Y., Kubo, S., Kobayashi, M., Hirano,T. (2005). Food–drug interaction between ferulic acid and nateglinide involving the fluorescein/H+cotransport system. *J Agric Food Chem*. 53, 2499-2502.

Itagaki, S., Kurokawa, T., Nakata, C., Saito, Y., Oikawa, S., Kobayashi, M., Hirano, T., Iseki, K. (2009). In vitro and in vivo antioxidant properties of ferulic acid: A comparative study with other natural oxidation inhibitors. *Food Chem*. 114, 466-471.

Jain, S., Chattopadhyay, S., Jackeray, R., Zainul Abid, C. V., Singh, H. (2013). Novel functionalized fluorescent polymeric nanoparticles for immobilization of biomolecules. *Nanoscale*. 5, 6883-6892.

Janes, K. A., Fresneau, M. P., Marazuela, A., Fabra, A., Alonso, M. J. (2001). Chitosan nanoparticles as delivery systems for doxorubicin. *J Control Release*. 73, 255-267.

Jang, K. I., Lee, H. G. (2008). Stability of chitosan nanoparticles for l-ascorbic acid during heat treatment in aqueous solution. *J Agric Food Chem*. 56, 1936-1941.

Jangra, A., Datusalia, A. K., Khandwe, S., Sharma, S.S. (2013). Amelioration of diabetes-induced neurobehavioral and neurochemical changes by melatonin and nicotinamide: Implication of oxidative stress–PARP pathway. *Pharmacol Biochem Behav.* 114–115, 43–51.

Janicke, B., Hegardt, C., Krogh, M., Onning, G., Akesson, B., Cirenajwis, H. M., Oredsson, S. M. (2011). The antiproliferative effect of dietary fiber phenolic compounds ferulic acid and p-coumaric acid on the cell cycle of Caco-2 cells. *Nutr Cancer*. 63, 611-622.

Jayakumar, R., Reis, R. L., Mano, J. F. (2007). Synthesis and characterization of pH-sensitive thiol-containing chitosan beads for controlled drug delivery applications. *Drug Deliv*. 14, 9-17.

Jayaprakasam, B., Vanisree, M., Zhang, Y., Dewitt, D. L., Nair, M. G. (2006). Impact of alkyl esters of caffeic and ferulic acids on tumor cell proliferation, cyclooxygenase enzyme, and lipid peroxidation. *J Agric Food Chem*. 54, 5375-5381.

Jeong, Y. C., Jae, H. M., Keun, H. P. (2000). Isolation and identification of 3-methoxy-4-hydroxybenzoic acid and 3-methoxy-4- hydroxycinnamic acid from hot water extracts of Hoveniadulcis Thumb and confirmation of their antioxidative and antimicrobial activity. *Korean J Food Sci Technol*. 32, 1403-1408.

Jung, E. H., Kim, S. R., Hwang, I. K., Ha, T. Y. (2007). Hypoglycemic effects of a phenolic acid fraction of rice bran and ferulic acid in C57BL/KsJ-db/db mice. *J Agric Food Chem*. 55, 9800-9804.

Just, M. J., Recio, M. C., Giner, R. M., Cullar, M. J., Manez, S., Bilia, A. R. (1998). Antiinflammatory activity of unusual Lupane saponins from Bupleurum fruticescens. *Plant Med*. 64, 404-407.

Kaloti, M., Bohidar, H. B. (2010). Kinetics of coacervation transition versus nanoparticle formation in chitosan–sodium tripolyphosphate solutions. *Colloids Surf B Biointerfaces*. 81, 165-173.

Kampa, M., Alexaki, V. I., Notas, G., Nifli, A. P., Nistikaki, A., Hatzoglou, A., Bakogeorgou, E., Kouimtzoglou, E., Bleka, G., Boskou, D., Gravanis, A., Castanas, E. (2004). Antiproliferative and apoptotic effects of selective phenolic acids on T47D human breast cancer cells: potential mechanisms of action. *Breast Cancer Res*. 6, 63-74.

Kanaze, F. I., Bounartzi, M. I., Georgarakis, M., Niopas, I. (2006). Pharmacokinetics of the citrus flavanone aglycones, hesperetin and naringenin after single oral administration in human subjects. *Eur J Clin Nutr*. 61(4), 472-477.

Kanski, J., Aksenova, M., Stoyanova, A., Butterfield, D. A. (2002). Ferulic acid antioxidant protection against hydroxyl and peroxyl radical oxidation in synaptosomal and neuronal cell culture systems in vitro: structure–activity studies. *J Nutr Biochem.* 13, 273-281.

Karthikeyan, S., Kanimozhi, G., Prasad, N. R., Mahalakshmi, R. (2011). Radiosensitizing effect of ferulic acid on human cervical carcinoma cells in vitro. *Toxicol In Vitro*. 25, 1366-1375.

Kawabata, K., Yamamoto, T., Hara, A., Shimizu, M., Yamada, Y., Matsunaga, K., Tanaka, T., Mori, H. (2000). Modifying effects of ferulic acid on azoxymethane-induced colon carcinogenesis in F344 rats. *Cancer Lett*. 157(1), 15-21.

Kayahara, H., Miao, Z., Fujiwara, G. (1999). Synthesis and biological activities of ferulic acid derivatives. *Anticancer Res*. 19, 3763-3768.

Keawchaoon, L., Yoksan, R. (2001). Preparation, characterization and in vitro release study of carvacrol-loaded chitosan nanoparticles. *Colloids Surf B Biointerfaces*. 84, 163-171.

Khan, W., Sharma, S. S., Kumar, N. (2013). Bioanalytical method development, pharmacokinetics, and toxicity studies of paromomycin and paromomycin loaded in albumin microspheres. *Drug Test Anal.* 5(6), 453-460.

Khanduja, K. L., Avti, P. K., Kumar, S., Mittal, N., Sohi, K. K., Pathak, C. M. (2006). Antiapoptotic activity of caffeic acid, ellagic acid and ferulic acid in normal human peripheral blood mononuclear cells: a Bcl-2 independent mechanism. *Biochim Biophys Acta.* 1760, 283-289.

Ko, J. A., Park, H. J., Hwang, S. J., Park, J. B., Lee J. S. (2002). Preparation and characterization of chitosan J. A. Microparticles intended for controlled drug delivery. *Int J Pharm.* 249, 165-174.

Koh, P. O. (2012). Ferulic acid modulates nitric oxide synthase expression in focal cerebral ischemia. *Lab Anim Res.* 28, 273-278.

Kojic, E. M., Darouiche, R. O. **(**2004). Candida infections of medical devices. *Clin Microbiol Rev*.17**,** 255-267.

Kondo, T., Mizuno, K. Kato, T. (1990). Cell wall-bound p-coumaric acids in Italian ryegrass. *Can J Plant Sci*. 71, 495-499.

Konishi, Y., Shimizu, M. (2003). Transepithelial transport of ferulic acid by monocarboxylic acid transporter in Caco-2 cell monolayers. *Biosci Biotechnol Biochem*. 67, 856-862.

Konishi, Y., Zhao, Z. H., Shimizu, M. (2006). Phenolic acids are absorbed from the rat stomach with different absorption rates. *J Agric Food Chem*. 54(20), 7539-7543.

Kroon, P. A., Garcia, C. M. T., Fillingham, I. J., Williamson, G. (1999). Release of ferulic acid dehydrodimers from plant cell walls by feruloylesterases. *J Sci Food Agric.* 79(3), 428-434.

Kuenzig, W., Chau, J., Norkus, E., Holowaschenko, H., Newmark, H., Mergens, W. (1984). Caffeic and ferulic acid as blockers of nitrosamine formation. *Carcinogenesis*. 5, 309-313.

Kumamoto, C. A. (2002). Candida biofilms. *Curr Opin Microbiol*. 5, 608-611.

Kumamoto, C. A., Vinces, M.D. (2005). Alternative Candida albicans lifestyles: Growth on Surfaces. *Annu Rev Microbiol.* 59, 113-133.

Kumar, A., Srivastavaa A., Galaevb, I. Y., Mattiasson, B. (2007). Smart polymers: physical forms and bioengineering applications. *Prog Polym Sci*. 32, 1205-1237.

Kumar, N., Kumar, S., Abbat, S., Nikhil, K., Sondhi, S. M., Bharatam, P. V., Roy, P., Pruthi, V. (2016). Ferulic acid amide derivatives as anticancer and antioxidant agents: synthesis, thermal, biological and computational studies. *Med Chem Res*. 25, 1175-1192.

Kumar, P., Mishra, S., Malik, A., Satya, S. (2014). Preparation and characterization of PEG-Mentha oil nanoparticles for housefly control. *Colloids Surf B Biointerfaces*. 116, 707-713.

Kumar, U., Sagar, R., Bhandari, A., Srivastava, A. K. (2015). Evaluation of anti-inflammatory activity of methanolic and toluene extract of Dipteracanthus prostrates nees. *Int J Pharmacognosy and Phytochem Res.* 7(3), 435-439.

Kumari, A., Yadav, S. K., Yadav, S. C. (2010). Biodegradable polymeric nanoparticles based drug delivery systems. *Colloids Surf B Biointerfaces*. 75, 1-18.

Kyoungho, S., Yun-Hee, K., Inik, C. (2001). IFNK sensitizes ME-180 human cervical cancer cells to TNFK-induced apoptosis by inhibiting cytoprotective NF-UB activation. *FEBS Lett*. 495, 66–70.

Labrecque, L., Lamy, S., Chapus, A., Mihoubi, S., Durocher, Y., Cass, B. (2005). Combined inhibition of PDGF and VEGF receptors by ellagic acid, a dietary derived phenolic compound. *Carcinogenesis*. 26(4), 821-826.

LaFleur, M. D., Kumamoto, C. A., Lewis, K. (2006). Candida albicans biofilms produce antifungal-tolerant persister cells. *Antimicrob Agents Chemother*. 50, 3839-3846.

Lam, T. B., Iiyama, K., Stone, B. A. (1994). Determination of etherified hydroxycinnamic acids in cell-walls of grasses. *Phytochemistry*. 36, 773-775.

Lam, T. B., Kadoyab, K., Iiyama. K. (2001). Bonding of hydroxycinnamic acids to lignin: ferulic and p-coumaric acids are predominantly linked at the benzyl position of lignin, not the b-position, in grass cell walls. *Phytochemistry*. 57, 987-992.

Lane, R. K., Matthay, M. A. (2002). Central line infections. *Curr Opin Crit Care*. 8, 441-448.

Lee, D. S., Woo, J. Y., Ahn, C. B., Je, J. Y. (2014). Chitosan hydroxycinnamic acid conjugates: Preparation, antioxidant and antimicrobial activity. *Food Chem*. 148, 97-104.

Lee, J. S., Kim, G. H., Lee, H. G. (2010). Characteristics and antioxidant activity of Elsholtzia splendens extract-loaded nanoparticles. *J Agric Food Chem*. 58, 3316-3321.

Li, O. U., Ling Y., Kong, Zhang, X., Niwa, M. (2003). Oxidation of Ferulic acid by momordica charantia peroxidase and related anti-inflammation activity changes. *Biol Pharm Bull.* 26(11), 1511-1516.

Li, Z., Jiang, H., Xu, C., Gu, L. (2015). A review: using nanoparticles to enhance absorption and bioavailability of phenolic phytochemicals. *Food Hydrocoll*. 43, 153-164.

Liang, J., Li, F., Fang, Y., Yang, W., An, X., Zhao, L., Xin, Z., Cao, L., Hu, Q. (2011). Synthesis, characterization and cytotoxicity studies of chitosan-coated tea polyphenols nanoparticles. *Colloids Surf B Biointerfaces.82*, 297-301.

Lin, F. H., Lin, J. Y., Gupta, R. D., Tournas, J. A., Burch, J. A., Selim, M. A. (2005). Ferulic acid stabilizes a solution of vitamins C and E and doubles its photoprotection of skin. *J Invest Dermatol.* 125, 826-832.

Liu, H., Du, Y., Wang, X., Sun, L. (2004). Chitosan kills bacteria through cell membrane damage. *Int J Food Microbiol*. 95, 147-155.

Liu, J., Wen, X., Lu, J., Kan, J., Jin, C. (2014). Free radical mediated grafting of chitosan with caffeic and ferulic acids: structures and antioxidant activity. *Int J Biol Macromol*. 65, 97-106.

Liu, N., Chen, X. G., Park H. J., Liu, C. G., Liu, C. S., Meng, X. H., Yu, L. J. (2006). Effect of MW and conc. of chitosan on antibacterial activity of *Escherichia Coli*. *Carbohydr Polym*. 64, 60-65.

Liu, R. H. (2003). Health benefits of fruits and vegetables are from additive and synergistic combination of phytochemicals. *Am J Clin Nutr*. 78, 517S-520S.

Liu, Z., Jiao, Y., Wang, Y., Zhou, C., Zhang, Z. (2008). Polysaccharides-based nanoparticles as drug delivery systems. *Adv Drug Deliv Rev.* 60, 1650-1662.

Lo, H. H., Chung, J. G. (1999). The effects of plant phenolics, caffeic acid, chlorogenic acid and ferulic acid on arylamine*N*-acetyltransferase activities in human gastrointestinal microflora. *Anticancer Res.* 19, 133-139.

Lorenzo-Lamosa, M. L., Remunan-Lopez, C., Vila-Jato, J. L., Alonso, M. J. (1998). Design of microencapsulated chitosan microspheres for colonic drug delivery. *J. Control Release.* 52, 109-118.

Luo, Y., Wang, Q. (2013). Recent advances of chitosan and its derivatives for novel applications in food science. *J Food Processing & Beverages*. 1(1): 13.

Maezaki, Y., Tsuji, K., Nakagawa, Y., Kawai, Y., Akimoto, M. (1993). Hypocholesterolemic effect of chitosan in adult males. *Biosci Biotechnol Biochem*. 57, 1439-1444.

Mamiya, T., Kise, M., Morikawa, K. (2008). Ferulic acid attenuated cognitive deficits and increase in carbonyl proteins induced by buthionine-sulfoximine in mice. *Neurosci Lett*. 430, 115-118.

Manach, C., Scalbert, A., Morand, C., Rémésy, C., Jiménez, L. (2004). Polyphenols: food sources and bioavailability. *Am J Clin Nutr. 79,* 727-747.

Mancuso, C., Santangelo, R. (2014). Ferulic acid: pharmacological and toxicological aspects. *Food Chem Toxicol.* 65, 185-195.

Mathew, S., Abraham, T. E. (2006). Bioconversions of ferulic acid, a hydroxycinnamic acid. *Crit Rev Microbiol*. 32, 115-125.

Mathew, S., Abraham, T. E. (2008). Characterisation of ferulic acid incorporated starche chitosan blend films. *Food Hydrocoll*. 22, 826-835.

Mattila, P., Hellstrom, J. (2007). Phenolic acids in potatoes, vegetables, and some of their products. *J. Food Comp Anal.* 20(3-4), 152-160.

Mattila, P., Pihlava, J. M., Hellstrom, J. (2005). Contents of phenolic acids, alkyl- and alkenylresorcinols, and avenanthramides in commercial grain products. *J Agric Food Chem.* 53(21), 8290-8295.

Maurya, D. K., Devasagayam, T. A. (2010). Antioxidant and prooxidant nature of hydroxycinnamic acid derivatives ferulic and caffeic acids. *Food Chem Toxicol*. 48, 3369-3373.

Merlin, J. P., Prasad R. N., Shibli, S. M. (2012). Ferulic acid loaded poly-d, l-lactide-co-glycolide nanoparticles: systematic study of particle size, drug encapsulation efficiency and anticancer effect in non-small cell lung carcinoma cell line in vitro. *Biomed Prev Nutr*. 2, 69-76.

Mi, F. L., Shyu, S. S., Kuan, C. Y., Lee, S. T., Lu, K. T., Jang, S. F. (1999a). Chitosan-polyelectrolyte complexation for thepreparation of gel beads and controlled release of anticancer drug. I. Enzymatic hydrolysis of polymer. *J Appl Polym Sci.* 74, 1868-1879.

Mori, H., Kawabata, K., Yoshimi, N., Tanaka, T., Murakami, T., Okada, T., Murai, H. (1999). Chemopreventive effects of ferulic acid on oral and rice germ on large bowel carcinogenesis. *Anticancer Res.* 19, 3775-3778.

Mori, T., Koyama, N., Guillot-Sestier, M. V., Tan, J., Town, T. (2013). Ferulic acid is a nutraceutical b-secretase modulator that improves behavioral impairment and alzheimer-like pathology in transgenic mice. *PLoS One*. 8(2), e55774.

Mukherjee, P. K., Maiti, K., Mukherjee, K., Houghton, P. J. (2006). Leads from Indian medicinal plants with hypoglycemic potentials. *J Ethnopharmacol.* 106, 1-28.

Mukhopadhyay, P., Sarkar, K., Chakraborty, M., Bhattacharya, S., Mishra, R., Kundu. P. P. (2013). Oral insulin delivery by self-assembled chitosan nanoparticles: In vitro and in vivo studies in diabetic animal model. *Mater Sci Eng C*. 33, 376-382.

Müller, R. H., Jacobs, C., Kayser, O. (2001). Nanosuspensions as particulate drug formulations in therapy rationale for development and what we can expect for the future. *Adv Drug Deliv Rev.* 47, 3-19.

Munin, A., Levy, F. E. (2011). Encapsulation of natural polyphenolic compounds; a review. *Pharmaceutics*. 3, 793-829.

Murakamia, A., Nakamurab, Y., Koshimizua, K., Takahashia, D., Matsumotoa, K., Hagiharaa, K., Taniguchic, H., Nomurac, E., Hosodac, A., Tsunod, T., Marutad, Y., Kime, H. W., Kawabatae, K., Ohigashi, H. (2002). FA15, a hydrophobic derivative of ferulic acid, suppresses inflammatory responses and skin tumor promotion: comparison with ferulic acid. *Cancer Lett*. 180, 121–129.

Nagpal, K., Singh, S. K., Mishra, D. N. (2010). Chitosan nanoparticles: a promising system in novel drug delivery. *Chem Pharm Bull.* 58(11), 1423-1430.

Nair, H. B., Sung, B., Yadav, V. R., Kannappan, R., Chaturvedi, M. M., Aggarwal, B. B. (2010). Delivery of antiinflammatory nutraceuticals by nanoparticles for the prevention and treatment of cancer. *Biochem Pharmacol*. 80, 1833-1843.

Nallamuthu, I., Devi, A., Khanum F. (2014). Chlorogenic acid loaded chitosan nanoparticles with sustained release property, retained antioxidant activity and enhanced bioavailability. *Asian J Pharm Sci*. 1-9.

Noumura, E., Kashiwada, A., Hosoda, A., Nakamura, K., Morishita, H., Tsuno, T., Tanigushi, H. (2003). Synthesis of amide compounds of ferulic acid and their stimulatory effects on insulin secretion in vitro. *Bioorg Med Chem*. 11(17), 3807-3813.

Ohnishi, M., Matuo, T., Tsuno, T., Hosoda, A., Nomura, E., Taniguchi, H., Sasaki. H., Morishita. H. (2004). Antioxidant activity and hypoglycemic effect of ferulic acid in STZ-induced diabetic mice and KK-Ay mice. *Bio Factors*. 21, 315-319.

Ohsaki, A.Y., Shirakawa, H., Koseki, T., Komai, M. (2008). Novel effects of a single administration of ferulic acid on the regulation of blood pressure and the hepatic lipid metabolic profile in stroke-prone spontaneously hypertensive rats. *J Agric Food Chem.* 56, 2825-2830

Ohta, T., Semboku, N., Kuchii, A., Egashira, Y., Sanada, H. (1997). Antioxidant activity of corn bran cell-wall fragments in the LDL oxidation system. *J Agric Food Chem*. 45, 1644-1648.

Omamoto, H., Hiroskitckan, U. Y. (1981). STZ and alloxan induces DNA strand breaks and poly (ADP ribose) synthatase in pancreatic islets. *Nature*. 294(19), 284-286.

Onoue, S., Ochi, M., Yamada, S. (2011). Development of (-)-epigallocatechin-3- gallate (EGCG)-loaded enteric microparticles with intestinal mucoadhesive property. *Int J Pharm.* 410(1-2), 111-113.

Orsolic, N., Gajski, G., Garaj-Vrhovac, V., Dikic, D., SpacirPrskalo, Z., Sirovina, D. (2011). DNA-protective effects of quercetin or naringenin in alloxan-induced diabetic mice. *E J Pharmocol*. 656, 110-118.

Ortega, M., Marco, F., Soriano, A., Almela, M., Martı´nez, J. A., Lopez, J., Pitart, J., Mensa, C. (2011). Candida species bloodstream infection: epidemiology and outcome in a single institution from 1991 to 2008. *J Hosp Infect.* 77, 157-161.

Ou, S., Kwok, K. C. (2004). Ferulic acid: pharmaceutical functions, preparation and applications in foods. *J Sci Food Agric*. 84, 1261-1269.

Padiya, R., Khatua, T. N., Bagul, P. K., Kuncha, M., Banerjee, S. K. (2011). Garlic improves insulin sensitivity and associated metabolic syndromes in fructose fed rats. *Nutr Metab*. 8:53.

Palacios, J. P. C. (1990). Poly (ferulic acid) by oxalyl chloride activated polycondensation. *New Polymeric Materials*. 2, 167-174.

Pan, Y, Li, Y. J., Zhao, H. Y. (2002) Bioadhesive polysaccharide in protein delivery system: chitosan nanoparticles improve the intestinal absorption of insulin in vivo. *Int J Pharm*. 249(1-2), 139-147.

Pannala, A. S., Razaq, R., Halliwell, B., Singh, S., Rice-Evans, C. A. (1998). Inhibition of peroxynitrite dependent tyrosine nitration by hydroxycinnamates: nitration or electron donation? *Free Radic Biol Med*. 24, 594-606.

Panwar, R., Sharma, A. K., Dutt, D., Pruthi, V. (2015). Phenolic acids from Parthenium hysterophorus: evaluation of bioconversion potential as free radical scavengers and anticancer agents. *Adv Biosci Biotechnol*. 6,11-17.

Papadimitriou, S., Bikiaris, D., Avgoustakis, K., Karavas, E., Georgarakis, M. (2008). Chitosan nanoparticles loaded with dorzolamide and pramipexole. *Carbohydr Polym*. 73, 44-54.

Park, J. H., Saravanakumar, G., Kim, K., Kwon, I. C. (2010). Targeted delivery of low molecular drugs using chitosan and its derivatives. *Adv Drug Deliver Rev*. 62, 28-41.

Pauli, A. (2006). Anticandidal low molecular compounds from higher plants with special reference to compounds from essential oils. *Med Res Rev*. 26, 223-68.

Pemmaraju, S. C., Pruthi, P. A., Prasad, R., Pruthi, V. (2013). Candida albicans biofilm inhibition by synergistic action of terpenes and fluconazole. *Ind J Exp Biol*. 51, 1032-1037.

Poquet, L., Clifford, M. N., Williamson, G. (2008) Transport and metabolism of ferulic acid through the colonic epithelium. *Drug Metab Dispos*. 36,190-197.

Prabhakar, P. K., Doble, M. (2008). A target based therapeutic approach towards diabetes mellitus using medicinal plants. *Curr Diabetes Rev*. 4, 291-308.

Prabhakar, P. K., Prasad, R., Ali, S., Doble, M. (2013). Synergistic interaction of ferulic acid with commercial hypoglycemic drugs in streptozotocin induced diabetic rats. *Phytomedicine*. 20, 488-494.

Punyani, S., Singh, H. (2008). Synthesis, characterization, and antimicrobial properties of novel quaternary amine methacrylate copolymers. *J Appl Polym Sci*. 107 (5), 2861- 2870.

Qi, L. F., Xu, Z. R. (2006). In vivo antitumor activity of chitosan nanoparticles. *Bioorg Med Chem Lett*. 16, 4243-4245.

Qi, L. F., Xu, Z. R., Jiang, X., Li, Y., Wang, M. Q. (2005a). Cytotoxic activities of chitosan nanoparticles and copper-loaded nanoparticles. *Bioorg Med Chem Lett*. 15, 1397-1399.

Qi, L. F., Xu, Z. R., Li, Y., Jiang, X., Han, X. Y. (2005b). In vitro effects of chitosan nanoparticles on proliferation of human gastric carcinoma cell line MGC803 cells. *World J Gastroenterol*. 11(33), 5136-5141.

Qi, L. F., Xua, Z. R., Chen, M. (2007). In vitro and in vivo suppression of hepatocellular carcinoma growth by chitosan nanoparticles. *Eur J Cancer*. 43, 184-193.

Qi, L., Xu, Z., Jiang, X., Hu, C., Zou, X. (2004). Preparation and antibacterial activity of chitosan nanoparticles. *Carbohydr Res*. 339, 2693-2700.

Qin, C., Li, H., Xiao, Q., Liu, Zhu J., Du, Y. (2006). Water-solubility of chitosan and its antimicrobial activity. *Carbohydr Polym.* 63, 367-374.

Ralph, J., Helm, R. F. (1993). Lignin-hydroxycinnamoyl model compounds related to forage cell wall structure. 2. Ester-linked structures. *J Agric Food Chem. 41* (4) 570–576

Ramage, G., Saville, S. P., Thomas, D. P., Ribot, J. L. (2005). Candida biofilms: an update. *Eukaryot Cell*. 4, 633-638.

Ramage, G., Wickes, J. B., Lopez, L. (2001). Biofilms of *Candida albicans* and their associated resistance to antifungal agents. *Am Clin Lab*. 20, 42-44.

Ramar, M., Manikandan, B., Raman, T., Priyadarsini, A., Palanisamy, S., Velayudam, M., Munusamy, A., Prabhu, M. N., Vaseeharan, B. (2012). Protective effect of ferulic acid and resveratrol against alloxan-induced diabetes in mice. *Eur J Pharmacol*. 690(1-3), 226-235.

Raut, J. S., Shinde, R. B., Chauhan, N. M., Karuppayil, S. M. (2014). Phenylpropanoids of plant origin as inhibitors of biofilm formation by *Candida albicans*. *J Microbiol Biotechn.* 24, 1216-1225.

Roehm, N., Rogers, G., Hatfield, S., Glasebrook, A. (1991). An improved colorimetric assay for cell proliferation and viability utilizing the tetrazolium salt XTT. J. *Immunol Methods.*142, 257-265.

Roller, S., Covill, N. (1999). The antifungal properties of chitosan in laboratory media and apple juice. *Int J Food Microbiol*. 47, 67-77.

Rondini, L., Peyrat-Maillard, M. N., Marsset-Baglieri, A., Fromentin, G., Durand, P., Tome, D., Prost, M., Berset, C. (2004). Bound ferulic acid from bran is more bioavailable than the free compound in rat. *J Agric Food Chem*. 52, 4338-4343.

Rosazza, J. P., Huang, Z., Dostal, L., Volm, T., Rousseau, B. (1995). Biocatalytic transformations of ferulic acid: An abundant aromatic natural product. *J Industrial Microbiol Biotechno*. 15: 457−471

Rossi, C., Schoubben, A., Ricci, M., Perioli, L., Ambrogi, V., Latterini, L., Aloisi, G. G., Rossi, A. (2005). Intercalation of the radical scavenger ferulic acid in hydrotalcite-like anionic clays. *Int J Pharm*. 295, 47-55.

Roy, S., Metya, S. K., Sannigrahi, S., Rahaman, N., Ahmed, F. (2013). Treatment with ferulic acid to rats with streptozotocin-induced diabetes: effects on oxidative stress, pro-inflammatory cytokines, and apoptosis in the pancreatic b cell. *Endocrine*. 44, 369-379.

Saija, A., Tomaino, A., Lo Cascio, R., Trombetta, D., Proteggente, A., De Pasquale, A. (1999). Ferulic and caffeic acids as potential protective agents against photooxidative skin damage. *J Sci Food Agr.* 79, 476-480.

Saija, A., Tomaino, A., Trombetta, D., De Pasquale, A., Uccella, N., Barbuzzi, T., Paolino, D., Bonina, F. (2000). In vitro and in vivo evaluation of caffeic and ferulic acids as topical photoprotective agents. *Int J Pharm.* 199, 39-47.

Saini, A. K., Arun, K. H., Sharma, S. S. (2007). Preventive and curative effect of edaravone on nerve functions and oxidative stress in experimental diabetic neuropathy. *Eur J Pharmacol*. 568, 164-172.

Saini, P., Gayen, P., Nayak, A., Kumar, D., Mukherjee, N., Pal, B. C., Santi, P., Babu, S. (2012). Effect of ferulic acid from Hibiscus mutabilis on filarial parasite Setariacervi: Molecular and biochemical approaches. *Parasitol Int.* 61, 520-531.

Sakai, S., Kawamata, H., Kogure, T., Mantani, N., Terasawa, K., Umatake, M., Ochiai, H. (1999). Inhibitory effect of ferulic acid and isoferulic acid on the production of macrophage inflammatory protein-2 in response to respiratory syncytial virus infection in RAW264.7 cells. *Mediat Inflamm*. 8, 173-175

Salmaso, S., Bersani, S., Semenzato, A., Caliceti, P. (2007). New cyclodextrin bioconjugates for active tumour targeting. *J Drug Target*. 15, 379-390.

Salunke, G. R., Ghosh, S., Santos, K. J., Khade, S., Vashisth, P., Kale, T., Pruthi, V., Kundu, G., Bellare, J. R., Chopade, B. A. (2014). Rapid efficient synthesis and characterization of silver, gold, and bimetallic nanoparticles from the medicinal plant Plumbagozeylanica and their application in biofilm control. *Int J Nanomedicine*. 9, 2635-2653.

Scalbert, A., Monties, B., Lallemand, J. Y., Guittet, E., Rolando, C. (1985). Ether linkage between phenolic acids and lignin fractions from wheat straw. *Phytochemistry*. 24, 1359-1362.

Scavariello, E. M., Ardlano, D. B. (1998). g-Oryzanol: an important component in rice bran oil. *Arch Latinoam Nutr*. 48, 7-12.

Schroder, F. H., Hugosson, J., Roobol, M. J., Tammela, T. L., Ciatto, S., Nelen, V. (2009). Screening and prostate-cancer mortality in a randomized European study. *N Engl J Med.* 360(13), 1320-1328.

Seiwert, T. Y., Salama, J. K., Vokes, E. E. (2007). The concurrent chemoradiation paradigm-general principles. *Natl Clin Pract Oncol*. 4, 86-100.

Sharma, D. R., Wani, W. Y., Sunkaria, A., Ramesh, J. L., Kandimalla., Verma, D., Cameotra, S. S., Gill, K. D. (2013). Quercetin protects against chronic aluminum-induced oxidative stress and ensuing biochemical, cholinergic, and neurobehavioral impairments in rats. *Neurotox Res*. 23, 336-357.

Singh, N., Pemmaraju, S. C., Pruthi, P. A., Cameotra, S. S., Pruthi, V. (2013). Candida biofilm disrupting ability of di-rhamnolipid (rl-2) produced from Pseudomonas aeruginosa DSVP20. *Appl Biochem Biotech*. 169, 2374-2391.

Singh, R., Shedbalkar, U. U., Wadhwani, S. A., Chopade, B. A. (2015). Bacteriagenic silver nanoparticles: synthesis, mechanism, and applications. *Appl Microbiol Biotechnol*. 4579-4593.

Singh, T., Vesentini, D., Singh, A. P., Daniel, G. (2008). Effect of chitosan on physiological, morphological, and ultrastructural characteristics of wood-degrading fungi. *Int Biodeterior Biodegrad.* 62, 116-124.

Smith, M. M., Hartley, R. D. (1983). Occurrence and nature of ferulic acid substitution of cell-wall polysaccharides in graminaceous plants. *Carbohydr Res.118*, 65-80.

Soane, R. J., Frier, M. (1999). Evaluation of the clearance characteristics of bioadhesive systems in humans. *Int J Pharm*. 178, 55-65.

Sofia, P., Dimitrios, B., Konstantinos, A., Evangelos, K., Manolis, G. (2008). Chitosan nanoparticles loaded with dorzolamide and pramipexole. *Carbohydr Polym*. 73, 44-54.

Sohn, Y. T., Oh, J. H. (2003). Characterization of physicochemical properties of ferulic acid, *Arch Pharm Res*. 26, 1002-1008.

Sornalakshmi, V., Soris P. T., Paulpriya, K., Lincy, P. M., Mohan, V. R. (2016). Oral glucose tolerance test (OGTT) in normal control and glucose induced hyperglycemic rats with hedyotis leschenaultiana DC. *International Journal of Toxicological and Pharmacological Research.* 8(1), 59-62.

Spencer, J. P., Chowrimootoo, G., Choudhury, R., Debnam, E. S., Srai, S.K., Rice-Evans, C. (1999). The small intestine can both absorb and glucuronidate luminal flavonoids. *FEBS Letters*. 458, 224-230.

Spinas, G. A. (1999). The dual role of nitric oxide in islet ß-cells. *News Physiol Sci.* 14: 49-54.

Srinivasan, M., Rukkumani, R., Ram Sudheer, A., Menon, V. P. (2005). Ferulic acid, a natural protector against carbon tetrachloride-induced toxicity. *Fundam Clin Pharmacol*. 19, 491-496.

Srinivasan, M., Sudheer, A. R., Menon, V. P. (2007). Ferulic acid: therapeutic potential through its antioxidant property. *J Clin Biochem Nutr*. 40, 92-100.

Srinivasan, M., Sudheer, A. R., Pillai, K. R., Kumar, P. R., Sudhakaran, P. R., Menon, V. P. (2006). Influence of ferulic acid on gamma-radiation induced DNA damage, lipid peroxidation and antioxidant status in primary culture of isolated rat hepatocytes. *Toxicology*. 228, 249-258.

Subburayan, K., Govindhasamy, K., Nagarajan, R. P., Rajendran, M. (2011). Radiosensitizing effect of ferulic acid on human cervical carcinoma cells in vitro. *Toxicol In Vitro*. 25:1366–1375.

Sudheer, A. R., Muthukumaran, S., Kalpana, C., Srinivasan, M., Menon, V. P. (2007). Protective effect of ferulic acid on nicotine-induced DNA damage and cellular changes in cultured rat peripheral blood lymphocytes: a comparison with Nacetylcysteine. *Toxicol In Vitro*. 21, 576-585.

Suleyman, H., Demirezer, L. O., Kuruuzum, A., Banoglu, Z. N., Gocer, F., Ozbakir, G., Gepdiremen, A. (1991). Antiinflammatory effect of the aqueous extract from Rumexpatientia L. roots. *J Ethnopharmacol*. 65, 141-148.

Suzuki, K., Mikami, T., Okawa, Y., Tokoro, A., Suzuki, S., Suzuki, M. (1986). Antitumor effect of hexa-N-acetylchitohexaose and chitohexaose. *Carbohydr Res.* 151, 403-408.

Tada, Y., Ikeda, T., Takahashi, H., Yano, N., Yuzawa, K., Nagasawa, A. (2001). Subchronic toxicity test of ferulic acid, natural food additive, in F344 rats. *Tokyo Metropolitan Research Laboratory of Public Health*. 52, 267-271.

Tada, Y., Tayama, K., Aoki, N. (1999). Acute oral toxicity of ferulic acid, natural food additive, in rats. *Tokyo Metropolitan Research Laboratory of Public Health*. 50, 311-313.

Tan, H., Ma, R., Lin, C., Liu, Z., Tang, T. (2013). Quaternized chitosan as an antimicrobial agent: antimicrobial activity, mechanism of action and biomedical applications in orthopedics. *Int J Mol Sci.* 14, 1854-1869.

Tilay, A., Bule, M., Kishenkumar, J., Annapure, U. (2008). Preparation of ferulic acid from agricultural wastes: its improved extraction and purification. *J Agric Food Chem*. 56, 7644-7648.

Tokoro, A., Tatewaki, N., Suzuki, K., Mikami, T., Suzuki, S., Suzuki, M. (1988). Growth-inhibitory effect of hexa-N-acetylchitohexaose and chitohexaose against meth-A solid tumor. *Chem Pharm Bull.* 36, 784-790.

Trombino, S., Cassano, R., Ferrarelli, T., Barone, E., Picci, N., Mancuso, C. (2013). Transferulic acid-based solid lipid nanoparticles and their antioxidant effect in rat brain microsomes. *Colloids Surf B: Biointerf*. 109, 273-279.

Tsou, M. F., Hung, C. F., Lu, H. F., Wu, L. T., Chang, S. H., Chang, H. L., Chen, G. W., Chung, J. G. (2000). Effects of caffeic acid, chlorogenic acid and ferulic acid on growth and arylamineNacetyltransferase activity in *Shigellasonnei* (group D). *Microbios.* 101, 37-46.

Ugochukwu, N. H., Babady, N. E. (2003). Antihyperglycemic effect of aqueous and ethanolic extracts of Gongronema latifolium leaves on glucose and glycogen metabolism in livers of normal and streptozotocin-induced diabetic rats. *Life Sci*. 73, 1925-1938.

Vashisth, P., Sharma, M., Kumar, N., Singh, H., Panwar, R., Pruthi, P. A., Pruthi, V. (2015). Antiproliferative activity of ferulic acid encapsulated electrospun PLGA/PEO nanofibers against MCF- 7 human breast carcinoma cells. *3 Biotech*, 5, 303-315.

Vemula, P. K, Li, J., John, G. (2006). Enzyme catalysis: tool to make and break amygdalin hydrogelators from renewable resources: a delivery model for hydrophobic drugs. *J Am Chem Soc*. 128, 8932-8938.

Vllasaliu, D., Exposito-Harris, R., Heras, A., Casettari, L., Garnett, M., Illum, L., et al. (2010). Tight junction modulation by chitosan nanoparticles: comparison with chitosan solution. *Int J Pharm*. 400(1-2), 183-193.

Vrignaud, S., Benoit, J. P., Saulnier, P. (2011). Strategies for the nanoencapsulation of hydrophilic molecules in polymer-based nanoparticles. *Biomaterials*. 32, 8593-8604.

Wang, B., Ouyang, J., Liu, Y., Yang, J., Wei, L., Li, K. (2004). Sodium ferulate inhibits atherosclerogenesis in hyperlipidemia rabbits. *J Cardiovasc Pharm*. 43, 549-554.

Wicki, A., Witzigmann, D., Balasubramanian, V. K., Huwyler, J. (2015). Nanomedicine in cancer therapy: Challenges, opportunities, and clinical applications. *J Control Release*. 200, 138-157.

Wilson, T. A., Nicolosi, R. J., Woolfrey, B., Kritchevsky, D. (2007). Rice bran oil and oryzanol reduce plasma lipid and lipoprotein cholesterol concentration and aortic cholesterol ester accumulation to a greater extent than ferulic acid in hypercholesterolemic hamsters. *J Nutr Biochem*. 18, 105-112.

Wimardani, Y. S., Suniarti, D. F., Freisleben, H. J., Wanandi, S. I., Ikeda, M. A. (2012). Cytotoxic effects of chitosan against oral cancer cell lines is molecular weight-dependent and cell-type-specific. *Int J Oral Res.* 3, 1-10.

Woranuch, S., Yoksan, R. (2013a). Preparation, characterization and antioxidant property of water-soluble ferulic acid grafted chitosan. *Carbohydr Polym*. 96, 495-502.

Woranuch, S., Yoksan, R. (2013b). Eugenol-loaded chitosan nanoparticles: I. Thermal stability improvement of eugenol through encapsulation. *Carbohydr Polym*. 96, 578-585.

Wu, W., Lee, S. Y., Wu, X, Tyler, J. Y., Wang, H., Ouyang, Z., Park, K., Xu, X., Cheng, J. (2014). Neuroprotective ferulic acid (FA) eglycol chitosan (GC) nanoparticles for functional restoration of traumatically injured spinal cord. *Biomaterials*. 35, 2355-2364.

Wydro, P., Krajewska, B., Hac-Wydro K. (2007). Chitosan as a lipid binder: a langmuir monolayer study of chitosan-lipid interactions. *Biomacromolecules*. 8, 2611-2617.

Xia, W., Liu, P., Zhan, J., Chen, J. Biological activities of chitosan and chitooligosaccharides. *Food Hydrocoll*. 25 (2011) 170-179.

Xu, Y., Wen, Z., Xu, Z. (2010). Chitosan nanoparticles inhibit the growth of human hepatocellular carcinoma xenografts through an antiangiogenic mechanism. *Anticancer Res*. 30, 5103-5110.

Yagi, K., & Ohishi, N. (1979). Action of ferulic acid and is derivatives as antioxidants. *J Nutr Sci Vitaminol*. 25, 127–130.

Yang, C., Tian, Y., Zhang, Z. J., Xu, F. G., Chen, Y. (2007). High-performance liquid chromatography-electrospray ionization mass spectrometry determination of sodium ferulate in human plasma. *J Pharm Biomed Anal*. 43, 945-950.

Yen, M. T., Yang, J. H., Mau, J. L. (2008). Antioxidant properties of chitosan from crab shells. *Carbohydr Polym*. 74, 840-844.

Yu, D. G. Qian, W., Wang, X., Li, Y., Lu, W., Zhang, Y. (2013). Ferulic acid-loaded shellac microparticles prepared using electrohydrodynamic atomization. *Adv Mat Res*. 675, 326-330.

Yuan, Q., Shah, J., Hein, S., Misra, R. K. (2010). Controlled and extended drug release behavior of chitosan-based nanoparticle carrier. *Acta Biomaterialia*. 6, 1140-1148.

Yuan, W. P., Liu, B., Liu, C. H., Wang, X. J., Zhang, M. S. (2009). Antioxidant activity of chito - oligosaccharides on pancreatic islet cells in streptozotocin induced diabetes in rats. *World J. Gastroenterol*. 15, 1339-1345.

Zhang, A. Y., Camp, W. L., Elewski, B. E. (2007). Advances in topical systemic antifungals. *Dermatol Clinics*. 25, 165-183.

Zhao, Z., Egashira, Y., Sanada, H. (2003). Ferulic acid sugar esters are recovered in rat plasma and urine mainly as the sulfoglucuronide of ferulic acid. *J Nutr*. 133, 1355-1361.

Zhao, Z., Egashira, Y., Sanada, H. (2004). Ferulic acid is quickly absorbed from rat stomach as the free form and then conjugated mainly in liver. *J Nutr*. 134, 3083-3088.

Zhao, Z., Moghadasian, M. H., (2010). Bioavailability of hydroxycinnamates: a brief review of in vivo and in vitro studies. *Phytochem Rev*. 9, 133-145.

Zheng, L. Y., Zhu, J. F. (2003). Study on antimicrobial activity of chitosan with different molecular weights. *Carbohydr Polym.* 54(4), 527-530.

Zheng, R. L., Zhang, H. (1997). Effects of ferulic acid on fertile and asthenozoospermic infertile human sperm motility, viability, lipid peroxidation, and cyclic nucleotides. *Free Radic Biol Med*. 22, 581-586.

Zhou, K., Xia, W., Zhang, C., Yu, L. (2006). In vitro binding of bile acids and triglycerides by selected chitosan preparations and their physico-chemical properties. *LWT-Food Sci Technol*. 39: 1087-1092.

Zhou, S. H., Hong, Y., Fang, G. J. (2007). Preparation, characterization and anticancer effect of chitosan nanoparticles. *J Clin Rehab Tiss Engin Res*. 11(48), 9688-9691.

List of Publications

Panwar, R., Pemmaraju, S.C., Sharma, A.K., Pruthi, V. (2016). Efficacy of ferulic acid encapsulated chitosan nanoparticles against *Candida albicans* biofilm. *Microbial Pathogenesis,* 95, 21-31.

Panwar, R., Sharma, A.K., Kaloti, M., Dutt, D., Pruthi, V. (2015). Characterization and anticancer potential of Ferulic acid loaded chitosan nanoparticles against ME-180 human cervical cancer cell lines. *Applied Nanoscience, http://dx.doi.org/10.1007/s13204-015-0502-y.*

Panwar, R., Sharma, A.K., Dutt, D., Pruthi, V. (2015). Phenolic acids from *Parthenium hysterophorus*: Evaluation of bioconversion potential as free radical scavengers and anticancer agents. *Advances in Biosciences and Biotechnology,* 6, 11–17.

Vashisth P., Sharma M., Kumar N., Singh H., **Panwar R.,** Pruthi P.A., Pruthi V. (2015). Antiproliferative activity of ferulic acid-encapsulated electrospun PLGA/PEO nanofibers against MCF-7 human breast carcinoma cells. *3 Biotech* 5:303–315.

Pemmaraju, S.C., Sharma, D., Singh, N., **Panwar, R.,** Cameotra, S.S., Pruthi, V. (2012). Production of Microbial Surfactants from Oily Sludge-Contaminated Soil by *Bacillus subtilis* DSVP23. *Applied Biochemistry and Biotechnology*. 167, 1119-1631.

Singh, N., Agarwal, V., Pemmaraju, S.C., **Panwar, R.,** Pruthi, V. (2011). Impact of infectious *Candida albicans* biofilm on biomaterials. *Indian Journal of Biotechnology*. 10, 417-422.